UNIVERSITY OF CALIFORNIA
RIVERSIDE

Heavy Duty Diesel Particulate Matter and Fuel Consumption Modeling for Transportation Analysis

A Dissertation submitted in partial satisfaction
of the requirements for the degree of

Doctor of Philosophy

in

Chemical and Environmental Engineering

by

George Alexander Scora

March 2012

Dissertation Committee:
Dr. Matthew Barth, Chairperson
Dr. Joseph Norbeck
Dr. David Cocker

The Dissertation of George Alexander Scora is approved:

_____

_____

_____

Committee Chairperson

University of California, Riverside

Acknowledgements

I would like to express my appreciation to several people who have helped me during the pursuit of my degree starting with my dissertation committee, Dr. Matthew Barth, Dr. Joseph Norbeck and Dr. David Cocker, who have always provided me with incredible knowledge, support and encouragement. I would like to specifically thank my graduate advisor Dr. Matthew Barth who provided me with and continues to provide me with excellent guidance in my areas of research.

Many thanks go out to fellow group members in the Transportation Systems Research group at CE-CERT who were invaluable to my research. I would like to specifically thank Michael Todd, Kanok Boriboonsomsin and Guoyuan Wu for their support and many helpful discussions concerning my research work as well as work outside of the scope of this dissertation.

This work would not be possible without the data provided by CE-CERT's Mobile Emissions Lab and the trailer team. My thanks go out to Kent Johnson and Don Pacocha for helping me with my data needs.

Finally, I would like to thank my parents and family for their patience and support. I would like to sincerely thank my father who has been extremely supportive in many ways and a great source of motivation for me.

ABSTRACT OF DISSERTATION

Heavy Duty Diesel Particulate Matter and Fuel Consumption Modeling for Transportation Analysis

by

George Alexander Scora

Doctor of Philosophy, Graduate Program in Chemical and Environmental Engineering
University of California, Riverside, March 2012
Dr. Matthew Barth, Chairperson

One of the most important issues concerning transportation is the impact of vehicle emissions on air quality and human health. Vehicle emission modeling is used to predict and evaluate the relationship between transportation activity and transportation emissions for many applications. The first part of this dissertation builds on previous emission modeling work and focuses on the development of a microscale HDD emission model for particulate matter (PM), one of the primary diesel pollutants of concern. In this work, a hybrid approach is used in which a physically based fuel and emission model is coupled with a statistical model to produce PM estimates at the microscale level. The microscale model is calibrated using measured on-road real-time data from UC Riverside's Mobile Emissions Laboratory (MEL). Microscale modeling errors are less than 3% for fuel consumption and less than 17% for PM over a 2.5 hour validation cycle. PM emissions from compression release braking events were also observed, quantified in the data set, and modeled to improve the overall PM emissions estimation.

A key factor in HDD fuel use and carbon dioxide estimation is the *operational variability* associated with heavy duty truck use. With a better understanding of this variability, it is possible to alter vehicle operation in order to reduce CO_2. The second part of this dissertation focuses on operational parameters and the development of a mesoscale fuel consumption and emission model that accounts for road grade and vehicle weight in addition to velocity. Model development and validation for this portion of work are based on simulated data from the microscale HDD model of measured activity and various road grade and vehicle weight combinations. Mesoscale modeling errors for the validation data set are less than 2% for fuel consumption and less than 12% for PM emissions.

In the final portion of this dissertation, the usefulness of this new mesoscale fuel and emissions model for transportation applications is demonstrated by its implementation in an environmentally friendly navigation (EFNav) application. The focus of EFNav is to decrease the amount of wasted energy (or increased emissions) due to poor routing choices. Routing today is typically based on minimizing the distance or duration traveled. With the inclusion of the new mesoscale fuel/emissions model, vehicle routing can now be based on fuel consumption or emissions that vary with average real-time link speed, average link road grade, and vehicle weight. The application of the mesoscale model is supported by a digital roadway map that integrates real-time traffic data from multiple sources. Vehicle testing of the mesoscale model with EFNav demonstrates the sensitivity of the system to road grade and vehicle weight and the ability

of the system to accurately predict fuel consumption and emissions, making it a useful tool for HDD routing.

Table of Contents

List of Tables

List of Figures

Nomenclature

Selected Acronyms

ADAS	Advanced Driver Alert System
API	Application Programming Interface
ARTEMIS	Assessment and Reliability of Transport Emission Models and Inventory Systems
ATA	American Trucking Association
CARB	California Air Resources Board
CART	Classification and Regression Tree
CE-CERT	UC Riverside's Bourns College of Engineering Center for Environmental Research and Technology
CFD	Computational Fluid Dynamics
CFR	Code of Federal Regulations
CLI	Command Line Interface
CMEM	Comprehensive Modal Emissions Model
CMEM	Comprehensive Modal Emissions Model
CO	Carbon Monoxide
CO_2	Carbon Dioxide
COST	European Cooperation in the field of Scientific and Technical Research
DDC	Detroit Diesel Corporation
DMM	Dekati Mass Monitor
DOC	Diesel Oxidation Catalyst
DPF	Diesel Particulate Filter
DynaNet	Dynamic Roadway Network
EC	Elemental Carbon
ECM	Engine Control Module
ECU	Engine Control Unit
EFNav	Environmentally Friendly Navigation

EMFAC	Emission Factor Model
EPA	Environmental Protection Agency
FTP	Federal Test Procedure Cycle
GHG	Greenhouse Gas
GIS	Global Information System
GPS	Global Positioning System
GUI	Graphical User Interface
H_2SO_4	Sulfuric Acid
HBEFA	Handbook of Emission Factors for Road Transport
HC	Hydrocarbons
HDD	Heavy-Duty Diesel
HDDEM	Heavy-Duty Diesel Emission Model
HDDTC	Heavy-Duty Diesel Test Cycle
HO_2	Hydroperoxyl Radical
Hz	Hertz
ITS	Intelligent Transportation Systems
LD	Light Duty
LDV	Light Duty Vehicle
LHV	Lower Heating Value
MEC	Modal Emission Cycle
MEL	Mobile Emissions Laboratory
MLR	Multiple Linear Regression
MOE	Measure of Effectiveness
MOVES	Motor Vehicle Emission Simulator
N_2	Nitrogen
NCHRP	National Cooperative Highway Research Program
NN	Neural Networks
NO	Nitrogen Oxide
NO2	Nitrogen Dioxide
NOx	Oxides of Nitrogen

O	Oxygen
OH	Hydroxyl Radical
OTAQ	Office of Transportation and Air Quality
PAH	Polycyclic Aromatic Hydrocarbons
PEMS	Portable Emission Systems
PHEM	Passenger Car and Heavy Duty Emission Model
PM	Particulate Matter
POLA	Port of Los Angeles California
POLB	Port of Long Beach California
RMSE	Root Mean Square Error
RMSE	Root Mean Square Error
RPM	Revolutions Per Minute
RTP	Regional Transportation Plan
SIP	State Implementation Plan
SOF	Soluble Organic Fraction
TAC	Toxic Air Contaminant
TDC	Top Dead Center
TEM	Transmission Electron Microscope
TIP	Transportation Improvement Plan
TSP	Total Suspended Particulate
TSR	Transportation Systems Research
US06	Supplemental Federal Test Procedure
US EPA	United States Environmental Protection Agency
VMT	Vehicle Miles Traveled
VRP	Vehicle Routing Problem
VSP	Vehicle Specific Power

Selected Symbols

Δt	Change in time
ε	Constant term
θ	Grade
ρ_a	Density of air
a	Vehicle acceleration
A_f	Frontal area of vehicle
b_x	Regression coefficient where $x = 0,1,2,3 \ldots n$
C_d	Coefficient of aerodynamic drag
C_r	Coefficient of rolling resistance
da/dt	Change in acceleration with time (jerk)
dF/dt	Change in fuel rate with time
dF/dt-	Negative portion of dF/dt
dF/dt+	Positive portion of dF/dt
F	Fuel use rate
g	Gravity, grade
k	Release constant
M	Mass of vehicle
n	Number of elements, order
PM_{Idle}	Idle PM value
$PM_{r,t}$	PM released at time t
$PM_{c,t}$	PM in the cylinders at time t
$PM_{c,t=0}$	PM in the cylinders at the start of the braking event
r	Pearson's Correlation Coefficient
R^2	Coefficient of Determination
v	Vehicle speed
w	Weight
x	Independent/explanatory variable
Y	Dependent variable

1.0 Introduction

The estimation of emissions from transportation sources is critical for air quality management and control. The ability to relate emissions and specific transportation activity is useful for various purposes including policymaking and the development and evaluation of Intelligent Transportation System (ITS) ideas and technologies. To date, there has been much effort put into the development of emission models for a variety of LD vehicles, but not as much for HDD vehicles, even though their contribution to freight movement and the emission inventory is significant. The most recent developments in on-highway truck emission certification standards in the United States called for significant reductions in NO_x emission for 2007 and for significant PM reductions for 2010 (EPA, 1997). These new on-highway HDD emission standards are forcing improvements in HDD emission controls such as the use of exhaust after-treatment devices, most notably the diesel-particulate filter (DPF) for PM emissions. Improvements in emission control technologies for new vehicles further increase the variation in emission performance between new and old HDD vehicles.

Part of the objective of this research is the development of an HDD PM emission model that can be used for transportation analysis at the microscale level. A new modeling methodology has been implemented as a hybrid approach in which a parameterized physical model, vehicle characteristics and different aspects of vehicle operation are used to calculate energy and fuel consumption which are then related to PM emissions through a statistical model. One of the key benefits of the microscale modeling

approach, in comparison to the more traditional mesoscale or macroscale modeling approaches, is the ease of integration with traffic simulation software with similar time resolutions.

In addition, concerns over limiting Green House Gas (GHG) emissions has put added attention on heavy duty trucks and improving their fuel economy thereby reducing their CO_2 emissions. Most of the focus to date has been placed on specific vehicle technologies and alternative fuels. Another key area, which is often overlooked, is the operational variability associated with heavy-duty truck use and how vehicle operation can affect CO_2 and other emissions. In the second portion of this dissertation, operational parameters such as vehicle speed, road grade and vehicle weight, and their influence on fuel consumption and emissions are examined. A modeling data set is created based on simulated microscale fuel and emissions results for measured activity and various road grade and vehicle weight combinations. A statistical mesoscale fuel model which utilizes not only average speed, but road grade and vehicle mass, is developed and calibrated from the modeling data set.

In the final portion of this dissertation, the mesoscale model is applied in an EFNav application. It has been shown that a significant amount of CO_2 reductions can be achieved by traffic operation improvements (Barth & Boriboonsomsin, 2008). One of the means of implementing these ideas is EFNav which focuses on optimizing driver routing choices and driving behavior based on a variety of operational parameters and road conditions (Barth, Boriboonsomsin, & Vu, 2007). In many cases, the shortest or quickest

route will minimize fuel use and emissions, but this does not always hold true during congestion or with significant road grade. This is especially true for HDD vehicles due to their low power to weight ratios. In this portion of work, the model's ability to predict fuel use and emissions based on average roadway speed, average road grade and vehicle mass are utilized by the EFNav routing algorithm.

Intellectual Merit: HDD engine emissions are known to cause adverse health as well as environmental effects and according to the California Air Resource Board (CARB) about 70% of the cancer risk in California from breathing toxic air pollutants stems from diesel exhaust particles (CARB, 2000). HDD emissions also contribute significant amounts of CO_2, the most important GHG. Characterizing HDD emission sources and understanding operational conditions affecting HDD emissions is an important step in developing control strategies and HDD related policy decisions. Mobile source emission models are a necessary part of transportation analysis and are used widely in a number of applications at the federal, local and private level to quantify and characterize vehicle emissions. Microscale emission models function at a higher time scale resolution than traditional transportation emission models and are more suited for the development and analysis of numerous ITS strategies, which will likely be an increasingly important part of future vehicle emission control strategies and up-and-coming driver's aids, which can utilize EFNav technologies.

Broader Impacts This research combines elements of environmental engineering, transportation engineering and public policy. Given the recent focus on HDD emissions

and the current global interest in reducing greenhouse gases, results from this work would be helpful in developing strategies to address these issues as they relate to on-highway heavy-duty transportation. Methods of analysis and modeling used and developed in this work may also be applicable elsewhere.

1.1 Research Objectives

The three key goals of this research are: 1) to develop a microscale modeling tool for HDD PM emissions; 2) to evaluate vehicle operational parameters for HDD and develop a mesoscale emission model that accounts for these operational parameters; and 3) to demonstrate the usefulness of the mesoscale model for transportation applications with an example implementation in an Environmentally Friendly Navigation (EFNav) application. The specific objectives of the research are listed below.

- Develop a modeling tool that estimates second-by-second HDD fuel use and PM emissions calibrated with a unique set of real-time emission and activity data gathered by UCR's Mobile Emission Lab.
- Further the understanding of operational parameters in relation to HDD emissions through data analysis. Develop a unique comprehensive modeling dataset for the HDD operational parameters of vehicle speed, vehicle weight and road grade for use in data analysis and mesoscale model development. Utilizing the modeling data set, develop a mesoscale emission model based on the key operational parameters of vehicle speed, road grade and vehicle weight.

- Demonstrate the usefulness of the mesoscale model for transportation applications by implementing it in an example EFNav application, thereby improving the EFNav application, extending its capabilities, and making it applicable to HDD vehicles. Evaluate the performance of the mesoscale model in the EFNav application for HDD vehicles.

1.2 Impact of Research

The lack of real-time HDD PM emissions data and the limited availability of real-time HDD emission data measured in-situ in general has made the development of HDD microscale emission models difficult in the past. This research utilizes a unique set of HDD emission data to develop an emission model with new capabilities as well as increasing the general knowledge of HDD on-road emission factors. This research also presents a method of HDD routing based on vehicle mass and road grade, an important parameter not utilized in commercially available truck routing software.

1.3 Overview of Dissertation

This dissertation begins with an introduction in Chapter 1.0 which focuses on the research objectives and impact of this work. Chapter 2.0 gives background data for the area of research including the area of transportation and how it relates to HDD as well as vehicle emission modeling and EFNav. Chapter 0 presents the development of the microscale HDD PM emissions model including discussions on the modeling approach and the measured data set used for development and validation. Chapter 4.0 describes the

use of the HDD microscale emission model to create a modeling data set, the evaluation of operational parameters based on measured data and the modeling data set, and the application of the modeling data set in the development of a mesoscale model for HDD vehicles. In Chapter 5.0, the use of the mesoscale model in an EFNav application is demonstrated and initial results are presented. The dissertation concludes in Chapter 6.0 with a discussion of results and areas for future work.

2.0 Background and Rationale

This chapter describes some basic background information relating to the areas of research, namely transportation, how transportation and more specifically HDD vehicles contribute to air pollution as well as the methods to model these emission contributions. Environmentally friendly navigation is also introduced as one way to reduce certain transportation related emissions.

2.1 Transportation and Heavy Duty Trucks

Transportation is an important part of the US energy picture, accounting for roughly 27% of the total US energy consumption and 72% of the petroleum use in 2009 as seen in Figure 2-1 (AEI, 2010). Petroleum accounts for 94% of the energy source for the transportation sector (AEI, 2010).

A large portion of the fuel used in the transportation sector is from heavy-duty trucks. According to the U.S. Department of Transportation, heavy-duty trucks accounted for roughly 67% of the total tonnage carried by all modes of domestic freight transportation in 2009 and the demand for truck transport is expected to increase by nearly 68% between 2009 and 2040 at which point heavy-duty trucks will account for roughly 79% of the total estimated tonnage moved by transportation in the U.S. (FHWA, 2011).

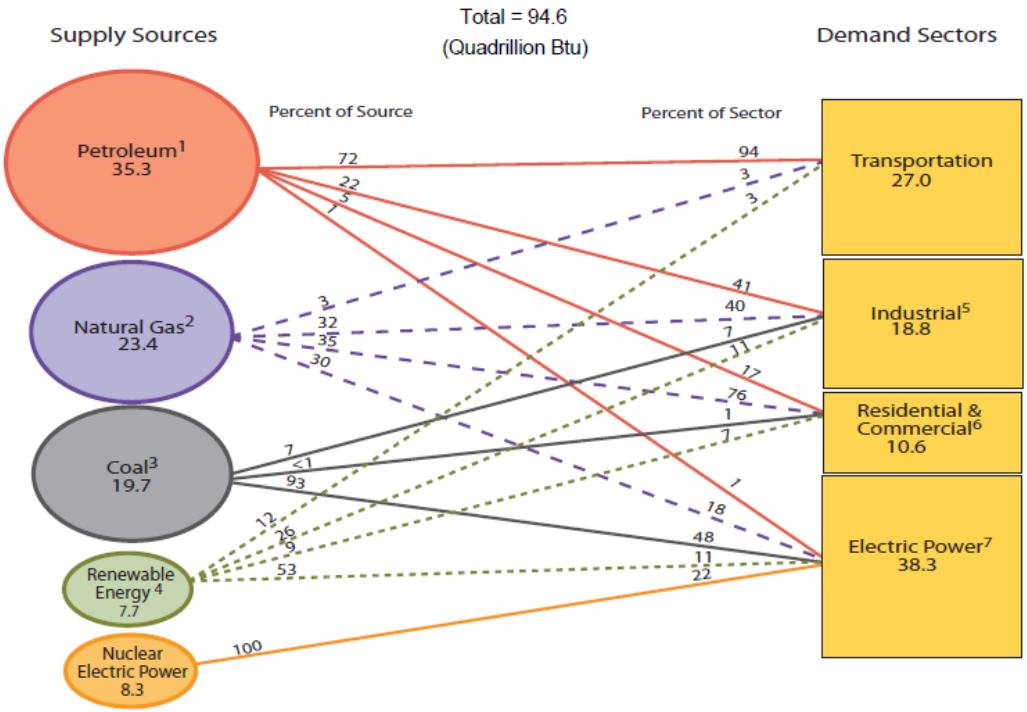

Figure 2-1 U.S. energy consumption by source and sector in quadrillion BTU in 2009 (AEI, 2010).

Figure 2-2 shows the breakdown of transportation related greenhouse gas emissions which are primarily CO_2. Since most of the carbon in fuel is converted to CO_2 during the combustion process (only a small portion remains partially oxidized or unoxidized), CO_2 is closely correlated to fuel use. Figure 2-2 shows that in 2008 roughly 20% of transportation related GHG emissions in California were produced by heavy trucks.

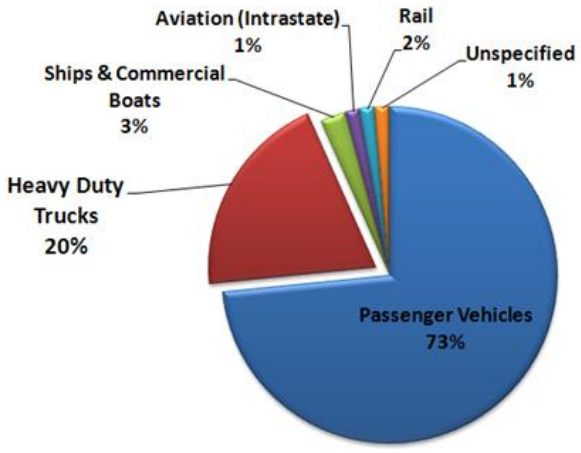

Figure 2-2 Transportation related greenhouse gas emissions for California in 2008. (CARB, 2010)

Heavy-duty trucks rely primarily on diesel engines as their power source due to the fuel efficiency, reliability and low end torque characteristics of diesel engines. As a result of the high power requirements and heavy loads carried by heavy-duty trucks, the fuel economy for these trucks is around 6 miles per gallon of diesel fuel and has not changed significantly in the last 30 years as shown in Figure 2-3 (AEI, 2010). The reliability of diesel engines is improved due to the lack of an electrical ignition system, their robust nature to handle high compression combustion, and the lower engine speeds at which they operate.

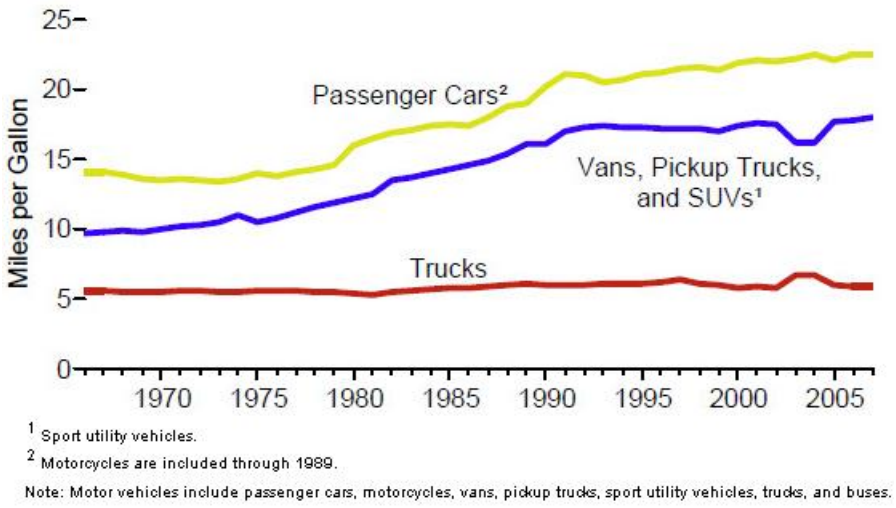

Figure 2-3 Vehicle fuel economy (EIA, 2010).

Although heavy-duty diesel trucks have a lower mile per gallon fuel economy value than light-duty vehicles as shown in Figure 2-3, they are more fuel efficient in terms of work per gallon of fuel. Diesel engines have higher conversion efficiencies than gasoline engines since they operate at higher compression ratios and temperatures. Their abundant use in the transportation sector, however, makes them the largest contributors to the freight emission inventory, accounting for an estimated 66.8% of the NO_x emissions and 64.7% of the PM emissions (FHWA, 2011).

Diesel engines operate under lean conditions (excess oxygen) and therefore emit relatively low levels of carbon monoxide (CO) in relation to their gasoline counterparts. Gaseous hydrocarbons (HC) emissions from diesel engines are typically 5 times lower than those of gasoline engines (Heywood, 1988). Diesel engines are a significant source of oxides of nitrogen (NO_x) and particulate matter (PM). In the diesel engine combustion process, fuel is injected into the cylinder just before combustion and the fuel distribution

is non-uniform resulting in hot spots and areas of incomplete combustion, which strongly affects pollutant formation. Elevated levels of NO_x emissions in diesel engines are a result of the oxidation of atmospheric nitrogen at high combustion temperatures and PM is primarily from the incomplete combustion of hydrocarbon compounds from the fuel or lubricating oil resulting in soot and absorbed organic compounds (Heywood, 1988). One of the problems in controlling engine out NO_x and PM emissions in diesel engines is the inverse relationship that exists between the two emissions. Measures that reduce combustion temperatures in an effort to reduce NO_x such as retarding fuel injection timing or fuel-water emulsions will also result in more incomplete combustion thereby increasing HC, CO and predominantly PM emissions.

2.2 Greenhouse Gases and Pollutant Emissions

Air pollution can be generally defined as the presence of one or more contaminants in the air in such quantities and duration that it causes damage to human life, plant life, animal life or property, or that it interferes with the comfortable enjoyment of life or property (Wark & Warner, 1981). The effects of air pollution can be divided into two basic categories; those having local impacts and those having more of a global impact. Historically, vehicle emissions standards were put in place to control gaseous emissions associated with local air quality problems such as poor visibility and respiratory illness. NO_x and PM emissions have been the main criteria pollutants of concern for heavy-diesel vehicles since they are produced in greater quantities relative to

HC and CO in the diesel engine. PM in particular was listed by the California Air Resources Board (CARB) as a Toxic Air Contaminant (TAC) in 1998 (CARB, 1998).

2.2.1 Carbon Dioxide

Currently, there is an emphasis on reducing GHG emissions whose increasing levels in the atmosphere are believed to affect climate change on a global scale. In California, landmark climate-change legislation (AB 32) was signed into law in 2006 with the intent of creating programs to reduce California's GHG emissions to below 1990 levels by 2020 (CARB, 2009). In December 2008, the CARB adopted the Heavy-Duty Greenhouse Gas Emission Reduction Regulation which requires California trucks and trucks operating in California to meet certain performance requirements between 2011 and 2023. Under the new rule, diesel exhaust filters must be installed on diesel trucks with almost all vehicles upgraded by 2014 and truck engines older than 2011 will have to be replaced during a phase in period between 2012 and 2022 (ARB, 2008).

One of the primary GHG pollutants of concern is CO_2 which is a byproduct of fuel combustion. The amount of CO_2 emission produced from the combustion of fuel is directly related to the carbon content of fuel. The carbon content of fuel varies, but the typical carbon content of diesel fuel is roughly 2,778 grams of carbon per gallon of fuel in comparison to gasoline which has around 2,421 grams of carbon per gallon of fuel (EPA, 2005).

2.2.2 Carbon Monoxide

CO emissions are a product of incomplete combustion and are controlled primarily by the air-fuel ratios occurring during combustion (Heywood, 1988). The formation of CO is typical for a rich air-fuel ratio where excess fuel is present and an insufficient amount of air to combust it. Diesel engines typically run under lean air-fuel conditions which means they have an excess amount of air for the quantity of fuel they are burning. Under these conditions, incomplete combustion is less common and therefore diesel CO emissions are extremely low unlike gasoline engines which run close to stoichiometry and which run rich at full load. It has been shown that for diesel engines, CO does not vary significantly with the air-fuel ratio (Heywood, 1988). Due to its low levels, diesel CO is not considered to be of great concern.

2.2.3 Hydrocarbons

Engine HC emissions in general are primarily a result of unburned hydrocarbons due to combustion inefficiencies which can arise is several ways. During the compression stroke, unburned fuel can be forced into crevices between the piston rings and cylinder walls where the combustion flame is too large to enter. Unburned fuel in crevices can escape later during the exhaust stroke. Another source of unburned hydrocarbons is from a fuel layer “quench layer” left on the cylinder walls which remains unburned, not being reached by the combustion flame before it extinguishes. Yet another source for unburned HC emissions is from the adsorption and desorption of fuel by any lubricating oil left on any of the cylinder surfaces (Heywood, 1988).

For diesel engines, fuel is injected toward the end of the compression stroke, shortly prior to combustion. For this reason, fuel has a limited time to distribute and fuel distribution becomes critical for the combustion process. This results in unburned hydrocarbons in areas of the combustion flame where air-fuel mixtures either prevent combustion from starting or the fuel spray is quenched on the cylinder walls (Heywood, 1988).

2.2.4 Nitrogen Oxides

One of the primary emissions of concern for diesel engines are (Nitrogen Oxides) NO_x, the other being Particulate Matter (PM). NO_x is a collective term that refers to both Nitric Oxide (NO) and Nitrogen Dioxide (NO_2), but the predominant emission for diesel engines is NO. The primary source of NO_x in vehicle emissions is from the oxidation of N_2 from the atmosphere. Atmospheric air is composed of roughly 78% N_2. The basic mechanisms for the formation of NO during combustion are given in equations 2.1 and 2.2 and for NO_2 are given in equation 2.3 (Heywood, 1988).

$$N_2 + O = NO + N \quad \textbf{2.1}$$

$$N + O_2 = NO + O \quad \textbf{2.2}$$

$$NO + HO_2 = NO_2 + OH \quad \textbf{2.3}$$

The formation of NO_x emissions in diesel engines is well understood and is dependent mainly on the presence of sufficient oxygen and high temperatures (Heywood, 1988).

2.2.5 Particulate Matter

Diesel particulate matter refers to the aerosol portion of diesel exhaust. This is basically the portion of the exhaust that can be collected and measured on a sampling filter. A typical diesel generated PM particle is presented in the TEM picture in Figure 2-4.

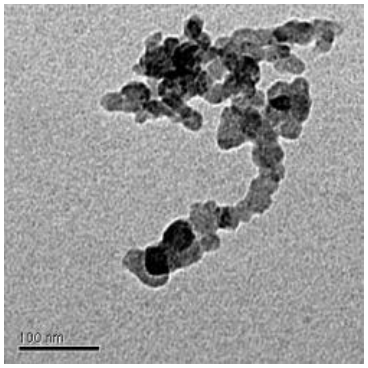

Figure 2-4 TEM image of diesel PM particle (Park, Cao, Kittelson, & McMurray, 2003).

Diesel PM consists of three main parts: elemental carbon (EC), the soluble organic fraction (SOF), and hydrated sulfuric acid. The various parts that make up a diesel PM particle are illustrated in Figure 2-5 (Twigg & Phillips, 2009). The elemental carbon portion of PM, also known as black carbon or soot, is the solid portion of diesel PM. The soluble organic fraction contains the heavier hydrocarbons. This portion contains any polycyclic aromatic hydrocarbons (PAH) that may be present in the emissions. Several PAHs are known carcinogens, especially the ones with four or more aromatic rings. The last portion is hydrated sulfuric acid and its portion will be directly related to the amount of sulfur in the diesel fuel.

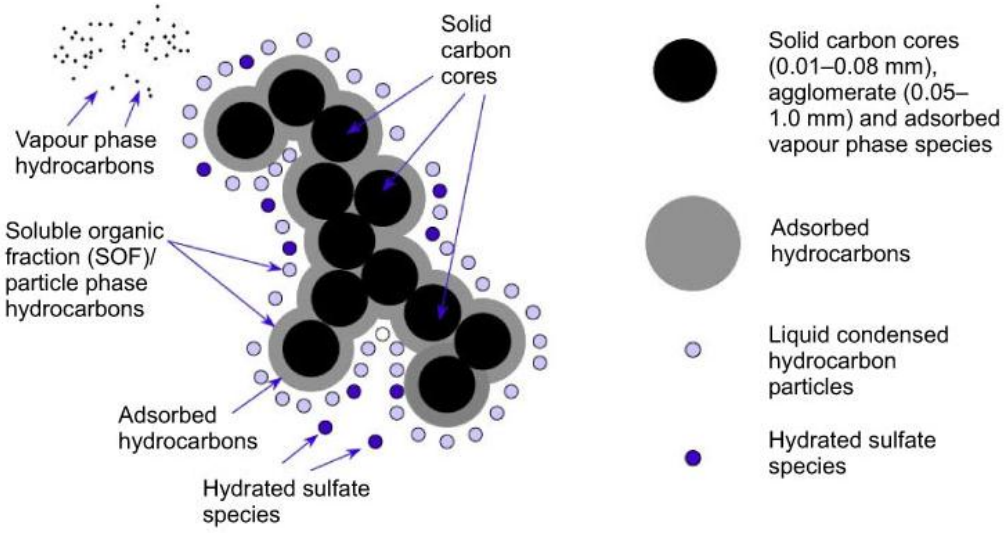

Figure 2-5 Schematic of diesel particulate matter composition (Twigg & Phillips, 2009).

PM ranges in size from a few nanometers to one micron. Some of the constituents in PM are in the nuclei mode and others are present in agglomerations of several nuclei particles. This creates a bimodal size distribution. PM under 2.5 microns in diameter is classified as fine and PM over 2.5 microns is considered coarse. Fine particulate has the characteristic of being able to penetrate deep into the respiratory system, which has serious health consequences (Seinfeld & Pandis, 1998).

Diesel PM has been classified by CARB in 1998 as a toxic air contaminant (TAC). In a 2000 study, CARB also attributed roughly 70% of the cancer risk from air contaminants to diesel PM (CARB, 2000). In addition to this, PM is known to be a respiratory irritant and is believed to be a precursor to serious respiratory illness.

Currently, diesel engines are being regulated to reduce PM and NO_x, and reducing CO_2 emissions has become an increasingly important goal. Some evidence suggests that

there is a fuel penalty associated with aftertreatment devices, such as diesel particulate filters (DPF), used to meet the more stringent current emission standards (Johnson, 2006) (Parks & Huff, 2007).

2.3 Vehicle Emission Modeling

Vehicle emission modeling is useful to evaluate and predict the relationship between vehicle activity and vehicle emissions for mobile source emission analysis. Vehicle emission modeling has long had a place at the local, state and federal levels as a tool to develop and evaluate transportation policy or for related decision making. This method of estimating the contributions of emissions from mobile sources has been used by the EPA to evaluate highway mobile source emission control strategies and by state, local and regional planning agencies like CARB in the development of control strategies for State Implementation Plans (SIP) under the Clean Air Act. In addition to this, emission modeling is used by metropolitan planning organizations and transportation departments for conformity analysis and transportation planning as well as by industry, academia and research organizations in many endeavors including the development of environmental impact statements (EPA, 2002). To date, there has been much effort put into the development of emission models for a variety of LD vehicles, but not as much for HDD vehicles. Vehicle emissions can be modeled at various levels of temporal resolution and generally fall into three major categories: macroscale, mesoscale and microscale.

2.4 Macroscale/Mesoscale Emission Models

Macroscale or large scale models are used to calculate emissions for large regional inventories. Regional to national models, such as the US EPA's MOBILE model (EPA, 2002) or CARB's EMFAC model (CARB, 2000), are large scale models and have been used for many years in evaluating fleet emissions. These models calculate vehicle emission rates under various conditions affecting in-use emissions such as ambient temperatures and average traffic speeds, based on user inputs.

Mesoscale traffic emission models estimate emissions at the roadway network link or corridor level based on mesoscopic parameters such as average link velocity. Results from mesoscale emission models as well as from higher resolution microscale modeling can be aggregated to produce macroscale emission results although this may be computationally intensive depending on the size of the network. Emission results from macroscale models cannot be reasonably broken down to the microscale level.

2.4.1 MOBILE and EMFAC

One of the primary functions of transportation emission models is to help generate emission inventories for the conformity analysis of transportation projects and air quality plans. Conformity analyses are necessary for the development of State Implementation Plans (SIP)'s which demonstrate the compliance of Regional Transportation Plans (RTPs) and Transportation Improvement Plans (TIPs) with the federal Clean Air Act. EPA's Highway Vehicle Emission Factor (MOBILE) model and CARB's Emission Factor (EMFAC) model have been the official models recognized by the federal and state

governments for these purposes for many decades. EPA's MOBILE model has been superseded by the MOVES model discussed in 2.6.1, however at this time it is not required for regional conformity analysis until March 2013 (EPA, 2011). EMFAC is used in California while MOBILE and MOVES are used in the remaining 49 states.

Emission model scales vary in level of resolution from macroscale to mesoscale to microscale. MOBILE and EMFAC are both macroscale emission models designed to estimate emissions from a wide area or region using vehicle average-speed emission factors. These emission models are based primarily on engine certification and dynamometer test data.

One of the drawbacks of macroscale emission models such as the MOBILE and EMFAC series is that they do a poor job at estimating emissions at smaller time scales. Macroscale models cannot be used to evaluate transportation designs or operational improvements at the vehicle level as is required for new Intelligent Transportation Strategies (ITS).

2.5 Microscale Emission Models

Large scale models, although good for predicting large inventories, are not well suited for evaluating operational effects that involved activity at the "microscopic" level, such as ramp metering, signal coordination, and many ITS strategies. These limitations have resulted in a need for emission models that consider emissions at a more fundamental level based on "modal" operation, i.e., emissions during activities of acceleration, deceleration, cruising, idle, etc. (Barth, Malcolm, & Scora, 2001).

Microscale models, also referred to as continuous or instantaneous models, address emissions at the shortest time scales, typically second-by-second. Unlike macroscale models, microscale models lend themselves well to analyzing the emission effects of changes in vehicle driving patterns on a small scale. Due to the similar resolution of timescales, microscale emission models are also useful for emission analysis with microscale traffic simulation software. The following subsections describe three microscale models and microscale modeling is discussed in further detail in Section 3.4.

2.5.1 Comprehensive Modal Emission Model (CMEM)

The Comprehensive Modal Emissions Model (CMEM) is a microscopic emissions model initially developed in the late 1990's by the College of Engineering Center for Environmental Research and Technology (CE-CERT) at the University of California Riverside. CMEM predicts fuel consumption and emissions from CO_2, CO, HC and NO_x on a second-by-second time scale given vehicle parameters and second-by-second vehicle activity information.

CMEM uses a physical, power-demand approach in which the fuel consumption and emissions process is broken down into general components that correspond to physical phenomena associated with vehicle operation and emissions production. Each component is modeled as an analytical representation consisting of various parameters that are characteristic of the process. These parameters vary according to vehicle type, engine technology, emission technology, and level of deterioration. One distinct advantage of this approach is that it is possible to adjust many of these physical

parameters to predict energy consumption and emissions of future vehicle models and applications of new technology (e.g., after-treatment devices).

The current version of CMEM (version 3.2) includes 28 light-duty vehicle/technology categories and 3 heavy-duty vehicle/technology categories (An F. , Barth, Scora, & Ross, 1998) (An F. , Barth, Scora, & Ross, 1999) (Barth M. , et al., 2000) (Barth, Scora, & Younglove, 2004). An HDD emission model for particulate matter (PM), one of the primary diesel emissions of concern, has been developed as part of this dissertation and is currently being incorporated into the CMEM modeling effort.

Model Background

The effort to develop CMEM began in 1996 with the four-year National Cooperative Highway Research Program (NCHRP, Project 25-11) for the development of a modal model for light duty vehicles. Over the years, CMEM has been maintained and updated with support from the U.S. EPA.

Initial development of the model was focused on emission from light-duty vehicles and the first version of CMEM contained 26 light-duty gasoline vehicle/technology categories characterized by emission control technologies, emission certification standards, mileage, power-to-weight ratios, and high emitting characteristics. These vehicle categories were developed based on dynamometer test data collected at CE-CERT for over 300 vehicles and three drive cycles. The model framework was extended later to include HDD trucks since emissions from HDD vehicles were attracting more and more attention and it is generally believed that transit buses and heavy trucks

will offer some of the earliest opportunities for public implementation of automated operations. With the combination of the light-duty and heavy-duty vehicle emission models, it is possible to estimate the total fuel consumption and emissions impact from ITS technologies and strategies on a systems-wide basis and allow for a more complete fleet emission inventory to be estimated.

In the past decade, there has been much interest in Intelligent Transportation Systems (ITS) and their potential to improve certain aspects of transportation. In order to evaluate these potential benefits, there arose a need for emission models that operate at a finer scale. This was a major impetus for the development of CE-CERT's Comprehensive Modal Emissions Model (CMEM) (Barth M. , An, Norbeck, & Ross, 1996). To facilitate the evaluation of the environmental impacts of ITS technologies and strategies, CMEM has been integrated with various ITS simulation models and analytical techniques (Barth, Malcolm, & Scora, 2001).

Model Structure

During the initial CMEM development, 26 different vehicle/technology categories, shown in Table 2-1, were developed from test data of an assortment of over 300 light duty vehicles. The various vehicle/technology categories were defined to serve as the basis for the model, as well as to guide the vehicle recruitment and testing performed. Vehicle/technology categories and the sampling proportions of each were chosen based on the emissions contribution of each group, as opposed to a group's actual population in the national fleet. This resulted in several distinct high-emitting

vehicle/technology categories; the remainder of the categories being based on vehicle class (e.g., car, truck), emission technology (e.g., no catalyst, catalyst, etc…), emission certification standard (e.g., Tier 0, etc…), power-to-weight ratio, and mileage.

Each of the test vehicles was recruited randomly within a category, tested on a dynamometer under the standard FTP test, the high-speed US06 cycle and the in-house developed Modal Emission Cycle, MEC. The MEC was designed to cover a wide range of operating conditions. More details on the dynamometer testing procedure can be found in (Barth, Wenzel, Scora, An, Ross, & Norbeck, 1997).

Table 2-1 Vehicle/technology modeled categories in CMEM.

Category #	Vehicle Technology Category
	Normal Emitting Cars
1	No Catalyst
2	2-way Catalyst
3	3-way Catalyst, Carbureted
4	3-way Catalyst, FI, >50K miles, low power/weight
5	3-way Catalyst, FI, >50K miles, high power/weight
6	3-way Catalyst, FI, <50K miles, low power/weight
7	3-way Catalyst, FI, <50K miles, high power/weight
8	Tier 1, >50K miles, low power/weight
9	Tier 1, >50K miles, high power/weight
10	Tier 1, <50K miles, low power/weight
11	Tier 1, <50K miles, high power/weight
24	Tier 1, >100K miles
	Normal Emitting Trucks
12	Pre-1979 (<=8500 GVW)
13	1979 to 1983 (<=8500 GVW)
14	1984 to 1987 (<=8500 GVW)
15	1988 to 1993, <=3750 LVW
16	1988 to 1993, >3750 LVW
17	Tier 1 LDT2/3 (3751-5750 LVW or Alt. LVW)
18	Tier 1 LDT4 (6001-8500 GVW, >5750 Alt. LVW)
25	Gasoline-powered, LDT (> 8500 GVW)
40	Diesel-powered, LDT (> 8500 GVW)
	High Emitting Vehicles
19	Runs lean
20	Runs rich
21	Misfire
22	Bad catalyst
23	Runs very rich

The generalized CMEM model is shown in Figure 2-6 and consists of six distinct modules that individually predict: 1) engine power; 2) engine speed; 3) air/fuel ratio; 4)

fuel-use; 5) engine-out emissions; and 6) catalyst pass fraction. The core of the CMEM model is fuel use which is determined based on engine power and engine speed. The modeling inputs include operating parameters such as vehicle trajectory and test conditions (e.g., temperature, soak time, etc…), and vehicle parameters both generally available and calibrated. Generally available parameters are those that typically define some physical characteristic of the car such as weight or engine power. These parameters are usually readily available. Calibrated parameters on the other hand are obtained from optimization procedures to calibrate these parameters from the second-by-second test data. Details of the model structure are given in (An F. , Barth, Norbeck, & Ross, 1997).

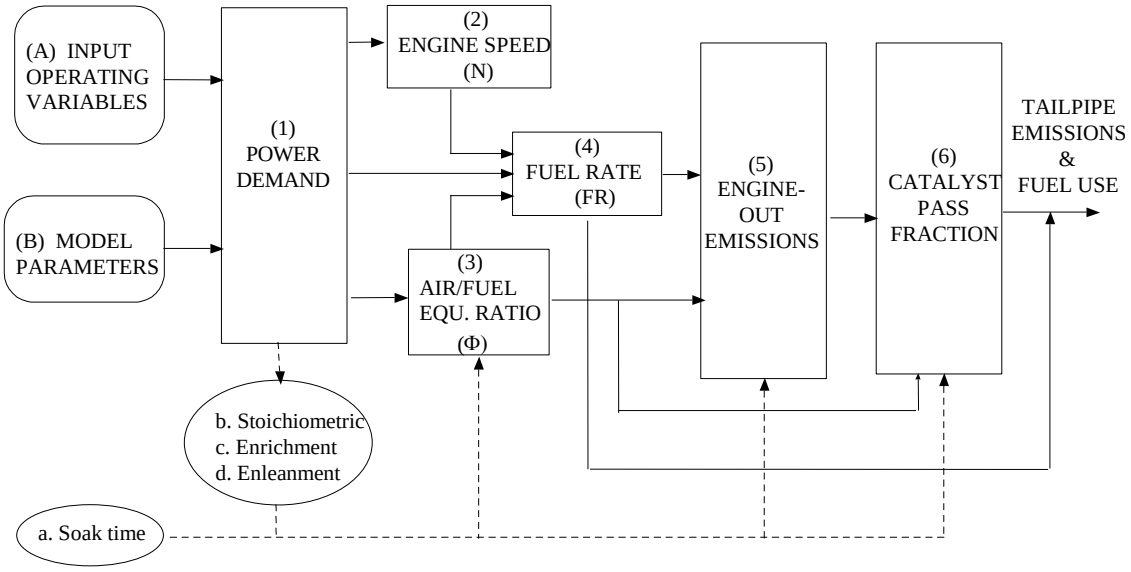

Figure 2-6 Generic CMEM model structure.

The CMEM model currently exists in several different formats. During development, the model was carried out in a research environment, using MATLAB (MathWorks, 2009) modeling/analysis tools and was subsequently coded in other formats

so that the model could be used outside of the MATLAB environment. For this a command line user interface was developed for the UNIX and PC environments. Since this time, a JAVA based Graphical User Interface has been added. Effort was also put into the integration of CMEM with transportation software. Further background on modal emission modeling and the NCHRP project is given in (An F. , Barth, Norbeck, & Ross, 1997) (An F. , Barth, Scora, & Ross, 1998) (Barth M. , et al., 2000) (Barth M. , An, Norbeck, & Ross, 1996).

2.5.2 VT-Micro

The Virginia Tech Microscopic (VT-Micro) model is a statistically based model, which uses a combination of speed and acceleration levels implemented in a dual-regime model to estimate fuel consumption and emission rates for light-duty vehicles. The modeling equation is presented as

$$\mathrm{MOE} = \begin{cases} \exp\left[\sum_{i=0}^{3}\sum_{j=0}^{3}\left(L_{i,j}^{e} \times s^{i} \times a^{j}\right)\right] & \text{for } a \geq 0 \\ \exp\left[\sum_{i=0}^{3}\sum_{j=0}^{3}\left(M_{i,j}^{e} \times s^{i} \times a^{j}\right)\right] & \text{for } a < 0 \end{cases} \qquad \textbf{2.4}$$

Where measure of effectiveness (MOE) is fuel consumption or emission rates including CO, HC, NOX, and CO_2. The coefficients $L^{e}_{i,j}$ and $M^{e}_{i,j}$ are given for each MOE, s^i is speed at speed exponent *i*, and a^j is acceleration at acceleration exponent *j* (Ahn, Rakha, Trani, Aerde, & M., 2002) (Rakha, Van Aerde, Ahn, & Tran, 2000) (Rakha, Ahn, & Trani, 2004).

The model is based on chassis dynamometer data for 101 LD vehicles. A subset of test data for 60-vehicles classified as normal was grouped homogeneously using Classification and Regression Tree (CART) analysis. CART analysis uses a regression tree method to search for patterns and relationships in data sets and identify classifiers. A tree of classifiers is built by continually splitting at active nodes based on split criterion until minimum split criteria are met. Calibration of the VT-Micro model involves the estimation of 32 parameters for each MOE.

2.5.3 PHEM

The Passenger Car and Heavy Duty Emission Model (PHEM) is an instantaneous emission model developed by TU Graz starting in 1999 under several international and national projects including the EU 5th research program ARTEMIS (Assessment and Reliability of Transport Emission Models and Inventory Systems) Work Project 400, the COST (European COoperation in the field of Scientific and Technical Research) 346 initiative and the German-Austrian-Swiss cooperation on the HandBook of Emission FActors for Road Transport (HBEFA) (Hausberger, Rodler, Sturm, & Rexeis, 2003). The model uses second-by-second vehicle speed, acceleration and grade as well as specific vehicle parameters to calculate driving resistance, transmission losses and engine speed which it then relates to fuel consumption and emissions through interpolation of steady state engine fuel consumption and emission maps. Emissions taken from engine maps are then adjusted with transient corrections to adapt the values to the actual driving cycle.

The diagram in Figure 2-7 shows the general process of the PHEM model (TU Graz, 2009).

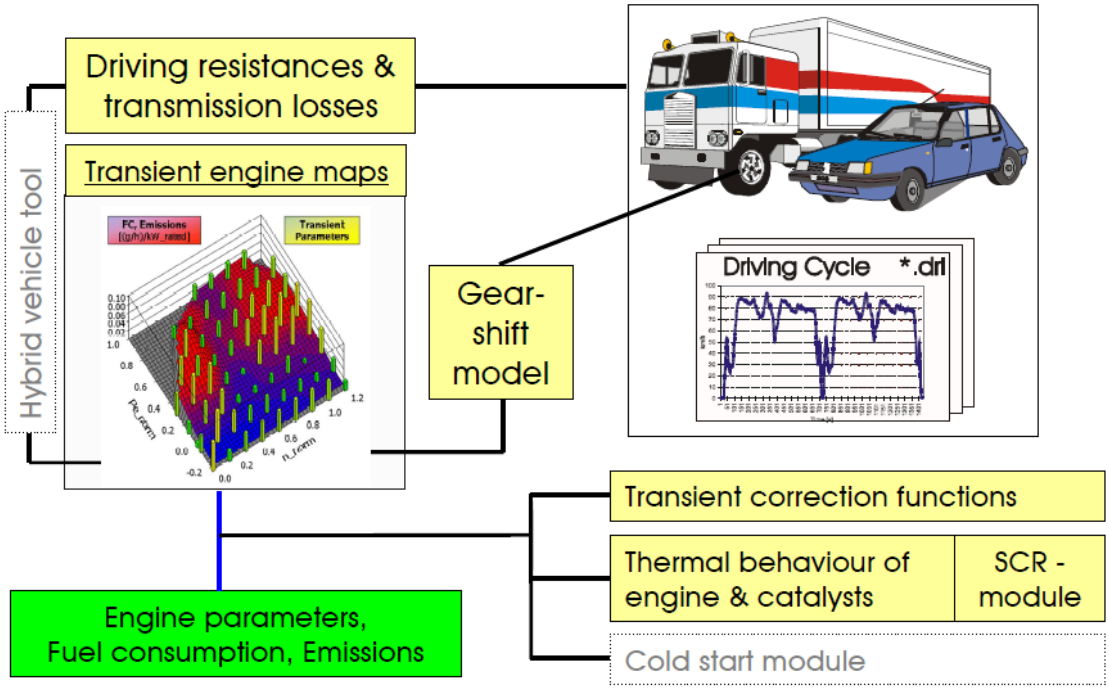

Figure 2-7 PHEM - Passenger car and heavy duty emission model (TU Graz, 2009)

2.5.4 Additional Modeling Efforts for Heavy-Duty Diesel

There are several notable modeling efforts specific to diesel vehicles. Two of these are presented here. Researchers from the University of California, Davis have developed a model that applies operational correction factors to emission rates from a mixed linear regression model. Model inputs include factors such as the measure of high power transient driving, idle time, and average speed. The test data set for this project was chassis dynamometer test data for HDD vehicles from the Coordinating Research Council's E55/E59 research project (Kear & Niemeier, 2006).

Researchers at Tsinghua University have investigated the development of an HDD specific emission model for China. This modeling effort analyzed test data from several HDD trucks and buses and compared emission rates on various external parameters. In this work a multivariable linear regression model based on vehicle specific power (VSP), CO_2 and a calculated variable called engine stress used for clustering was developed. Vehicle specific power is discussed in further detail in Section 3.5.2. Results show PM prediction results with a correlation of 0.73 and error of 29 % (Liu, He, Lents, & Wang, 2008).

2.6 Multi-scale Emission Models

Multi-scale emission models are flexible emission models that can estimate emissions at the microscale to the macroscale level. In general, results from microscale emission modeling can be aggregated spatially and temporally to produce mesoscale or macroscale emission estimates, making microscale modeling an important foundation for a multi-scale vehicle emission model structure. Depending on the available inputs, and the data demand and processing requirements of the microscale model, it is not always practical to aggregate microscale emissions to produce mesoscale or macroscale emission results.

2.6.1 MOVES

The Motor Vehicle Emission Simulator (MOVES), developed by the U.S. EPA's Office of Transportation and Air Quality (OTAQ), is the EPA's newest vehicle emission model. MOVES replaces MOBILE6.2, the latest version of MOBILE released in 2004, and is a multi-scale model lending itself to analysis at the microscopic level as well as at the regional and national level (Koupal, Cumberworth, Michaels, Beardsley, & Brzezinski, 2002) (Koupal, 2001). The MOVES model is based on emission factors binned by operating mode which is defined by vehicle-specific power (VSP) and speed range. Vehicle specific power is discussed in further detail in Section 3.5.2 and the operating mode bins used by the MOVES model are presented in Figure 2-8. The speed bin ranges help account for speed anomalies which were discovered by EPA during MOVES development (Nam, Giannelli, & Koupal, 2003).

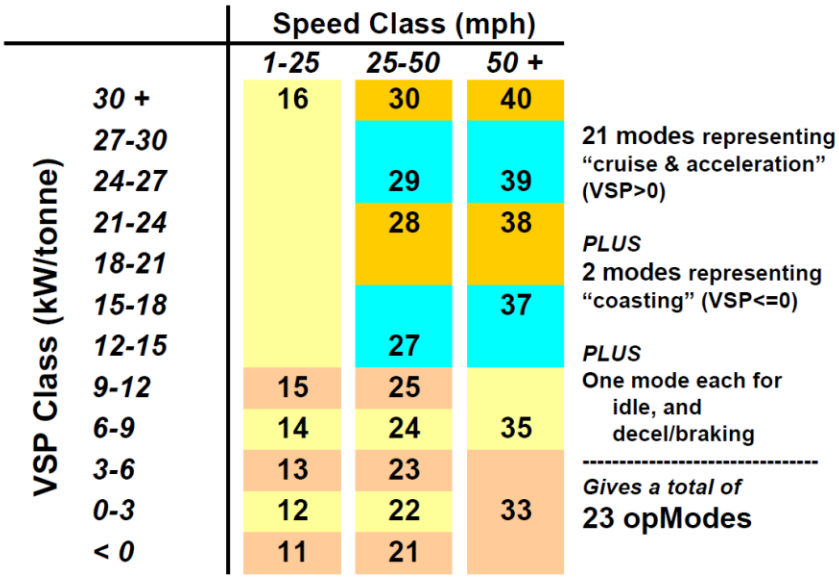

Figure 2-8 Overview of MOVES VSP based operating mode bins (Warila, Nam, Landman, & Kahan, 2011)

MOVES is supported by VSP binned tailpipe emission data from various sources including dynamometer data, remote sensing and PEMS measurement units. The model is primarily data driven and vehicle emission rates are generated from VSP based look-up tables organized by various parameters such as vehicle type, vehicle year, pollutant type, and fuel type.

The MOVES modeling methodology applies the VSP binned emission factor approach to multiple modeling scales from project level scale analysis to national inventory estimation. Some of the limitations to the binning approach are the need for large amounts of data, the difficulty in filling data gaps, and the difficulty in extrapolating beyond the collected set.

2.7 Environmentally-Friendly Navigation

Transportation is essential for work and commerce; however, it does have negative effects, most notably on the environment. Two of the primary areas of concern are energy consumption and emissions. Although energy consumption is a requirement for transportation, a certain amount of energy is wasted due to inefficiencies in the transportation process. Environmentally friendly navigation addresses some of these inefficiencies with improvements in trip scheduling, route choices and operating parameters such as vehicle weigh and speed. The key objective of EFNav is to optimize routing and driving behavior to minimize a vehicle's fuel consumption, emission production, contribution to human emission exposure, or other negative environmental effects.

Many businesses transport goods between a set of locations. It is important to manage these operations efficiently, both to reduce operating costs and to ensure that the pickups and deliveries meet certain criteria such as time and capacity constraints of clients and the company. In the U.S., a significant portion of goods is transported by heavy-duty trucks. These trucks consume a large amount of fuel each year, primarily due to the quantity of goods they transport and their high annual mileage. Fuel costs are one of the major cost components of total truck operating costs. The trucking industry has continued to look for ways to improve operations and reduce the amount of fuel consumption of their truck fleets.

One way of reducing fuel consumption from trucking operations is to perform the routing and scheduling efficiently. There are several commercially available software packages that allow truck routes to be predetermined, taking into account numerous variables including the driver hours-of-service rules, pick-up and delivery windows, vehicle size constraints, vehicle-product compatibility, vehicle-loading dock compatibility, vehicle route restrictions, and many others (e.g., (Rand McNally, 2011) (ORTEC, 2011) (TeleType Co, 2010) (ALK Technologies Inc., 2011) (ArcLogistics, 2009)). These software packages use sophisticated optimization models to solve this so called vehicle routing problem (VRP) (ArcLogistics, 2009). The key objective of these optimization models is to minimize the mileages traveled by trucks.

It is important to note that any measures that reduce fuel consumption will also reduce criteria pollutants such as NO_x and PM as well as the GHG emission CO_2 and thus, benefit the environment. In many cases, a shortest-distance route will also minimize fuel consumption and emissions (e.g. when all routes have similar conditions). However, in many other cases, this is not the case. A shortest-distance route may include roadway sections with steep grades, requiring more energy for the truck to climb the hills while producing more emissions in the process. The route may also have a truck travel through heavily congested roadways, resulting in longer time spent and higher fuel consumed. Similarly, a shortest-time route does not ensure the minimum fuel consumption or emissions (a shortest-time route is usually calculated based on typical vehicle speeds on different roadway types, for example, 60 mph for freeways, 35 mph for arterials, etc.). A

shortest-time route may have a truck travel longer distances, albeit on less congested roadways. Traveling at high speeds for longer distances will result in higher fuel consumption (and emissions) compared to a more direct route at lower speeds. This is especially true for heavy duty trucks whose power-to-weight ratio is low. A shortest distant route may also be less desirable when considering pollutant exposure and an EFNav application with emission estimation can also be used to optimize least exposure routing.

Researchers at CE-CERT have developed new navigation techniques that focus on minimizing energy consumption and pollutant emissions for light duty vehicles. These methods combine mobile-source energy and emission models with route minimization algorithms that are used for navigational purposes (Barth, Boriboonsomsin, & Vu, 2007). Most of the work in the area of EFNav deals with Advanced Driving Assistance Systems (ADAS) such as when to shift gears in order to optimize fuel economy (Huang, Bevly, & Li, 2007). Due to the scale of emission production, the number of Vehicle Miles Traveled (VMT) and the sensitivity to operational parameters, HDD trucks are well positioned to take advantages of EFNav.

3.0 Development of a Microscale HDD PM Model

The objective of this portion of work is to develop a microscale HDD Energy and Emission Model (HDDEM) with the ability to estimate second-by-second PM emissions based on real-time data. This builds on the author's previous emission modeling work in which a microscale HDD emission model was developed for the gaseous pollutants CO, HC and NO_x based on an initial data set of 11 HDD vehicles (Scora, 2007). This portion of work focuses on modeling PM emissions as a function of fuel use and readily available vehicle parameters.

3.1 Review of Microscale Emission Modeling Approaches

There are various approaches to modeling emissions at the microscale level which can be characterized generally as statistical or physically based approaches. Statistically based approaches relate explanatory variables to emissions using statistical techniques such as data binning, regression analysis, classification and regression trees or neural networks. In pure statistical modeling approaches, the parameters generated for the models often have little if any physical meaning and it is difficult to generalize the trend between emissions and vehicle characteristics.

Physically based modeling approaches focus on modeling various aspects of vehicle dynamics and the vehicle emission process. Although physically based modeling approaches may use statistical methods in some parts, such as regressions, the overall structure of these approaches is focused around general physical principles and the mathematical equations for these principles. Unlike in statistical modeling, many of the

parameters for physically based models have physical meanings and their effect in the model is often well understood and can be modified to accommodate new vehicle types or operating conditions. The number of inputs to physically based models is typically more than with statistical models due to the number of processes being modeled and it is also easy to add additional components to the model when the data to support them is available. For some applications, physically based models may be too data or computationally intensive, but this is becoming less so as computational power becomes greater.

3.1.1 Lookup Table Models

One of the most basic microscale modeling approaches is a multidimensional lookup table which stores emission values corresponding to a set of predictor variables typically speed and acceleration. The advantage of this type of emission modeling approach is that it is easy to implement, not computationally intensive, and consequently can generate results quickly. One of the major drawbacks of lookup table based models is that adding a new variable such as vehicle weight, road-grade or accessory load requires a new table or at least a set of correction factors. Emission lookup tables also cannot explicitly account for the emission effects of vehicle operating history such as the vehicle activity leading up to a particular moment.

3.1.2 Classification and Regression Tree Models

One statistical approach to microscale emission modeling is the use of a classification and regression tree (CART) model. This statistical technique creates a binary recursive decision tree that splits data into partitions based on conditional statements and uses regression analysis to relate explanatory variables to emission results within partitions. The CART algorithm decides how to partition data at each step, when to stop partitioning data and how to predict data within partitions (Razi & Athappilly, 2005). The CART approach requires an extensive amount of data to train the model, but the results are generally easy to interpret.

3.1.3 Artificial Neural Network Models

Another statistical approach used for microscale emission modeling is the use of artificial neural networks which are statistical modeling techniques, inspired by the function of the human brain, that identify non-linear function mapping between the independent input variables and the dependent output variables (Razi & Athappilly, 2005). Although this modeling technique has the potential to provide acceptable results, it also has several drawbacks. Much like many of the other more complicated statistical modeling methods, the primary drawbacks for neural network models are that the entire process is essentially a "black box" making it difficult to determine the influence of parameters on emissions.

3.1.4 Engine Emission Models

Another type of physical model worth noting is the detailed three-dimensional engine and emission model based on combustion theory and computational fluid dynamics (CFD), such as the modeling work that is done with the popular KIVA set of code developed by the Los Alamos National Laboratory. This type of modeling considers the detailed chemistry, chemical kinetics, thermodynamics and fluid dynamics of the engine and emission process to model details such as flame propagation, combustion chamber temperatures and emission production (Amsden, 1999). This level of modeling is important for engine research and design, but its application as a transportation emission model is highly impractical since it is computationally intensive and relies on a large number of detailed engine, fuel and environmental data which are not generally available even from traffic micro simulation software.

3.2 PM Emission Model Structure

The modeling approach used for the PM model is a combination approach that models the physical phenomena associated with vehicle operation leading up to fuel use and then relates the modeled fuel use and other predictor values to emissions primarily through multiple linear regression. The parameters required for this modeling consist of both, readily available parameters such as vehicle mass, engine size and aerodynamic drag coefficients, as well as parameters than can be determined based on the calibration of measured second-by-second emission data. There are several key advantages to a physically based modeling approach. One of these advantages is that the physical

modeling component can readily account for the effects of additional load producing inputs such as road grade, accessory power or vehicle weight. Another key advantage of this approach is that it is well suited to incorporate the emission effects of vehicle operation history.

3.2.1 The Physical Model

The general structure of the model is presented in Figure 3-1. The inputs to the emission model are of two general types: second-by-second operating parameters and vehicle parameters. Operating parameters describe the activity of the vehicle such as speed, acceleration and accessory usage as well as running conditions such as road grade, headwind or crosswind. A greater level of detail can be utilized here when available with the inclusion of second-by-second information for things such as road surface type, temperature, altitude, humidity and compression release braking activity discussed in Section 3.8.1. Vehicle parameters include all the parameters that characterize the vehicle itself such as weight, horsepower, and engine idle speed, as well as calibrated parameters for the emission behavior of the vehicle.

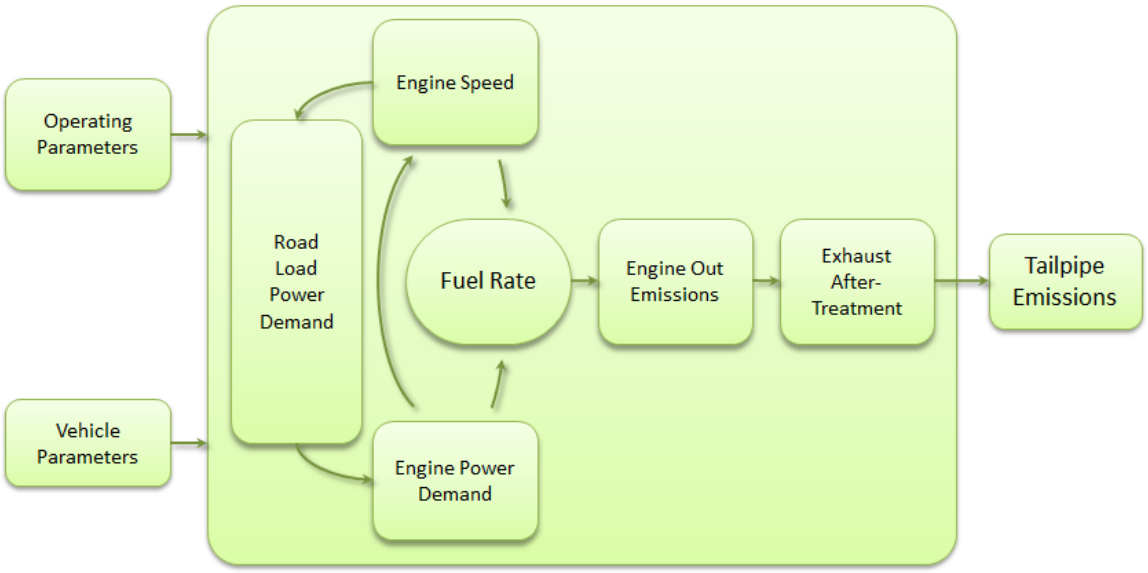

Figure 3-1 General HDD emission model structure

The subcomponents of the model calculate various intermediate variables such as tractive road load demand, gear selection and engine speed, which are used in subsequent submodels to determine fuel use and finally emissions. For information on the submodels, please refer to the author's previous emission modeling work (Scora, 2007).

3.2.2 Regression Based PM Submodel

The foundation of the HDD PM model developed for this research is a physical model that estimates data for several dynamic vehicle parameters such as fuel rate, engine speed and engine torque as discussed in Section 3.2. These dynamic parameters are then related to PM emissions through Multiple Linear Regression (MLR) modeling discussed in this section.

MLR is a statistical modeling method that is used to relate a dependent variable to one or more independent explanatory variables using a linear function. For a simple

linear regression between a dependent variable and a single predictor value, the fit between the variables is described by equation 3.1.

$$Y = b_0 + b_1 x_1 + \varepsilon \qquad 3.1$$

where:

Y = dependent variable

x_1 = independent value

b_0, b_1 = regression coefficients

ε = error term

Equation 2 can be extended to describe a MLR model. The format for a MLR model is the expression of a dependent or predicted variable as a linear function of one or more predictor variables and an error term as presented in equation 3.2.

$$Y = b_0 + b_1 x_1 + b_2 x_2 + b_3 x_3 + \ldots + b_n x_n + \varepsilon \qquad 3.2$$

where:

Y = dependent variable (PM)

$x_1, \ldots, x_n$ = independent variables (explanatory values)

$b_1, \ldots, b_n$ = regression coefficients

ε = error term

Although the format of the MLR model is a linear combination of predictor variables, the predictor variables may be non-linear. Examples of nonlinear terms are second and third order variables. The predictor values may also contain cross product or

interaction terms. In this case, the response of the dependent variable to a predictor value is scaled based on another predictor variable. The format for a MLR model with an interaction term would follow the format similar to equation 3.3.

$$Y = b_0 + b_1x_1 + b_2x_2 + b_4x_4x_5 + \varepsilon \qquad 3.3$$

where:

Y = dependent variable (PM)

$x_1, \ldots, x_5$ = independent variables (explanatory values)

$b_1, \ldots, b_4$ = regression coefficients

ε = error term

The regression coefficients are determined by minimizing the sum of the squared residuals, ordinary least squares analysis. The resulting equation is an empirical equation and may not have any understandable physical meaning. To minimize this, the analysis is constrained in part to variables which are more easily conceptualized such as fuel rate, the change in fuel rate and engine speed. Higher order terms such as fuel rate to the fourth order are not considered in the microscale model because they have little physical meaning. The development of the PM submodel is described in further detail in Sections 3.7 and 3.8.

3.3 Heavy Duty Diesel Data Collection

The microscale PM model is developed and calibrated from a unique set of measured second-by-second on-road test data. In the past, HDD emissions model development on a second-by-second basis was restricted by the lack of appropriate real-

world data. HDD engines are used in a variety of applications and for this reason are certified based on testing separate from the truck chassis and under laboratory conditions which may or may not be representative of the "real-world" conditions in which the engines will operate. Much of the data available for HDD engines has been engine certification data from laboratory test stands. The use of this data for the estimation of actual vehicle emissions under real-world driving conditions has its uncertainties.

In an attempt to address these uncertainties, the U.S. EPA and other research organizations have to develop systems for measuring emissions from HDD vehicles under real-world driving conditions, or conditions representative of real-world driving. These systems fall into the following categories: Heavy-duty chassis dynamometers, Portable Emission Systems (PEMS) (EPA, 2010), and trailer-based emission laboratories; the latter category being the source of data for this work.

3.3.1 CE-CERT's Mobile Emission Lab

CE-CERT's Mobile Emissions Laboratory (MEL) is a 53-foot class 8 trailer with the ability to measure instantaneous (i.e., modal) CO_2, CO, HC, NO_x and PM emissions in-situ. The trailer contains a full-scale dilution tunnel and analyzers for gaseous pollutants. Figure 3-2 shows a basic schematic of the MEL trailer. The various instruments are powered by an on-board generator making the entire lab mobile. The laboratory can measure emissions in a stationary position, such as is required when sampling from a back-up generator or engine dynamometer, or it can be towed by a class 8 tractor, measuring the tractor's emissions in traffic under real-world operating

conditions. In the latter setup, the truck's exhaust system is connected to the dilution system and the entire exhaust stream is captured. The laboratory is based on Code of Federal Regulations (CFR) standards for emissions certification measurement. Validation was performed by comparing MEL emission results with data from CARB's HDD test facility (Cocker, Shah, Johnson, Miller, & Norbeck, 2004).

Data collected by MEL also includes information from the vehicle's Engine Control Unit (ECU) as well as additional sensors. These data are very valuable for modeling purposes. The ECU provides, among other things, engine speed, percent engine load and fuel rate which are variables that are calculated or can be related to variables that are calculated in the modeling effort. This provides for an excellent intermediate validation of the modeling results.

In addition to this, a driver's aid was developed, which allows the truck operator to follow a standardized cycle if the road conditions permit. More information regarding MEL can be found in (Cocker, Shah, Johnson, Miller, & Norbeck, 2004) (Cocker, Shah, Johnson, Zhu, Miller, & Norbeck, 2004).

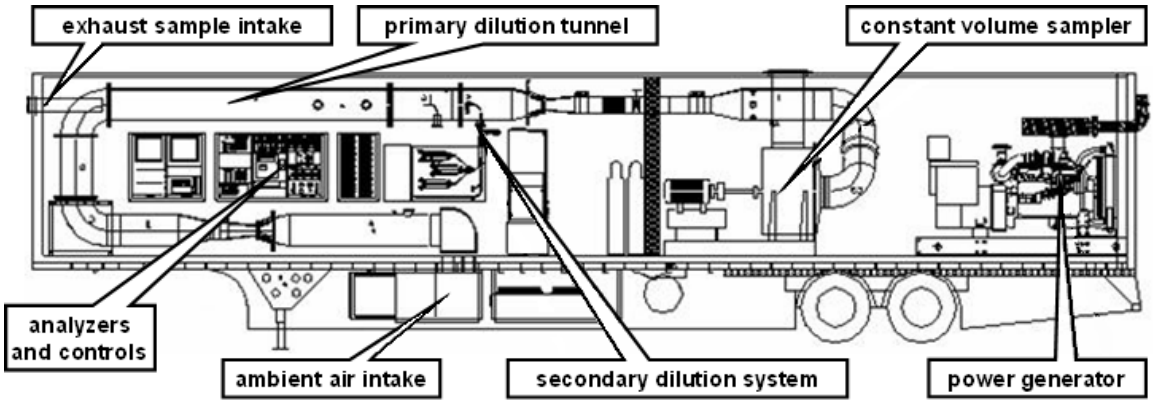

Figure 3-2 Schematic of CE-CERT's Mobile Emission Research Lab (After: Cocker, Shah, Johnson, Miller, & Norbeck, 2004)

3.3.2 Measuring PM

Real time emission data is crucial to the development of a microscale emission model. Second-by-second PM modeling has long been limited by a general lack of real-time emission data. Over the last several years however, real-time PM emission data is becoming more available making microscale PM modeling efforts possible.

CE-CERT's MEL provides three sets of PM data: gravimetric PM filter data and real-time PM data from a DustTrak® analyzer and a Dekati Mass Monitor analyzer (Cocker, Shah, Johnson, Zhu, Miller, & Norbeck, 2004). All three of these data sets are based on differing measurement principals and are discussed briefly below.

Gravimetric PM

Gravimetric PM measurements are obtained by weighing the mass of PM deposited on filters and are the classical method of obtaining integrated PM emissions for a given sampling period. During MEL testing, PM mass is collected on Teflon filters fed from the secondary dilution stream. The filters are loaded for the duration of a phase or cycle which is either preprogrammed or selected in real time. MEL has the ability to switch filter loading on and off during operation allowing for multiple measurements of selected driving sections on a single filter. The loaded PM filters are then weighed and the measurement is considered the "gold standard" which is used to calibrate and validate other PM measurements. The PM filter numbers provide integrated PM mass emission number for selected portions or phases of testing.

TSI DustTrak®

The DustTrak® is a real-time laser photometer from TSI Inc. (TSI, 2011), which is capable of recording in the range of 0.001 to 100 mg/m3. In this measuring device, shown in Figure 3-3, the diluted exhaust sample is drawn into the instrument continuously and separated into two streams, one of which is filtered and used as sheathing flow. The sample flow is illuminated by a sheet of laser light emitted from a laser diode and conditioned by a shaping lens. The scattered light is collected by a spherical mirror and focused onto a photodetector to produce a voltage that is proportional to the mass concentration of $PM_{2.5}$. This voltage response is then adjusted by a calibration constant to match with a known $PM_{2.5}$ concentration, typically Arizona Test

Dust (TSI, 2006) (TSI, 2009). Comparisons of the DustTrak test data from the MEL data set used in this work are presented in this section.

Figure 3-3 TSI DustTrak analyzer

Dekati Mass Monitor 230

The Dekati Mass Monitor model 230 or DMM-230, shown in Figure 3-4, is a real-time PM mass emission monitoring device that measures PM in the size range of 0-1.5 μm. The device operates on the principles of particle charging, density measurement, particle size classification with inertial impaction and electrical detection of charged particles. In this measuring device, the incoming sample flow is charged with a high voltage corona charger to give the particles a known charge. Following the charging region, a static electrical field deflects the smaller particles onto an electrode based on their electric mobility producing a measurable current. The larger remaining particles enter a 6-stage inertial impactor with electrical detection where they are separated based on their aerodynamic size. Mass number as well as number concentration can then be calculated based on information from the electric mobility of the smaller particles and the aerodynamic size of the larger particles (Dekati Ltd., 2010). Comparisons of the DMM test data from the MEL data set used in this work are presented in Section 3.3.3.

Figure 3-4 DMM 230 PM analyzer

Comparison of Real-time PM Measurements

For the selected data set, the MEL lab provides real-time PM data from the DustTrak and DMM-230 analyzers described in this section. In this section the real-time PM measurements from these two instruments are compared. Since these two analyzers operate on different measurement principles, their sensitivity to PM measurement varies. The DustTrak, like all aerosol photometers, detects PM by measuring the amount of light scattered by particles. The amount of light scattered by particles in the sample stream is a function of particle properties such as size, shape and the refraction index. Particles of different sizes scatter light disproportionately and there is an optimal size range of roughly 0.1 to 10 microns in which particles scatter significantly more light relative to their mass. Below 0.1 microns, the light scattering abilities of particles relative to their mass decreases sharply and for this reason, the DustTrak analyzer is not expected to capture PM mass in this size range (TSI, 2006).

In contrast to the DustTrak, the DMM-230 is expected to capture particles below 0.1 microns because of its ability to measure particles in part by their electric mobility. The agreement between the real-time PM mass measurements from the DustTrak and

DMM-230 will depend on the size distribution of PM in the sample stream and the amount of PM mass contributed by the smaller particles.

A comparison of typical real-time data from the Dustrak and DMM-230 is presented in Figure 3-5 for over 13000 data points. This data set is the calibration data set described in Section 3.3.3. In this figure, the data from the DustTrak has been aligned and scaled so that its integrated value matches that of the DMM-230. This figure shows that visually, the general agreement between the two analyzers can be relatively good for diesel exhaust. Figure 3-6 shows a smaller section of the same data set which illustrates that although the two analyzers do follow the same trend, they are not capturing the PM emission events in the same way. In this example, the DustTrak seems to over-estimate the larger emission event and under-estimate some of the lower emission events.

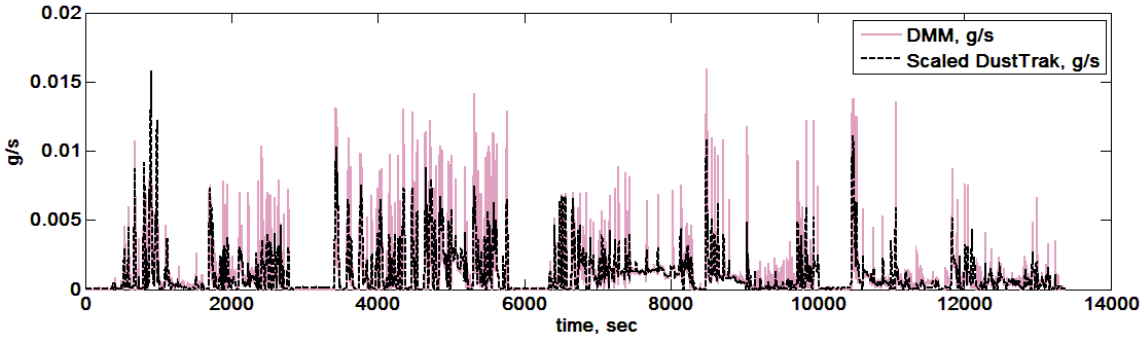

Figure 3-5 Comparison of DMM-230 and Dustrak real-time PM measurements

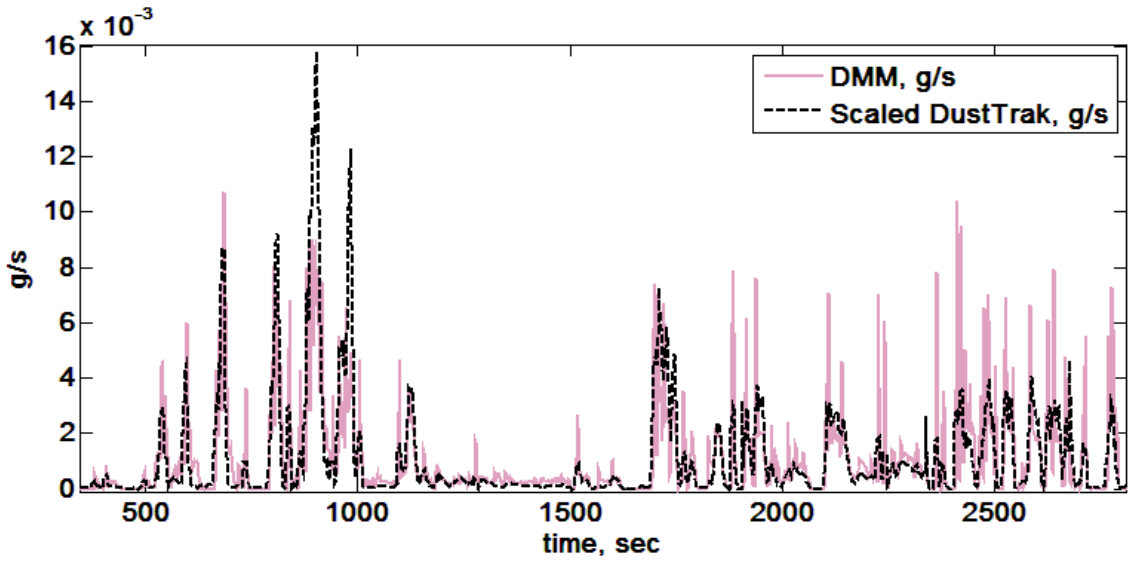

Figure 3-6 Comparison of DMM-230 and DustTrak real-time PM measurements

The plot in Figure 3-7 shows the correlation between the adjusted DustTrak PM data and that of the DMM-230. In this figure, as in the previous two, the data has been aligned for maximum correlation to the nearest second and shows the linear fit between the two data sets in relation to the line of parity with a coefficient of determination of 0.6 and slope near 0.7. A similar result is presented in a later discussion in Figure 3-25.

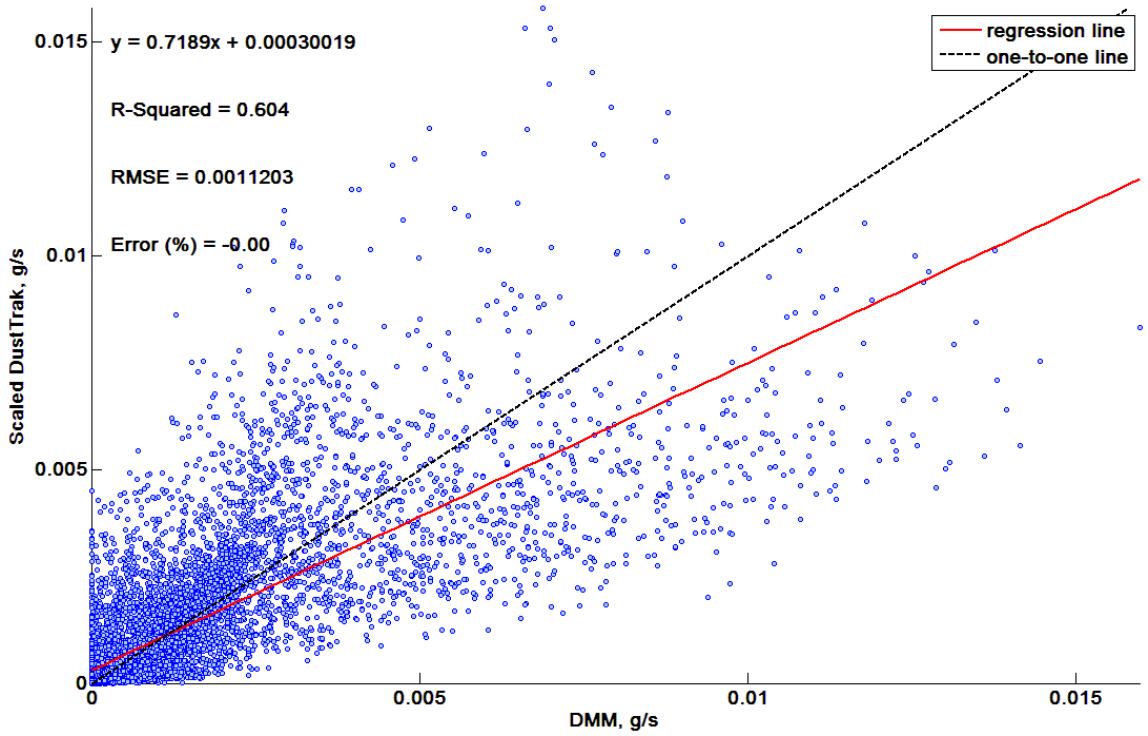

Figure 3-7 Correlation between adjusted and aligned DustTrak and DMM-230 real-time PM data

For the PM modeling work presented here, the DMM-230 data was chosen as a source of PM data over the DustTrak since the DMM-230 encompasses a greater range of particle sizes.

3.3.3 PM Data Set Description

Emission testing performed by MEL is ongoing and includes on-road testing as well as engine dynamometer and chassis dynamometer testing of vehicles and engines ranging in model years from 1989 to 2011. This breadth in range of HDD model years allows for the comparison of performance between new and old trucks and helps in the

evaluation of the newest after-treatment technologies such as diesel particulate filters (DPF).

Emission data collected from MEL is the foundation for the development and calibration of the PM modeling efforts in this work. For model development, the focus was narrowed down to a single vehicle, although the model applies to most HDD vehicles. The selected vehicle is a 1995 model year Class 8 tractor with a 12.7 L series-60 Detroit Diesel Corp. (DDC) engine. Selected information for the test vehicle and testing is presented in Table 3-1 followed by an image of the vehicle in Figure 3-8.

Table 3-1 Model development test vehicle details

Engine Make	Engine Model	Engine Displacement	Rated Power	Engine Year	Odometer	PM Control Device	Real-time PM	Test Location	Hours Tested
-	-	liters	hp@RPM	year	miles		yes/no		hours
Detroit Diesel	Series60	12.7	500	1995	342,907	none	YES	on-road	7.45

Figure 3-8 HDD test vehicle used for microscale PM model development

The selected data set includes PM emissions from two instruments discussed in Section 3.3.2, and encompasses a wide range of on-road driving activity within the span of couple of days. The short time frame helps to reduce various sources of testing variability such as those related to environmental conditions, vehicle conditions and lab conditions. In data sets that span greater lengths of time such as those that combine data from repeat testing of the same vehicle, ambient temperatures and humidities may differ, the vehicle may have deteriorated or malfunctioned, or the analyzer setup may have changed. All of these variables have the potential to influence the compatibility of the combined data set and for these reasons a shorter testing period is preferred.

For the purposes of this work, the data set was divided into two separate data sets: one for calibration and the other for validation. The routes for both data sets were similar and included roughly 80 miles of driving in the high desert of southern California between the Cajon junction on the I-15 and Newberry Springs on the I-40, a steep decent or ascent through the Cajon pass on the I-15, and roughly 70 miles of driving along the I-15, I-215, SR 91 and SR 60 freeways as well as the Van Buren arterial through Woodcrest, Riverside and Mira Loma. The test location for the calibration and validation data sets is shown in Figure 3-9.

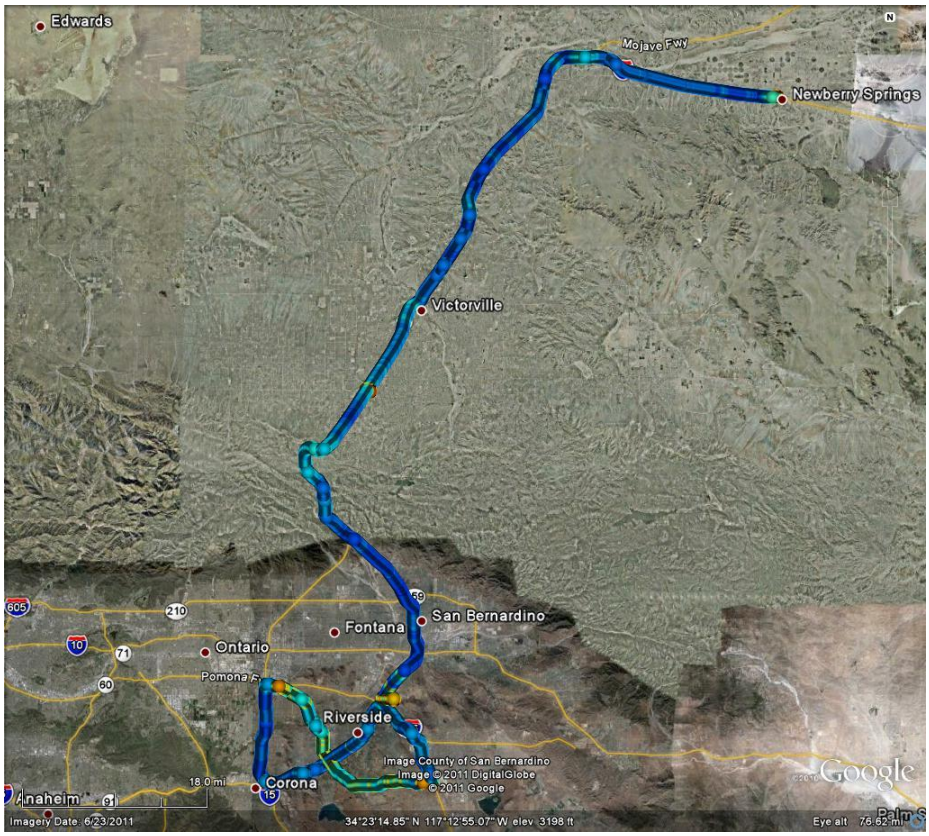

Figure 3-9 Test location for calibration and validation data runs in Southern California

Since vehicle activity has a significant influence on the relationship between PM emissions, it is important to develop a model based on a wide range of activity. Modeling work developed based on limited range of vehicle driving may not hold up outside of the range of vehicle activity it was developed on. Extrapolating beyond the test data range may produce unexpected results.

The vehicle activity distributions for the calibration and validation data sets are presented in the histograms in Figure 3-10 and Figure 3-11. The activity distributions are split into two ranges to accommodate the scales since they include a substantial amount

of driving at freeway speeds. The calibration data set contains 3.72 hours of test data and the validation data set contains 3.74 hours of test data.

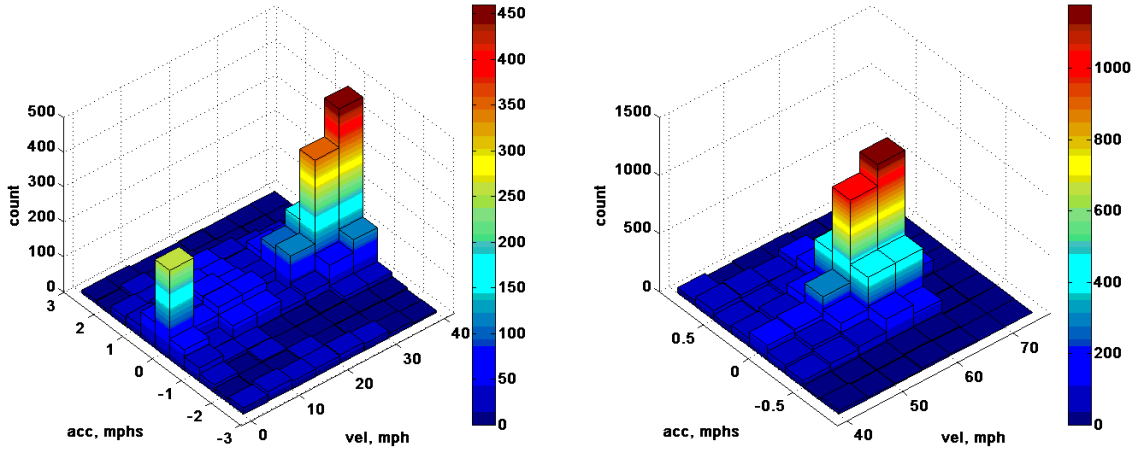

Figure 3-10 Activity distribution for calibration dataset excluding zero speed.

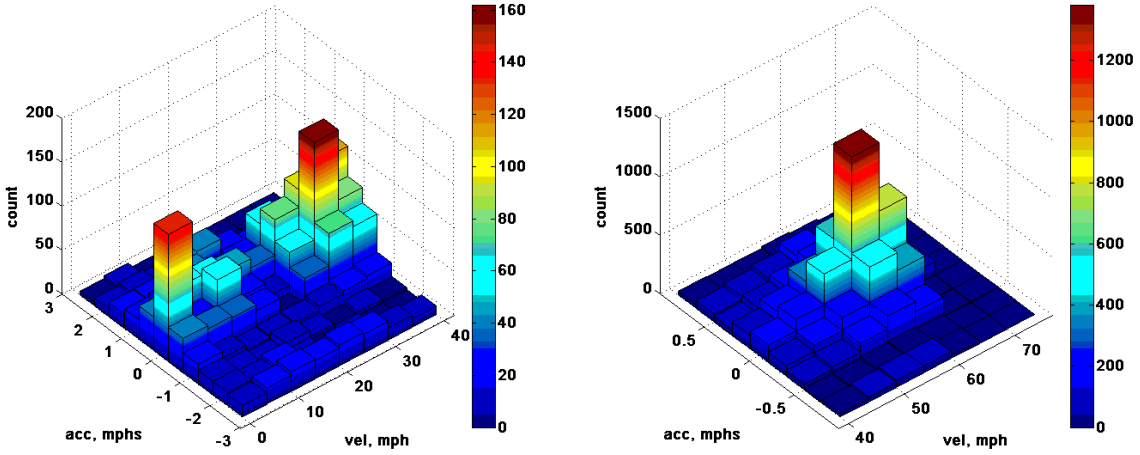

Figure 3-11 Activity distribution for validation dataset excluding zero speed.

3.3.4 Data Processing

The various sources of data collected from the MEL are processed in several ways before they are used for data analysis. Data processing helps to consolidate the data into one coherent data set, translate the data into a usable working environment and generally clean the data. Some of the data processing steps are reviewed below.

Data Storage

As part of the operation of MEL, raw second-by-second data from the vehicle's ECM and the various instruments and analyzers are processed to some extent and presented in separate comma delimited text files. In addition to the instantaneous data, scalar test values and test summary information are stored in a single database file. In order to further process the data and perform analysis and modeling, the data is translated into Matlab (discussed in Section 3.4) workspaces. Much of the data cleaning occurs during this conversion step. The resulting Matlab workspaces contain renamed vector variables for the cleaned second-by-second data as well as variables of type cell that contain all the scalar values for the cross-referenced summary data and test data. This makes all of the test information conveniently accessible. The entire conversion process is scripted into functions and can be rerun as needed to make corrections or additions to the data set.

Cleaning Data

Data obtained for each test comes from a variety of sources. In some cases this data may contain bad values. These values are either removed or replaced depending on

the situation. In most cases a script is written to identify these values and then either extrapolate between neighboring points or replace with the last correct value. In certain instances, where the use of filters is not practical, manual corrections are recorded in a script and are applied early in the processing step. Sometimes replacement of values was possible. In the data set described in Section 3.3.3 for example, some of the measured fuel data was missing or stuck on preceding values creating sections of flat or missing fuel data. This was probably a characteristic of the ECM connection or ECM itself, perhaps due to the age of the vehicle. In this case, fuel rate calculated from measured CO_2, which matches very well with the ECM broadcast fuel rate, was used to clean up the ECM fuel value.

Other data cleaning steps include the smoothing of rough data. Data smoothing may be applied to values that show a stepwise behavior or are somewhat noisy. This is especially helpful if the values are used to calculate difference values such as speed to calculate acceleration or elevation to calculate the second-by-second change in elevation and road grade.

Some commonly needed parameters are added to the basic Matlab workspaces during the conversion process such as acceleration and grade, as well as aligned, normalized, unit converted, or otherwise processed versions of certain parameters. This increases the workspace size, but eliminates the need for recalculating these values repeatedly. A rough grade value, for example, is calculated as the change in elevation in

meters over the distance traveled in meters. The distance traveled is calculated using the great-circle distance calculation from latitude and longitude values.

Data Alignment

Data alignment is an important aspect of processing data obtained from two separate systems. The primary concern for the MEL data set is aligning 1 Hz data that is broadcast from the ECM with mass emission data from the MEL facility. This is done in post processing using cross correlation functions in Matlab that analyze the correlation between two variables at various offsets. Data analysis and modeling is performed with 1 Hz data. In order to find the proper shift for time alignment at intervals less than 1 Hz, ECM and emission data are resampled at a rate of 10 Hz using interpolation prior to correlation. The resampled data is aligned based on the lag that produces the maximum correlation and the resulting data set is subsampled back to 1 Hz. In order to help minimize false correlations based on missing or bad data, a maximum lag was set up which defined the range of shifts the correlations were evaluated over.

True alignment of measured tailpipe mass emissions with ECM parameters depends in part on variances in the exhaust flow rate since the exhaust flow rate will dictate the time it takes for emissions to travel from the engine to the analyzer. At higher exhaust flow rates, emissions will take less time to reach the analyzers and have a shorter time shift relative to lower exhaust flow rates. Time alignment using the cross correlation method described above will be dominated by the larger emission events which are typically correlated to increased fuel combustion and consequently vehicle activity under

higher load and generally higher exhaust flows. Discrepancies in time alignment will be more noticeable at the lower emission levels. For this reason, constant time alignment using the cross correlation method described above is generally acceptable based on visual inspection of the data. A more sophisticated time resolution correction for emission measurement data which accounts for variances in exhaust flow rate would have to be applied to the concentration values prior to the conversion of the data to mass emission rates and was not employed for this analysis.

3.4 Data Analysis Software and Programming

The data collection, data analysis, model development and model calibration presented here was performed using various software programs; however, the majority of the work utilized the Matlab technical computing environment. Matlab is a high-level interactive object-oriented programming environment with strong graphing capabilities and is widely used in academia and industry. Matlab code is compiled during runtime and commands can be issued either line-by-line at the command prompt or from scripts (MathWorks, 2009). Data sets developed for this research are maintained in Matlab workspaces, comma separated text files or in R data files.

Following the research and development of algorithms for the emission model in Matlab, the C++ programming language is used to create a command line executable of the model for use in analysis work. Matlab provides a user friendly programming environment for model development; however, this level of simplicity comes at the expense of run-time performance. The C++ version of the model can be compiled into a

Windows Application Programming Interface (API) or an executable for the Linux kernel with improved run-time performance. Either of these command line executables can be called from the Matlab prompt, allowing for the creation of a Matlab wrapper program which executes the command line version of the model from within the Matlab environment.

3.5 Explanatory Variables for PM Modeling

The estimation of emissions for transportation applications is constrained by the availability of variables for emission modeling. For microscale applications in which specific vehicle behavior is of interest, second-by-second vehicle trajectory data are typically the basis for the analysis. This level of trajectory information can be obtained from measured or simulated vehicle activity. Second-by-second simulated vehicle activity and related parameters can come from a microscale traffic simulation model, a useful tool when integrated with an emission model for the evaluation of transportation related emissions (Scora, 2007). The following subsections discuss some of the basic parameters, apart from inputs to the physical core model, which were considered for PM modeling purposes at the microscale level. Some variables are included in both the core model and as potential explanatory values in the regression portion of the model. Additional parameters were also evaluated.

3.5.1 Velocity and Acceleration

Velocity is an important variable since it is the most basic characteristic of vehicle movement and it is the basis for the calculation of related parameters such as acceleration, vehicle specific power (VSP) and fuel consumption. Velocity is also relatively easy to obtain since it is generally broadcast from the engine control module (ECM) of a vehicle. Under real-world driving conditions it can also be calculated from GPS data and with chassis dynamometer testing it can be calculated from the dynamometer's roller speed. Simulated velocity is often available from microscale traffic simulation models. Velocity itself is positively correlated with emission production since an increase in velocity generally indicates an increase in fuel consumption and consequently emissions.

The second-by-second change in velocity is defined as acceleration which is also positively correlated with emission production. The rate at which a vehicle can accelerate decreases with increased speed as the resistive forces on the vehicle increase and the power required to overcome those forces increases. The third derivative of position or the rate of change of acceleration is known as jerk and is also considered as an explanatory variable.

The product of velocity and acceleration is also meaningful since it is proportional, by a factor equal to vehicle mass, to the power required to overcome the inertia of vehicle mass and accelerate the vehicle. A more detailed discussion on the forces acting on the vehicle and the modeled power demand is presented in (Scora, 2007).

3.5.2 Vehicle Specific Power

Vehicle Specific Power (VSP) is a value representing the road load on a vehicle. The application of VSP as an explanatory value for vehicle emissions has appeared in the literature for several years, highlighted in Jimenez-Palacios (Palacios, 1999). VSP is defined as the instantaneous power to move a vehicle per the mass of the vehicle. The calculation for VSP in kW/metric tons is based on the following equation, simplified from the power demand terms for a moving vehicle:

$$\mathrm{VSP} = v(1.1a + \mathrm{g}\sin(\theta) + \mathrm{g}\,\mathrm{C}_r) + \frac{\rho_a \mathrm{C}_d \mathrm{A}_f v^3}{2\mathrm{M}} \qquad 3.4$$

where

v = vehicle speed in m/s

a = vehicle acceleration in m/s^2

g = gravity (m/s^2)

θ = grade

C_r = coefficient of rolling resistance

ρ_a = density of air (kg/m^3) (~1.2 kg/m^3 at sea level and 20 °C)

C_d = coefficient of aerodynamic drag

A_f = frontal area of vehicle (m^2)

M = mass of vehicle (kg)

3.5.3 Fuel Use

The core of the PM model described in Section 3.4 is based on fuel consumption as the primary explanatory variable. In previous work, calculated fuel consumption was

used as the foundation for NO_x emission estimation due to the strong linear relationship that exists between the two parameters (Scora, 2007). Figure 3-12 shows NO_x versus fuel over a 1000 second drive cycle with two apparent driving regimes represented by the two regression lines in the second subplot. In this figure the same color points in each subplot represent the same points in both plots. It is evident that the vehicle is switching between two different engine regimes and that regardless of the engine regime; NO_x emissions maintain a strong linear relationship with fuel.

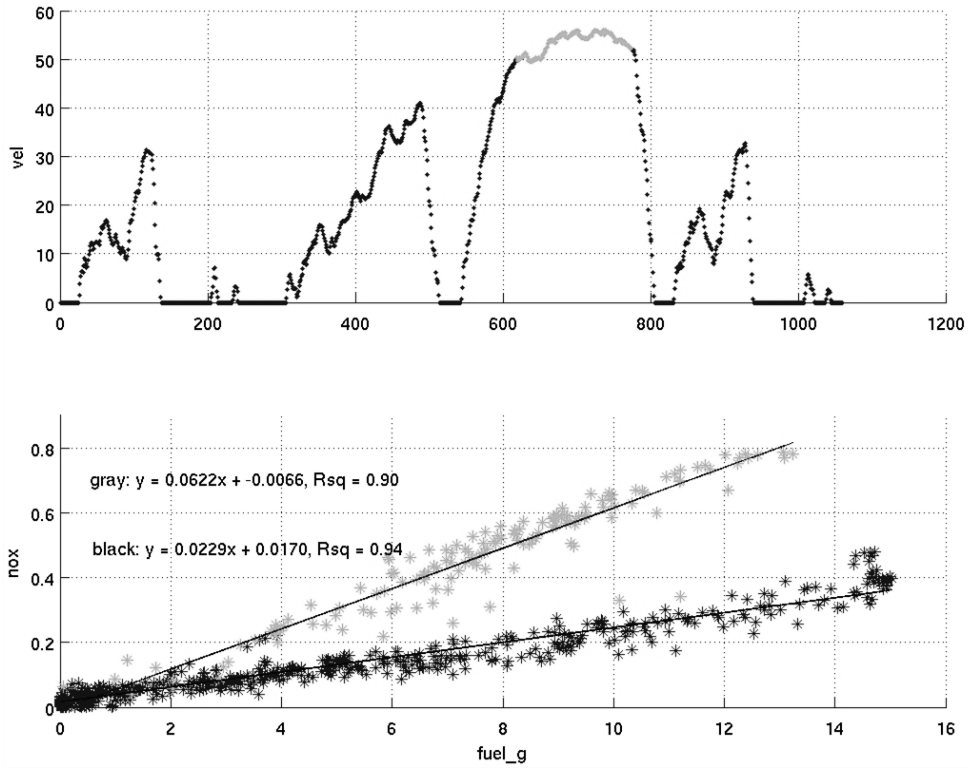

Figure 3-12 a) Velocity (mph) vs. Time (seconds) and b) NOx (grams) vs. fuel use rate (grams) with corresponding colors and associated regression lines.

The formation of NO_x emissions in diesel engines is well understood and is dependent mainly on the presence of sufficient oxygen and high temperatures. NO_x emissions may be reduced by decreasing in-cylinder temperatures which can be accomplished with retarded fuel injection timing at the expense of increased particulate emissions and reduced fuel economy. This relationship between NO_x, PM and fuel is commonly referred to as the NO_x, PM, fuel "trade-off". For this reason fuel injection timing strategies have a great impact on the formation of NO_x and PM emissions (Heywood, 1988).

Fuel injection timing refers to the point during the combustion process in which fuel is injected into the combustion chamber and it is usually measured in degrees of crank angle before top dead center (TDC). Retarding this timing lowers NO_x and promotes incomplete combustion, which leads to increased PM. There is also a fuel penalty associated with retarded ignition timing. Advancing the fuel injection timing lowers the PM produced. Advanced fuel injection creates higher in-cylinder pressures and higher fuel efficiency, but it increases combustion temperatures and as a result increases NO_x emissions and decrease PM emissions (Heywood, 1988).

As discussed, there are several factors that can influence PM emissions. The primary source of PM emissions, however, is from the combustion and incomplete combustion of fuel and for this reason fuel use and fuel related parameters are expected to be strong predictors of PM emissions. Figure 3-13 and Figure 3-14 show 300 seconds of MEL test data that exhibit a strong linear relationship between fuel use and PM

emissions. The coefficient of determination for this data set is roughly 0.7 as seen in Figure 3-14.

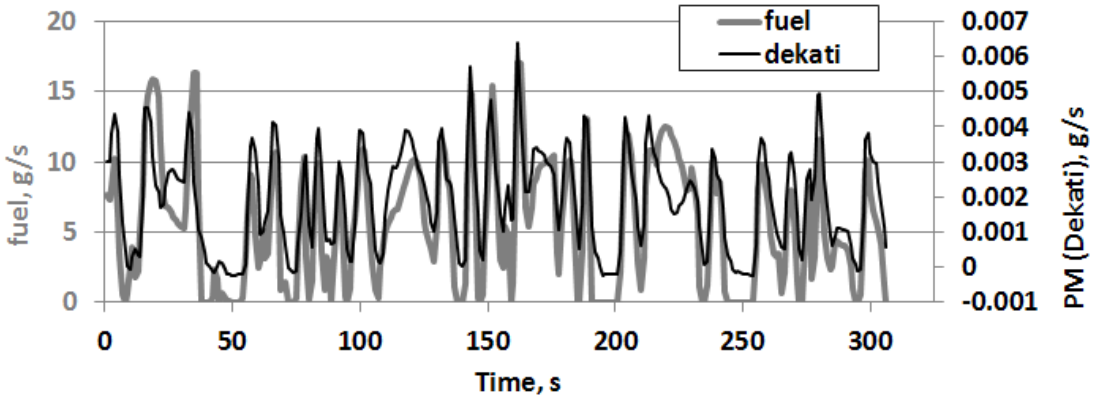

Figure 3-13 Sample data showing strong linear relationship between fuel rate in g/s and PM mass emission rate from the Dekati analyzer.

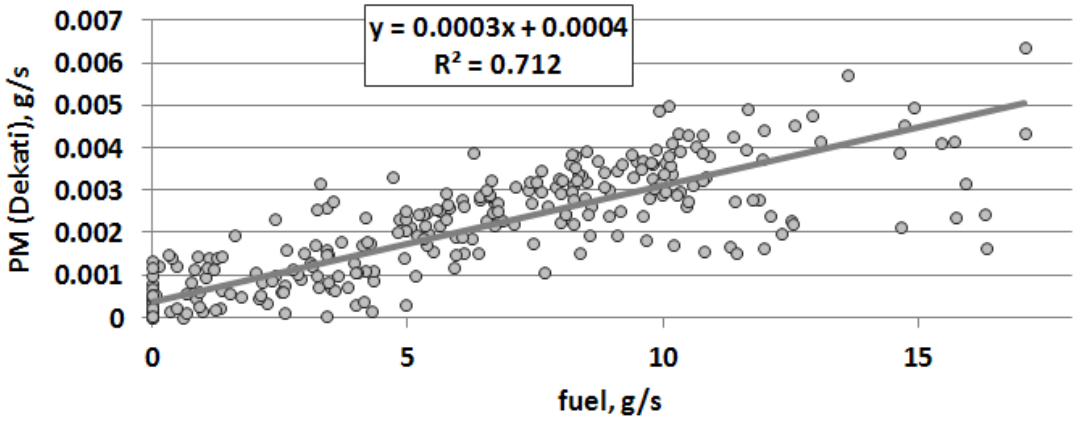

Figure 3-14 Sample data regression showing strong linear relationship between PM from the Dekati analyzer vs. fuel rate in g/s

In the data that were analyzed, fuel use did not always share the same linear relationship with PM that was observed for NO_x emissions or in Figure 3-14. Figure 3-15 and Figure 3-16 show sample test data which exhibits a weak fuel use vs. PM relationship. In Figure 3-15, the basic correlation between the fuel use and PM profile is

evident, as are certain deviations from this correlation. In the data presented in Figure 3-15, PM emissions spike with fuel use, but fall off rapidly. In the case that the fuel use event is shorter, the fuel use event and the PM event fall off together after the initial PM "puff". For some of the longer fuel use events the corresponding emissions profiles are somewhat different, such as the event near second 150 in Figure 3-15. The start of this event shows a similar PM puff which then falls off to a steady PM value at roughly one fifth of the PM spike for the remainder of the fuel use event. This seems to indicate that the change in fuel rate likely has an influence on PM emissions.

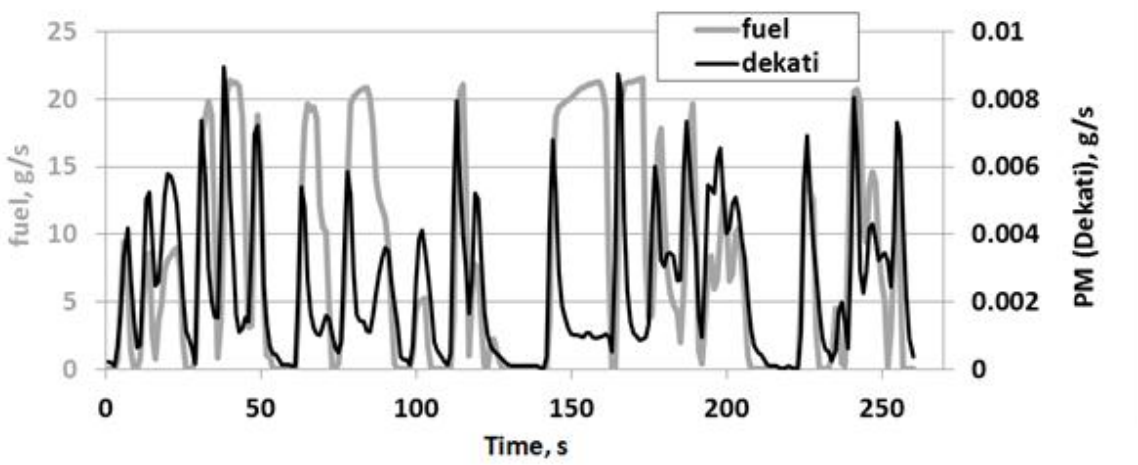

Figure 3-15 Sample data showing deviations from a linear relationship between fuel rate in g/s and PM mass emission rate from the Dekati analyzer.

Figure 3-16 shows the regression of PM versus fuel use for the data presented in Figure 3-15. The data for these two figures has been shifted by a precision of one tenth of a second for optimal time alignment based on a cross correlation function implemented in Matlab.

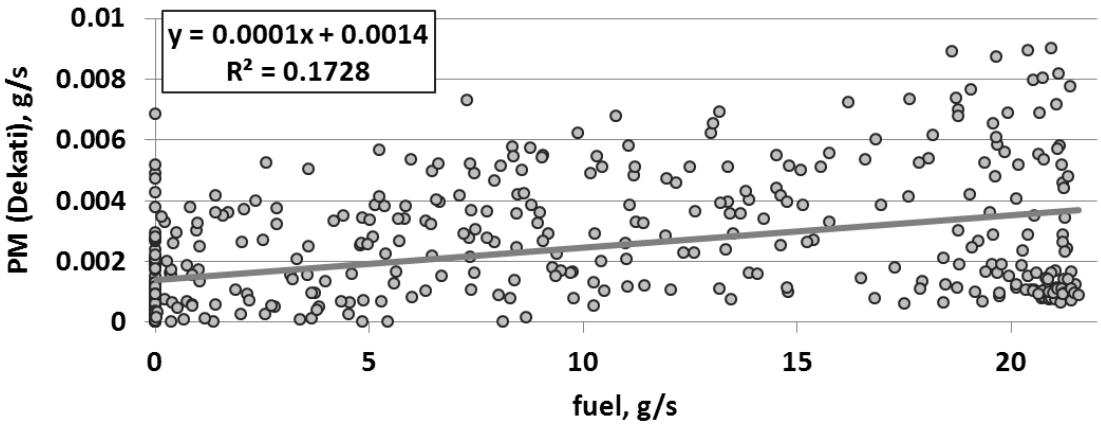

Figure 3-16 Sample data regression showing weak linear relationship between fuel rate in g/s and PM from the Dekati analyzer.

In order to improve the predictive power of fuel use for PM emission, other forms of the fuel use variable were included in the analysis such as the second and third order fuel use terms as well as the change in fuel rate and the second order of the change in fuel rate. The results of this analysis are discussed in Section 3.6.

3.5.4 Engine Speed

The speed of the engine is a parameter of interest in modeling PM emissions. It is easily obtained from the ECU data and is also part of the modeling output from previous modeling work (Scora, 2007). Since the displacement of the engine is a fixed quantity, the speed at which the engine crank rotates is an indicator of the exhaust flow rate through the engine. Engine speed is included in the analysis of explanatory variables below.

3.6 Explanatory Variable Correlations

The correlation coefficient (r) is a measure of the degree of association between two variables (Stone, 1996). The correlation coefficient provides a measure of how well explanatory values are associated with a target parameter, whether the relationship between the explanatory variable is positive or negative and also the degree of correlation between the explanatory variables themselves. Explanatory variables may be highly correlated if, for example, they are related to the same physical phenomenon. An example of this would be fuel rate and VSP, since both of these variables are closely related to engine load. Including highly correlated variables in the model does not take away from model performance, but it does increase model complexity, usually without adding significant explanatory value. It also makes it difficult to interpret the significance of individual parameters.

A correlation matrix for various parameters, summarized in Table 3-2, is presented in Table 3-3 through Table 3-7. The correlations were calculated based on the calibration data set defined in Section 3.3.3. For this analysis, “Fuel” is the truck’s fuel use rate as determined from the ECU. The variable “dFdt” is the change in fuel use rate with time and is partitioned into two parameters: “dFdt-” and “dFdt+”. The variable “dFdt-” represents the negative portions of the change in fuel rate with the positive values set to zero and the variable “dFdt+” represents the positive portions of the change in fuel rate with the negative values set to zero. In each of these lines, the excluded information is set to zero. The “dFdt” variable was partitioned into negative and positive values

because PM shows much higher correlation with the positive portion of the change in fuel rate than with the negative or combined portions. This is evident from the data in Table 3-3. The last column in the table shows the correlation of PM emissions with the explanatory values.

Table 3-2 Summary of explanatory values used in correlation matrices

Explanatory Value	Definition
vel	velocity
acc	acceleration
acc-	negative accelerations only
acc+	positive accelerations only
jerk	jerk value (da/dt)
jerk+	positive jerk values
grade	grade
fuel	fuel rate
$fuel^2$	fuel $rate^2$
$fuel^3$	fuel $rate^3$
VSP	vehicle specific power
dFdt	change in fuel rate (df/dt)
dFdt+	positive change in fuel rate
dFdt-	negative change in fuel rate
RPM	engine speed
load_1	VSP * RPM
load_2	cumulative VSP*RPM over last 2 seconds
fuel_s2	cumulative fuel use over last 2 seconds
fuel_s3	cumulative fuel use over last 3 seconds
fuel_s5	cumulative fuel use over last 5 seconds
PM	particulate matter

This data shows that across the data set PM shows the strongest correlation with the positive change in fuel rate ($r = 0.75$) and then with positive accelerations ($r = 0.52$) followed closely by the fuel rate itself ($r = 0.48$). From a physical perspective, a positive change in fuel rate would likely result in positive acceleration in many cases and so the variance explained by both of these parameters may overlap significantly. The correlation coefficient between these two parameters is 0.32. It is important to note that the values of

the correlation coefficients between these predictors (which range from r = 0.22 to 0.36) are less than those between the predictor values and PM.

Table 3-3 Matrix of coefficients of correlation for explanatory values. Stronger positive correlations have darker shading.

	vel	acc	acc-	acc+	jerk	jerk+	grade	fuel	$fuel^2$	$fuel^3$	VSP	dfdt	dfdt+	dfdt-	RPM	PM
vel	1	0.01	0.1	-0.14	-0.11	-0.13	-0.09	0.36	0.3	0.25	-0.04	-0.05	-0.01	-0.07	0.79	0.01
acc	0.01	1	0.89	0.67	0.13	-0.05	-0.14	0.38	0.33	0.3	-0.11	0.1	0.24	-0.07	0.28	0.38
acc-	0.1	0.89	1	0.25	0.11	-0.13	-0.11	0.27	0.22	0.2	-0.07	0.05	0.11	-0.02	0.22	0.18
acc+	-0.14	0.67	0.25	1	0.09	0.11	-0.12	0.36	0.33	0.31	-0.12	0.13	0.32	-0.1	0.24	0.52
jerk	-0.11	0.13	0.11	0.09	1	0.8	0	0.03	0.04	0.04	-0.01	0.41	0.27	0.34	-0.18	0.14
jerk+	-0.13	-0.05	-0.13	0.11	0.8	1	-0.03	-0.06	-0.06	-0.06	-0.03	0.27	0.27	0.14	-0.13	0.15
grade	-0.09	-0.14	-0.11	-0.12	0	-0.03	1	0.49	0.46	0.44	0.69	0	0.08	-0.07	-0.12	0.21
fuel	0.36	0.38	0.27	**0.36**	0.03	-0.06	0.49	1	0.97	0.92	0.5	0.11	0.22	-0.03	0.4	0.48
$fuel^2$	0.3	0.33	0.22	0.33	0.04	-0.06	0.46	0.97	1	0.99	0.5	0.13	0.14	0.06	0.32	0.4
$fuel^3$	0.25	0.3	0.2	0.31	0.04	-0.06	0.44	0.92	0.99	1	0.48	0.12	0.09	0.1	0.28	0.35
VSP	-0.04	-0.11	-0.07	-0.12	-0.01	-0.03	0.69	0.5	0.5	0.48	1	0	0.03	-0.03	-0.05	0.17
dfdt	-0.05	0.1	0.05	0.13	0.41	0.27	0	0.11	0.13	0.12	0	1	0.73	0.79	-0.1	0.45
dfdt+	-0.01	0.24	0.11	**0.32**	0.27	0.27	0.08	**0.22**	0.14	0.09	0.03	0.73	1	0.16	0.09	0.75
dfdt-	-0.07	-0.07	-0.02	-0.1	0.34	0.14	-0.07	-0.03	0.06	0.1	-0.03	0.79	0.16	1	-0.22	-0.01
RPM	0.79	0.28	0.22	0.24	-0.18	-0.13	-0.12	0.4	0.32	0.28	-0.05	-0.1	0.09	-0.22	1	0.21
PM	0.01	0.38	0.18	**0.52**	0.14	0.15	0.21	**0.48**	0.4	0.35	0.17	0.45	**0.75**	-0.01	0.21	1

The correlation matrices in Figure 3-5 through Figure 3-7 present selected variable correlations separated into three velocity ranges in much the same way that MOVES operating mode bins are separated into speed ranges described in Section 2.6.1. Correlations between variables for these same speed ranges were tested (Figure 3-5 through Figure 3-7) and show that variable correlations differ between ranges. The data indicate that there is generally a stronger correlation for most parameters with PM in the 0-25 mph speed range than in the others with the exception of road grade which increases significantly in the higher speed range. Fuel and the positive portion of acceleration are

significantly higher in the low speed range. It is interesting to note that vehicle speed shows a positive correlation with PM in the low speed range and then a negative correlation in the higher speed ranges.

Table 3-4 Correlation matrix for selected explanatory values for velocity between 0-25 mph. Stronger positive correlations have darker shading.

	vel	acc	acc-	acc+	grade	fuel	vsp	dfdt	dfdt+	eng	pm
vel	1	0.06	0.02	0.12	-0.02	0.43	0.08	0.05	0.21	0.4	0.34
acc	0.06	1	0.95	0.74	-0.06	0.6	0.01	0.18	0.42	0.62	0.52
acc-	0.02	0.95	1	0.49	-0.05	0.41	-0.01	0.08	0.27	0.53	0.36
acc+	0.12	0.74	0.49	1	-0.04	0.76	0.07	0.31	0.57	0.58	0.68
grade	-0.02	-0.06	-0.05	-0.04	1	0.15	0.62	0.04	0.08	-0.1	0.12
fuel	0.43	0.6	0.41	0.76	0.15	1	0.28	0.37	0.64	0.63	0.83
vsp	0.08	0.01	-0.01	0.07	0.62	0.28	1	0.06	0.15	-0.04	0.22
dfdt	0.05	0.18	0.08	0.31	0.04	0.37	0.06	1	0.83	0	0.45
dfdt+	0.21	0.42	0.27	0.57	0.08	0.64	0.15	0.83	1	0.31	0.73
eng	0.4	0.62	0.53	0.58	-0.1	0.63	-0.04	0	0.31	1	0.59
pm	0.34	0.52	0.36	0.68	0.12	0.83	0.22	0.45	0.73	0.59	1

Table 3-5 Correlation matrix for selected explanatory values for velocity between 25-50 mph. Stronger positive correlations have darker shading.

	vel	acc	acc-	acc+	grade	fuel	vsp	dfdt	dfdt+	eng	pm
vel	1	-0.02	0.08	-0.2	-0.04	0.08	0.15	0	-0.13	0.08	-0.16
acc	-0.02	1	0.92	0.68	-0.12	0.59	-0.02	0.09	0.21	0.46	0.41
acc-	0.08	0.92	1	0.33	0.06	0.49	0.09	0.06	0.14	0.43	0.28
acc+	-0.2	0.68	0.33	1	-0.41	0.48	-0.22	0.11	0.25	0.29	0.46
grade	-0.04	-0.12	0.06	-0.41	1	0.44	0.55	0.02	-0.12	0.05	0
fuel	0.08	0.59	0.49	0.48	0.44	1	0.31	0.16	0.09	0.39	0.39
vsp	0.15	-0.02	0.09	-0.22	0.55	0.31	1	-0.02	-0.05	0.1	0.03
dfdt	0	0.09	0.06	0.11	0.02	0.16	-0.02	1	0.7	-0.24	0.45
dfdt+	-0.13	0.21	0.14	0.25	-0.12	0.09	-0.05	0.7	1	-0.09	0.73
eng	0.08	0.46	0.43	0.29	0.05	0.39	0.1	-0.24	-0.09	1	0.03
pm	-0.16	0.41	0.28	0.46	0	0.39	0.03	0.45	0.73	0.03	1

Table 3-6 Correlation matrix for selected explanatory values for velocity greater than 50 mph. Stronger positive correlations have darker shading.

	vel	acc	acc-	acc+	grade	fuel	vsp	dfdt	dfdt+	eng	pm
vel	1	0.02	0.1	-0.14	-0.23	-0.14	-0.21	-0.1	-0.11	0.77	-0.23
acc	0.02	1	0.91	0.64	-0.22	0.31	-0.18	0.11	0.08	-0.02	0.22
acc-	0.1	0.91	1	0.27	-0.1	0.22	-0.07	0.09	0.04	0.05	0.11
acc+	-0.14	0.64	0.27	1	-0.32	0.32	-0.28	0.09	0.11	-0.13	0.31
grade	-0.23	-0.22	-0.1	-0.32	1	0.68	0.94	0.01	0.02	-0.3	0.27
fuel	-0.14	0.31	0.22	0.32	0.68	1	0.69	0.09	0.07	-0.22	0.48
vsp	-0.21	-0.18	-0.07	-0.28	0.94	0.69	1	0	0.01	-0.26	0.27
dfdt	-0.1	0.11	0.09	0.09	0.01	0.09	0	1	0.69	-0.13	0.42
dfdt+	-0.11	0.08	0.04	0.11	0.02	0.07	0.01	0.69	1	-0.13	0.64
eng	0.77	-0.02	0.05	-0.13	-0.3	-0.22	-0.26	-0.13	-0.13	1	-0.26
pm	-0.23	0.22	0.11	0.31	0.27	0.48	0.27	0.42	0.64	-0.26	1

Table 3-7 shows correlation coefficients for several additional parameters that were evaluated as potential predictors for PM. In this table fuel is included for reference. The parameter “load_1” and “load_2” are an attempt to represent the level of load on an engine leading up to an emission event in order to account for any influence this may have on emission production. The concept of “engine stress” is used in the IVE emission model to help partition VSP based emission bins (ISSRC, 2008). The parameter “load_1” is the product of engine speed and VSP and the parameter “load_2” is the cumulative value of the product of engine speed and VSP over the last two seconds. The cumulative value of this parameter for 5 second and 10 second ranges prior was also evaluated and showed no improvement. These values are not presented in Table 3-7.

Table 3-7 Correlation matrix for additional parameters. Stronger positive correlations have darker shading.

	fuel	load_1	load_2	fuel_s2	fuel_s3	fuel_s5	PM
fuel	1	0.49	0.5	0.99	0.97	0.93	0.48
load_1	0.49	1	0.99	0.49	0.49	0.49	0.17
load_2	0.5	0.99	1	0.5	0.5	0.51	0.16
fuel_s2	0.99	0.49	0.5	1	0.99	0.96	0.43
fuel_s3	0.97	0.49	0.5	0.99	1	0.98	0.38
fuel_s5	0.93	0.49	0.51	0.96	0.98	1	0.33
PM	0.48	0.17	0.16	0.43	0.38	0.33	1

In addition to the engine load parameter, cumulative fuel use over the previous 2, 3 and 5 second range was evaluated with the parameters "fuel_s2", "fuel_s3", and "fuel_s5". These values are calculated from the fuel rate and are highly correlated with the fuel rate. Unlike the change in fuel rate, which is also calculated from the fuel rate, the "fuel_s2", "fuel_s3" and "fuel_s5" parameters do not show any increased correlation with PM over the fuel rate itself.

3.7 Regression Model Descriptions

This section describes three general proposed emission models that were developed and evaluated for predicting PM at the microscale level. Each of these models were developed based in part on observations from the correlation matrix in Table 3-3 and have increasing complexity. The strongest predictor variables, as determined by the correlation coefficients and as discussed in Section 3.6, are the positive portion of the change in fuel rate, positive acceleration, and fuel rate. The fuel rate and the change in fuel rate are modeled using the physical approach presented in Section 3.4 and form the

basis for the regression component of the models developed in this section. The values of second-by-second velocity and acceleration are standard inputs to the microscale model and are used for partitioning regions in the PM models. The criteria for model development are model simplicity, intuitiveness and performance. The three proposed submodels are described in the following sections. Model A is the base model, model B is the base model applied to two separate acceleration regions and model C is the base model applied in three separate speed regions. Calibration and validation results are presented in Section 3.8.

3.7.1 Model A

The basic PM model developed in this research is presented in equation 3.5 and 3.6. Equation 3.6 is the main equation for all three models and was developed from the core parameter fuel and the positive change in fuel rate which showed the most predictive power for PM. This equation also seems to make sense conceptually since it incorporates fuel and the change in fuel rate which would be associated with transients and PM events. In this model, as well as the models following, the idle mode is separated out and modeled with a constant value, PM_{idle}.

$$PM = PM_{idle} \qquad \text{for v = 0 mph} \qquad (3.5)$$

$$PM = b_1F + b_2(dF/dt+) + \varepsilon \qquad \text{for v > 0 mph} \qquad (3.6)$$

where:

PM = HDD PM, g/s

PM_{idle} = HDD PM at velocity equal to zero, g/s

F = fuel use rate, g/s

$dF/dt+$ = positive portion of the change in fuel rate, g/s^2

b_1, b_2 = regression coefficients

ε = constant term

v = velocity, mph

3.7.2 Model B

The correlation matrices presented in Section 3.6 indicate that acceleration and the positive component of acceleration exhibit some of the higher correlations, among the variables tested, with PM. Model B, the second model that was developed and evaluated, is the basic model, Model A, separated into acceleration modes. Model B is presented in equations 3.7, 3.8 and 3.9.

$$PM = PM_{idle} \quad \text{for v = 0 mph} \quad (3.7)$$

$$PM = b_1F + b_2(dF/dt+) + \varepsilon \quad \text{for a <= 0 mph/s} \quad (3.8)$$

$$PM = b_3F + b_4(dF/dt+) + \varepsilon \quad \text{for a > 0 mph/s} \quad (3.9)$$

where:

PM = HDD PM, g/s

PM_{idle} = HDD PM at velocity equal to zero, g/s

F = fuel use rate, g/s

$dF/dt+$ = positive portion of the change in fuel rate, g/s^2

b_1, b_2, b_3, b_4 = regression coefficients

ε = constant term

v = velocity, mph

3.7.3 Model C

The third model that was developed and evaluated is the basic PM model, Model A, separated into three velocity ranges in much the same way that the MOVES operating mode bins are separated into speed ranges as described in Section 2.6.1 and discussed in Section 3.6. Model C is presented in equations 3.10 through 3.13.

$$PM = PM_{idle} \quad \text{for v = 0 mph} \quad 3.10$$

$$PM = b_1F + b_2(dF/dt+) + \varepsilon \quad \text{for v > 0 \& v <= 25 mph} \quad 3.11$$

$$PM = b_3F + b_4(dF/dt+) + \varepsilon \quad \text{for v > 25 \& v <= 50 mph} \quad 3.12$$

$$PM = b_5F + b_6(dF/dt+) + \varepsilon \quad \text{for v > 50 mph} \quad 3.13$$

where:

PM = HDD PM, g/s

PM_{idle} = HDD PM at velocity equal to zero, g/s

F = fuel use rate, g/s

$dF/dt+$ = positive portion of the change in fuel rate, g/s^2

b_1, b_2 = regression coefficients

v = velocity, mph

ε = constant term

3.8 Model Calibration and Validation

In practice, model calibration, data analysis and algorithm development are, to a large extent, performed together in an iterative fashion. During the calibration step, a subset of second-by-second data, described in Section 3.3.3 as the calibration data set, is used to determine model coefficients in both the physically based and the regression based portions of the model. The MEL data set contains continuous data for several intermediate variables such as engine speed, percent engine load and fuel use. These intermediated variables are used to help verify key modules in the physical model. The final PM model is developed and calibrated using ECM broadcast fuel and measured emissions from the calibration data set. Validation is performed in a second step using the validation data set described in Section 3.3.3.

Model validation is the assessment of how a model performs independent of input data and is an essential part in the model development process. It provides a better understanding of the capabilities of the model and also its limitations. The validation process is complicated by the fact that the data being used is real-world data and is subject to external forces which are often hard to quantify, such as wind speed, temperature, pressure and to some extent road grade.

The following sections discuss the model calibration and validation process in more detail. The measures of goodness-of-fit which are used are the coefficient of determination (R^2), the slope and intercept of the linear regression line between the modeled and measured data, and root-mean-square error (RMSE). The R^2 value is an

indicator of the precision of the model prediction while the slope of the linear regression line between the measured and modeled data is an indicator of the accuracy of the prediction. The RMSE value is also a common measure of accuracy and has the characteristic of having the same units of measure as the predicted and modeled values. Many of the measures of fit are based on comparisons at the second-by-second level and are very sensitive to time alignment issues discussed in Section 3.3.4.

3.8.1 Fuel Rate Model

Fuel rate and the change in fuel rate are the basis for the PM model and are the first step in the modeling process. The basic equation for the prediction of fuel rate from vehicle activity has been discussed previously (An & Ross, 1993) (An F. , Barth, Norbeck, & Ross, 1997) and a general overview of the physical model is presented in Section 3.2. Additional information on the HDD fuel model as well as the supporting models used in this work can be found in the author's previous work (Scora, 2007). Since measured fuel is one of the variables available from the ECU, the fuel rate model can be calibrated to the measured data. Many of the parameters associated with the fuel rate calculation are fixed based on the physical characteristics of the vehicle and the engine. Some parameters are not readily available for the particular test vehicle and can be adjusted within a known range of practical values to calibrate the model. Examples of adjustable parameters include engine friction terms, rolling resistance coefficients and to some extent the coefficient of aerodynamic drag.

The fuel model is calibrated to a 3% error over the calibration data set as presented in Figure 3-17. The resulting R^2 of 0.95 and the regression line slope of 1 indicate that the model does a very good job of explaining the variance in fuel rate especially considering the various sources of unexplained error which exist in on-road driving data set.

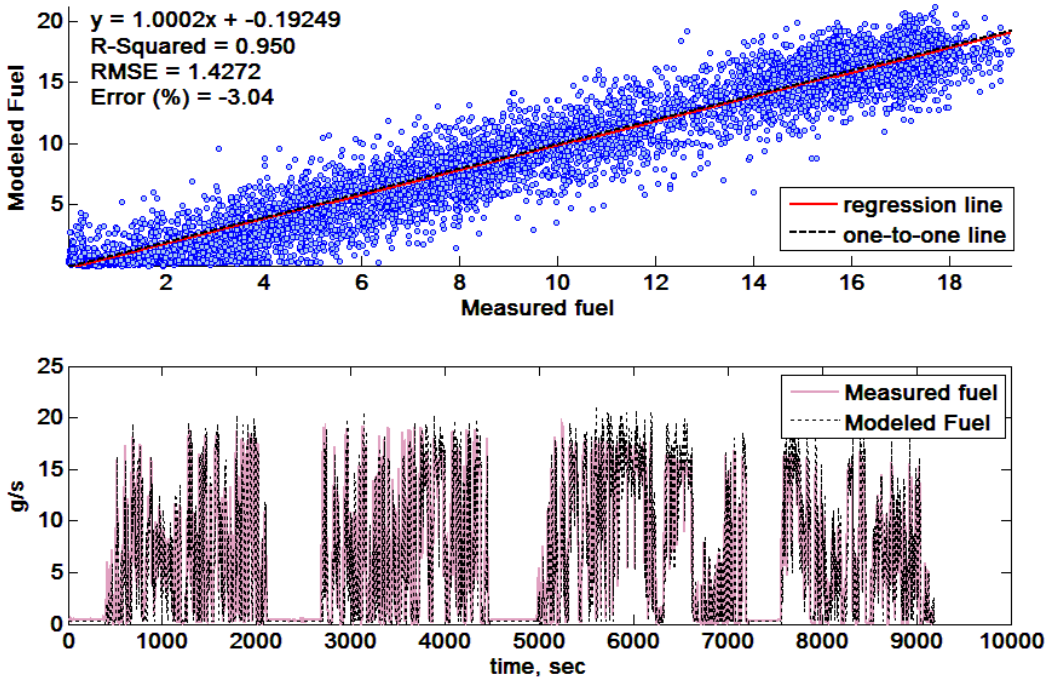

Figure 3-17 Comparison of modeled versus measured fuel use for the calibration data set, top: scatter plot showing regression statistics and one-to-one line, bottom: second-by-second time series of measured and modeled fuel.

Validation of the fuel rate model was performed using the validation data set and the calibrated parameters determined in the calibration step. The results of the validation step are presented in Figure 3-18 and indicate that the fuel rate model's performance hold up well to this independent data set with an R^2 value of 0.92 and a regression line slope near 0.98. Improvements in the testing parameters such as more precise grade and wind

information would likely reduce the model error further. At this point, grade information is obtained from GPS data and has limited accuracy, and wind data, obtained from local weather stations when available, is limited and very general.

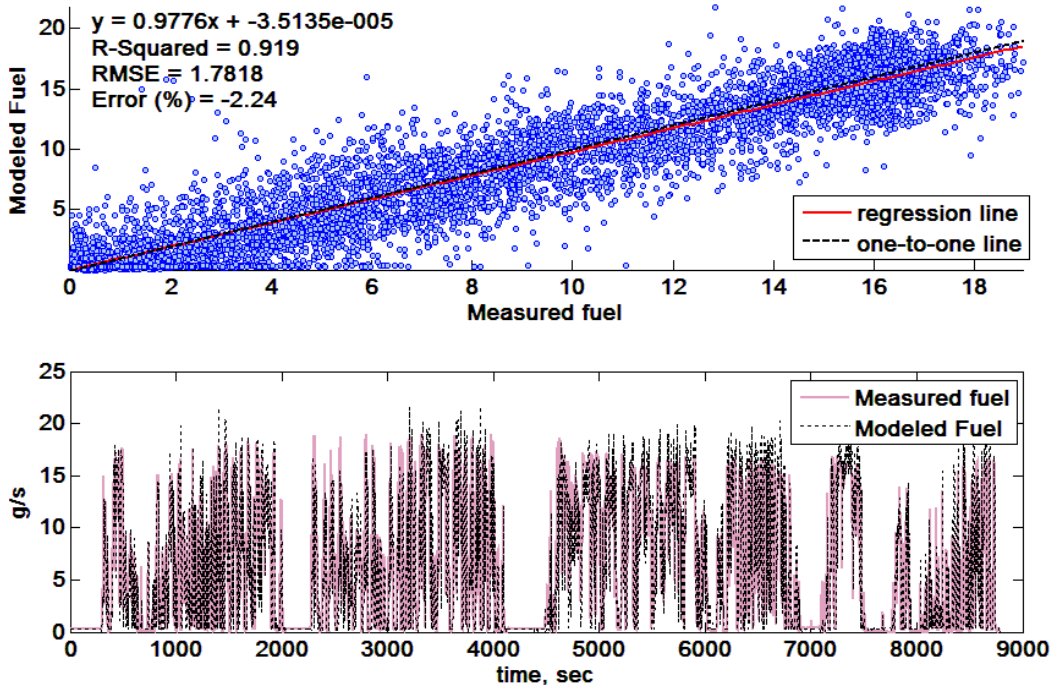

Figure 3-18 Comparison of modeled versus measured fuel use for the validation data set, top: scatter plot showing regression statistics and one-to-one line, bottom: second-by-second time series of measured and modeled fuel.

3.8.2 PM Model

In Section 3.7, three PM models were developed and presented; these models are evaluated in the following section. The three models are a variation of the base case model, Model A. Model B is differentiated by its use of an acceleration and deceleration regime while Model C is differentiated by its use of three speed regimes. The models are calibrated using a regression function using the standard least squares method. For the

regression analysis and calibration process, a matrix of explanatory variables is created as discussed in Section 3.5. In the case of Model B which consists of two acceleration regimes or Model C which consists of three speed regimes, a set of binary dummy variables was created for each regime to isolate the effects of coefficients to those regimes. The velocity equal to zero regimes, which exists in all three models, was also handled by a binary dummy variable. In all cases where model calibration and validation are concerned, the measured PM value used is from the Dekati analyzer.

Model A

Model A was calibrated using the calibration data set with measured predictor values and the results are presented in Figure 3-19. The R^2 for the basic regression is 0.6 with a RMSE of 0.0013 g/s. The calibration process includes a constant term which eliminates the total predicted error.

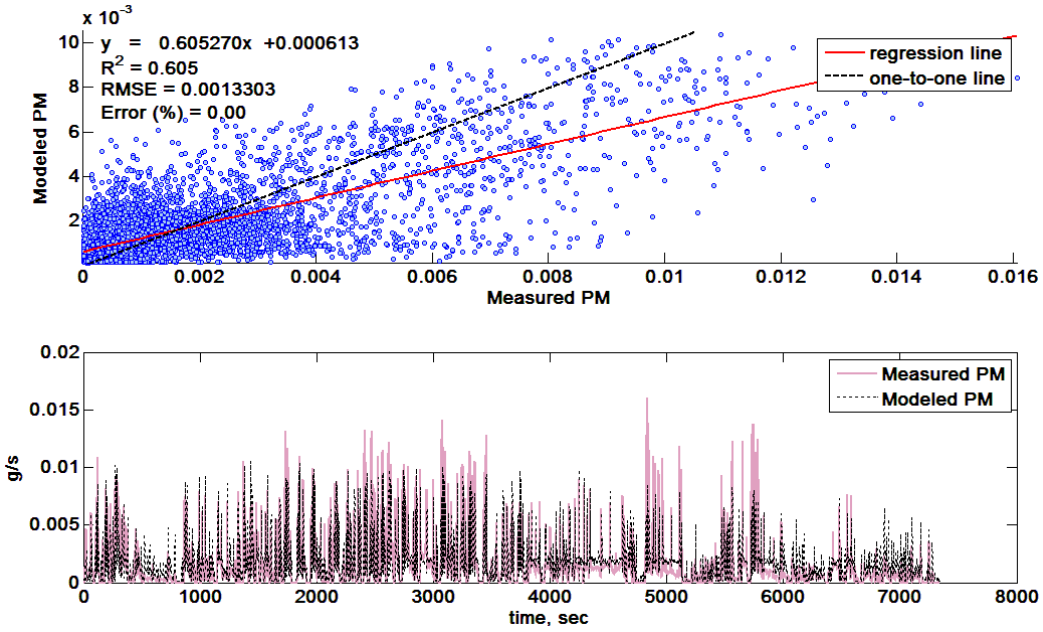

Figure 3-19 "Model A" predicted PM based on measured predictor values and the calibration data set.

The calibrated model was then applied to the validation data using only modeled predictor values and the comparison is presented in Figure 3-20. This step introduces additional error based on the variability between the calibration and validation data set as well as that between the measured and modeled predictor values. The R^2 value has dropped from 0.6 in the calibration step to 0.35 in the independent validation step and the RMSE has increased by roughly 65%. The total error is around -18%.

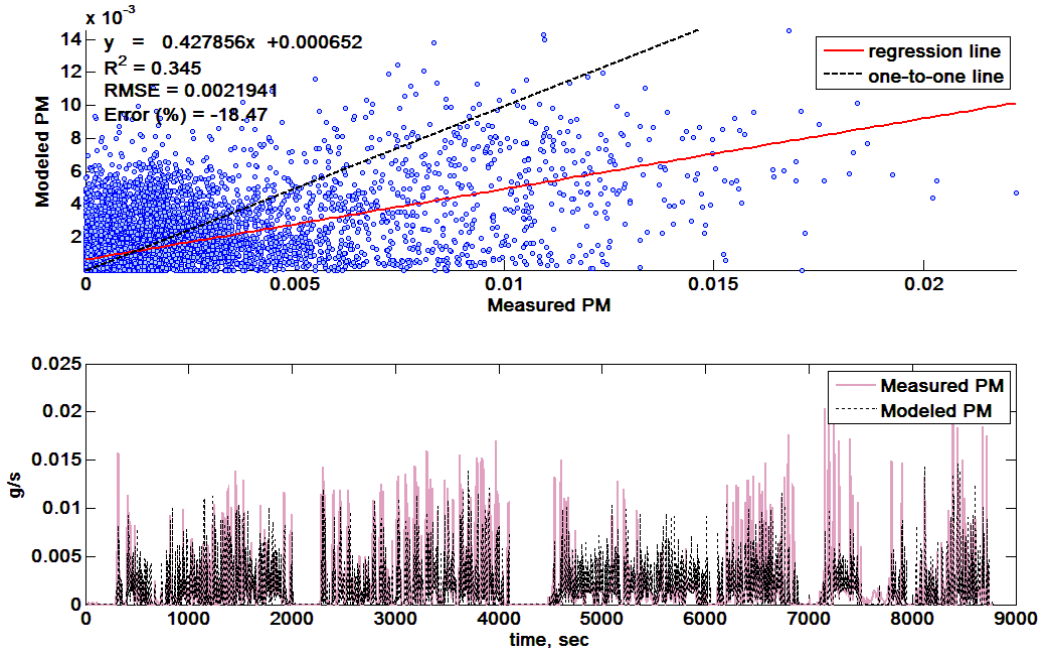

Figure 3-20 "Model A" predicted PM based on modeled predictor values and the validation data set.

Model B

The calibration process for Model B was the same as that for Model A and the results are presented in Figure 3-21. The R^2 for the basic regression is 0.62 with a RMSE of 0.0013 g/s. The results are similar to Model A.

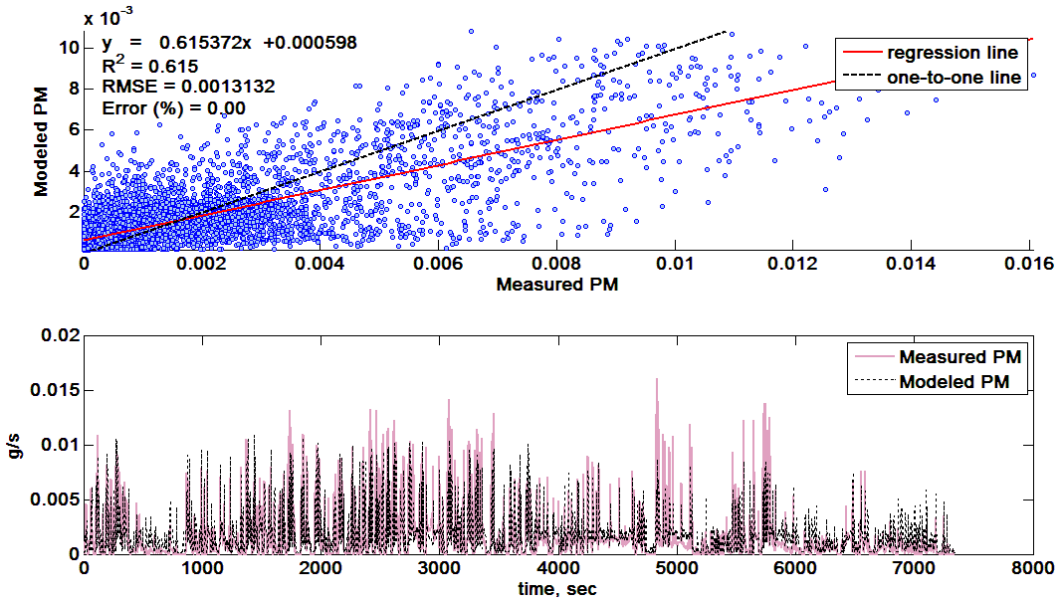

Figure 3-21 "Model B" predicted PM based on measured predictor values and the calibration data set.

The calibrated model was then applied to the validation data using only modeled predictor values and the comparison is presented in Figure 3-22. The R^2 value has dropped from 0.62 in the calibration step to 0.36 in the independent validation step and the RMSE has increased by roughly 65%. The total error is around -23%.

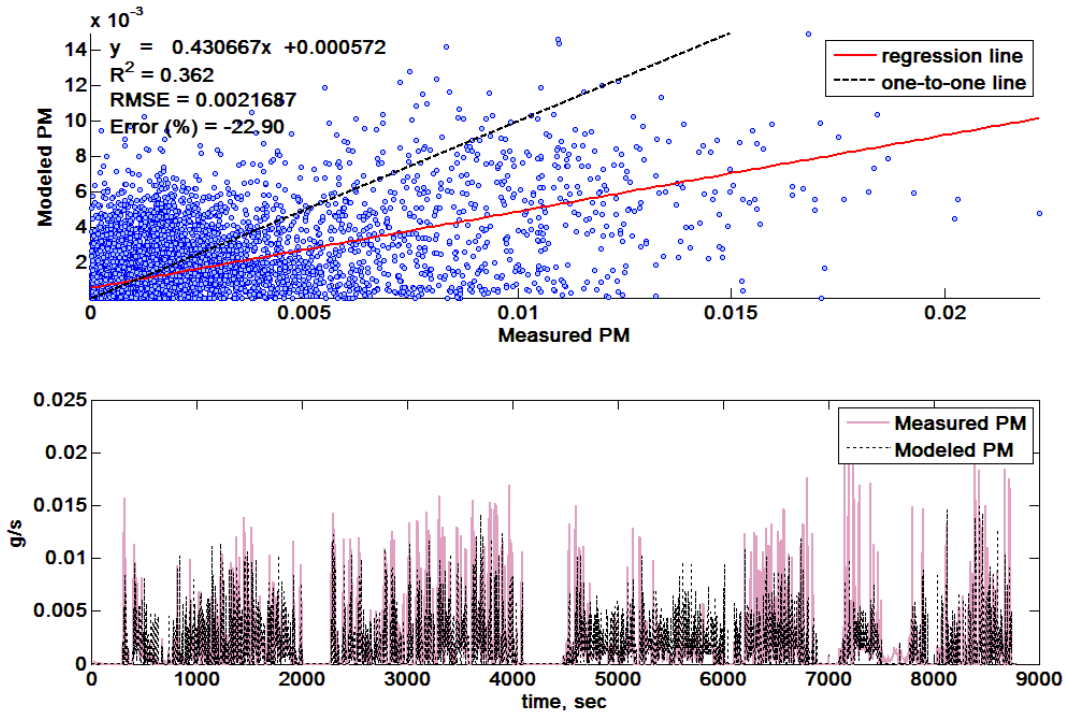

Figure 3-22 "Model B" predicted PM based on modeled predictor values and the validation data set.

Model C

Model C was calibrated in the same manner as Model A and B and the results are presented in Figure 3-23. The calibration process includes a constant term which eliminates the total predicted error. An R^2 value of 0.72 indicates that the model explains roughly 72% of the variance in the measured PM value.

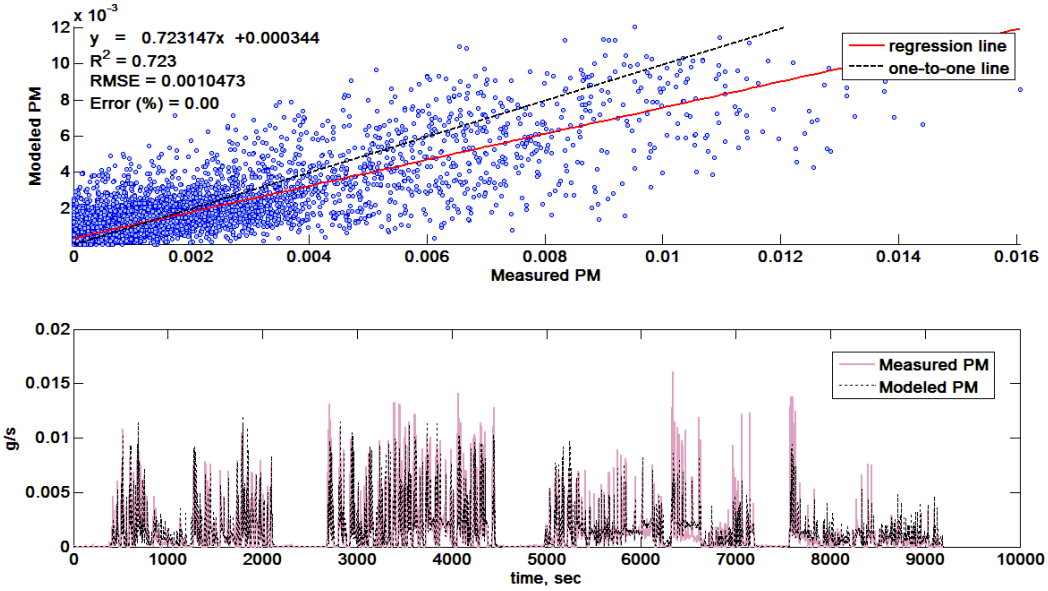

Figure 3-23 "Model C" predicted PM based on measured predictor values and the calibration data set.

The calibrated model was applied to the validation dataset and the results are presented in Figure 3-24. With the introduction of error from the modeled fuel step and the variability between the calibration and validation data sets, the R^2 value has dropped from 0.72 in the calibration step to 0.46 in the independent validation step. The RMSE has decreased by roughly 9% and the total error is around -17%.

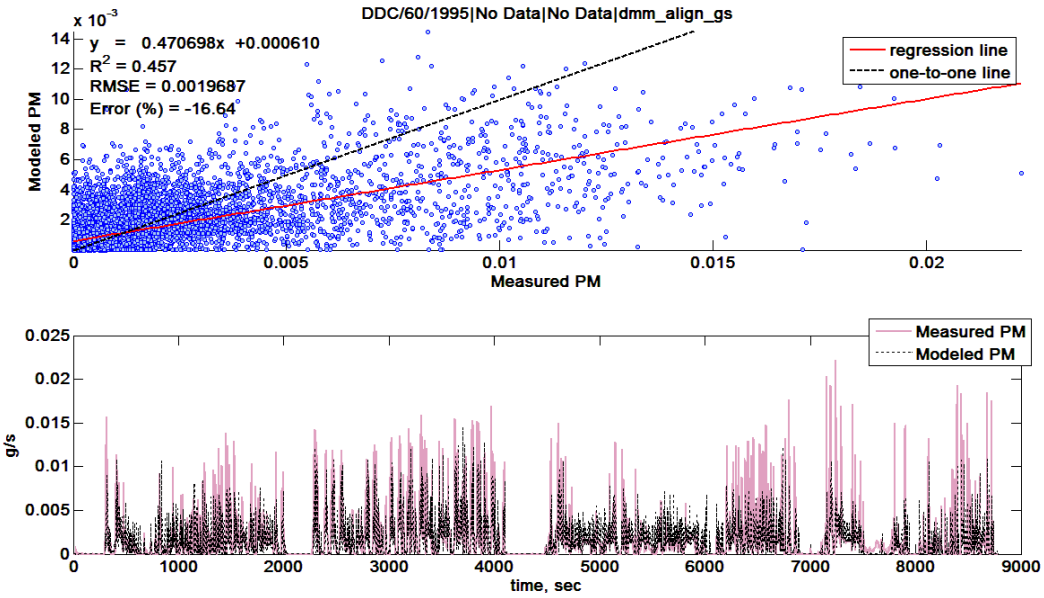

Figure 3-24 "Model C" predicted PM based on modeled predictor values and the validation data set.

For comparison, Figure 3-25 shows the performance of the DustTrak relative to the Dekati analyzer for the validation data set. The DustTrak data is scaled to match the cumulative Dekati data, so the overall error is zero. It is, however, evident that the performance of Model C relative to the Dekati data is not much less than that of the DustTrak with a difference in RMSE of less than 15%.

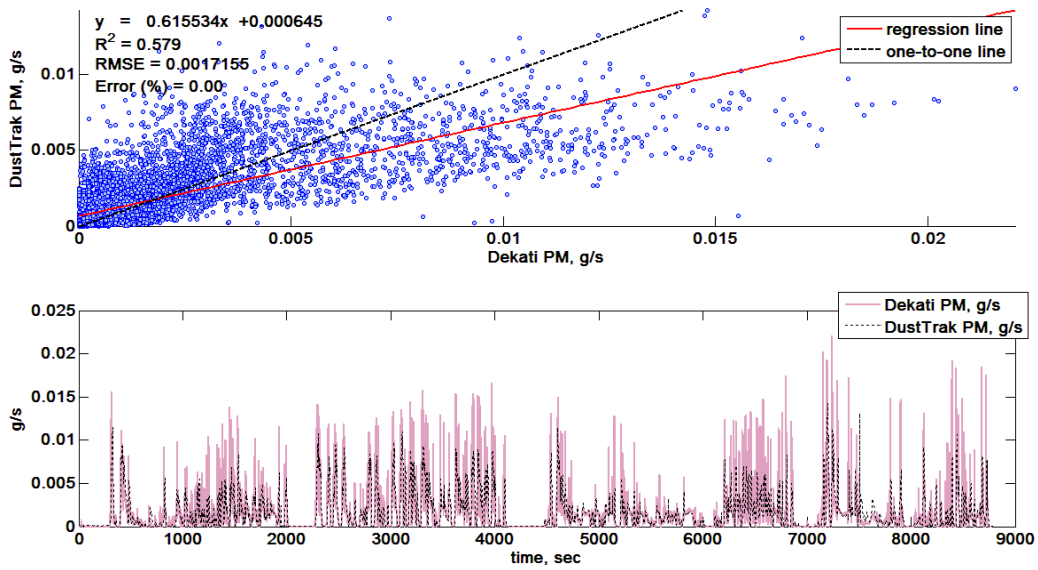

Figure 3-25 Comparison of DustTrak PM verses Dekati PM for the validation data set.

3.8.3 Modeling Trade Offs

Although Model C required the most parameters, the improvement over the base case model and the model partitioned by two acceleration regimes was substantial and warrants the inclusion of the additional parameters. The regression results for the validation data indicate the difficulty in accurately characterizing PM data on a second-by-second basis. The performance of the model based on known data from the ECU in the calibration data set indicates that the model performance may be greatly improved in an onboard vehicle application such as real-time on-board emission predictions. In the calibration step, model performance matches PM emissions from the Dekati far better than the scaled DustTrak data; with an improvement in RMSE of nearly 40% and an increase in R^2 from 0.58 to 0.72.

3.9 Compression Release Braking and PM in HDD Vehicles

It was found that compression release braking appears to have a significant effect on PM emissions. This section describes the special condition of compression release braking encountered in the MEL test data set, initial compression release braking analysis and a modeling methodology. A compression release brake is a mechanism common in diesel engines which uses the engine's compression force to aid in decelerating the vehicle. The term "Jake brake" refers to a popular brand of compression release brake and is often used to refer to this type of braking. In a diesel engine air is compressed during the compression stroke which absorbs energy from the system and if the vehicle is in gear this energy is taken from the vehicles forward motion. In an engine without compression release braking, this energy in transferred back to the piston during the following power stroke when the compressed air expands without the addition of fuel and fuel combustion. In this manner, most of the energy it took to compress the air in the cylinder is returned to the system and only a small net amount of engine braking force is created.

In an engine equipped with compression release braking, the cylinder valves are lifted at the top of the compression stroke which releases the compressed charge of air and returns very little energy back to the vehicle through the piston. This produces a much greater engine braking force. The characteristic chatter or popping noise from compression release braking is the release of compressed air near the top of the compression stroke.

3.9.1 Identifying Compression Release Braking Events

It was determined that during compression release braking there are PM emission events not associated with the instantaneous fuel use of the vehicle. This can be seen in Figure 3-26 during the deceleration event between seconds 100 and 115. During this event the truck is slowing down with no fuel input and producing a significant PM emission spike. At the same moment, the boost pressure is also observed to increase which is used as an indication of compression release braking.

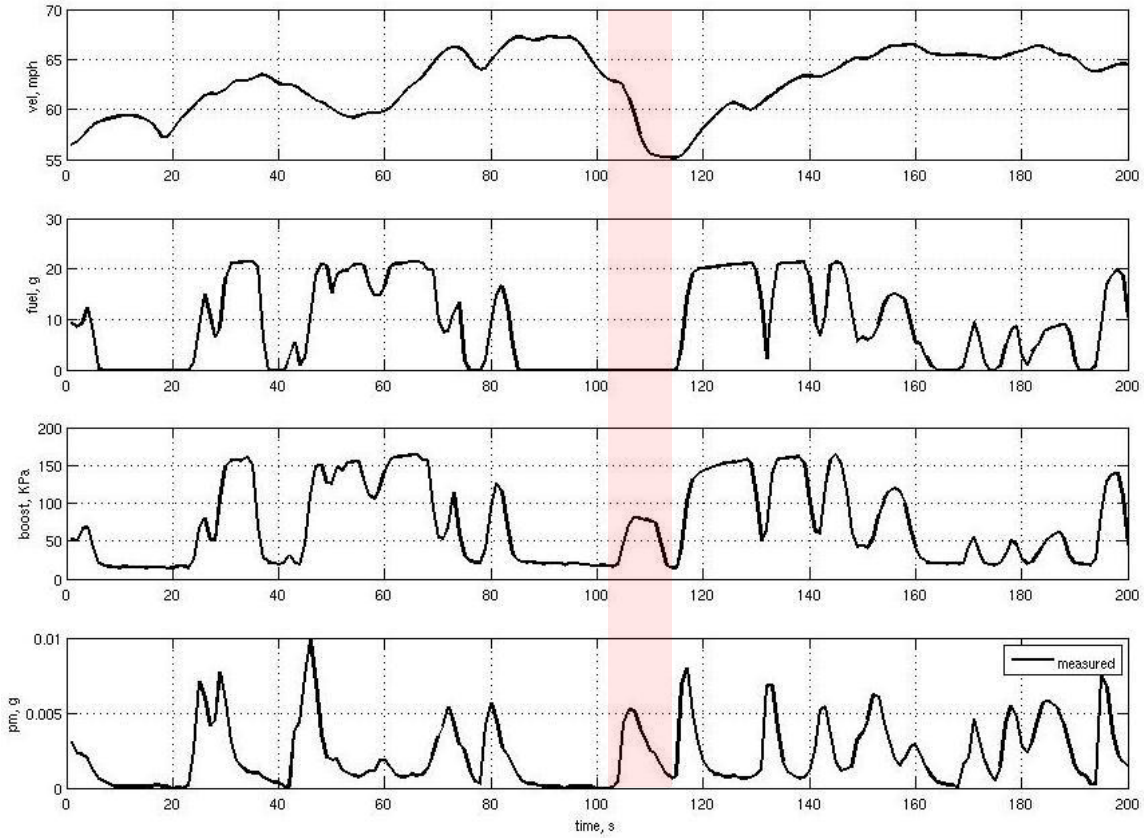

Figure 3-26 PM event over compression release braking event.

In addition to fuel use and boost pressure, the MEL data set also provides GPS location data. This data can be used to position the vehicle on a roadway network to gain additional information about the conditions the vehicle was tested under. Figure 3-27 shows a truck route for an emission test trace plotted in Google Earth with each data point being represented by a ring and scaled based on PM emissions. This helps visualize geospatially where emission spikes are occurring.

Figure 3-27 MEL PM measurement data visualized by location. Larger rings represent greater PM emissions.

A closer look at the location for the compression release event introduced in Figure 3-26 is presented in Figure 3-28. The upper portion of the figure shows increased PM emissions during the downhill event while the lower portion of the figure shows the elevation profile for the location. The direction of travel and the start of the compression release event are labeled in each portion of the figure.

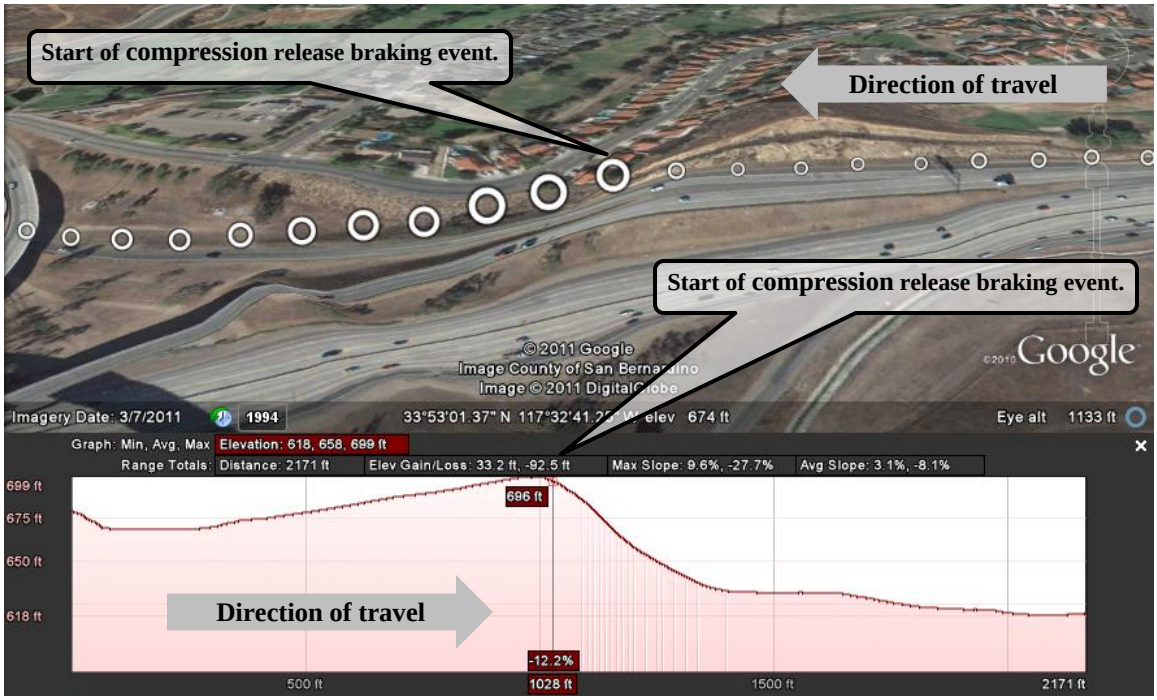

Figure 3-28 Map showing increased PM emissions during downhill event. Circles represent PM emissions and are scaled based on magnitude.

3.9.2 Modeling Compression Release Braking Events

It was determined that during compression release braking, either unburned fuel in the cylinder that has accumulated in the crevices or accumulated PM in the exhaust system is forced out during the decompression braking process. The amount of PM released at each second is theorized to be dependent on the amount of unburned fuel available in the cylinder or the amount of accumulated PM in the exhaust system and is modeled based on a first order exponential decay rate according to equation 3.14. The amount of PM released is subtracted from the current amount of PM producing material to determine the amount of PM producing material left in the system for further release according to equation 3.15.

$$PM_{r,t} = PM_{c,t}e^{-k\Delta t} \quad \textbf{3.14}$$

$$PM_{c,t+\Delta t} = PM_{c,t} - PM_{r,t} \quad \textbf{3.15}$$

Where

$PM_{r,t}$ = PM released at time t, grams

$PM_{c,t}$ = PM in the system at time t, grams

k = release constant in units of 1/second

Δt = change in time (1 sec for our modeling purposes)

$PM_{c,t=0}$ = PM in the system at the start of the braking event, grams

The last subplot in Figure 3-29 compares the measured PM emission profile with the PM emission profile for the standard PM model, both with and without the addition of compression release braking model. Since the core PM model presented here is based on the fuel rate and the change in fuel rate, the core PM model predicts zero PM emissions during a compression release braking event in which no fuel is consumed. The practical application of a compression release braking model requires a second-by-second compression release braking input flag and calibration parameters for the initial PM producing potential of the system during a compression release braking event and the release constant. The PM producing material in the system at the beginning of a compression release braking event appears to vary greatly and appears to be dependent on the vehicle activity leading up to the braking event and how many cylinders the Jake brake is being applied to. Typically, the user has multiple switches to select the number of active cylinders for braking, for example 2, 4, or 6.

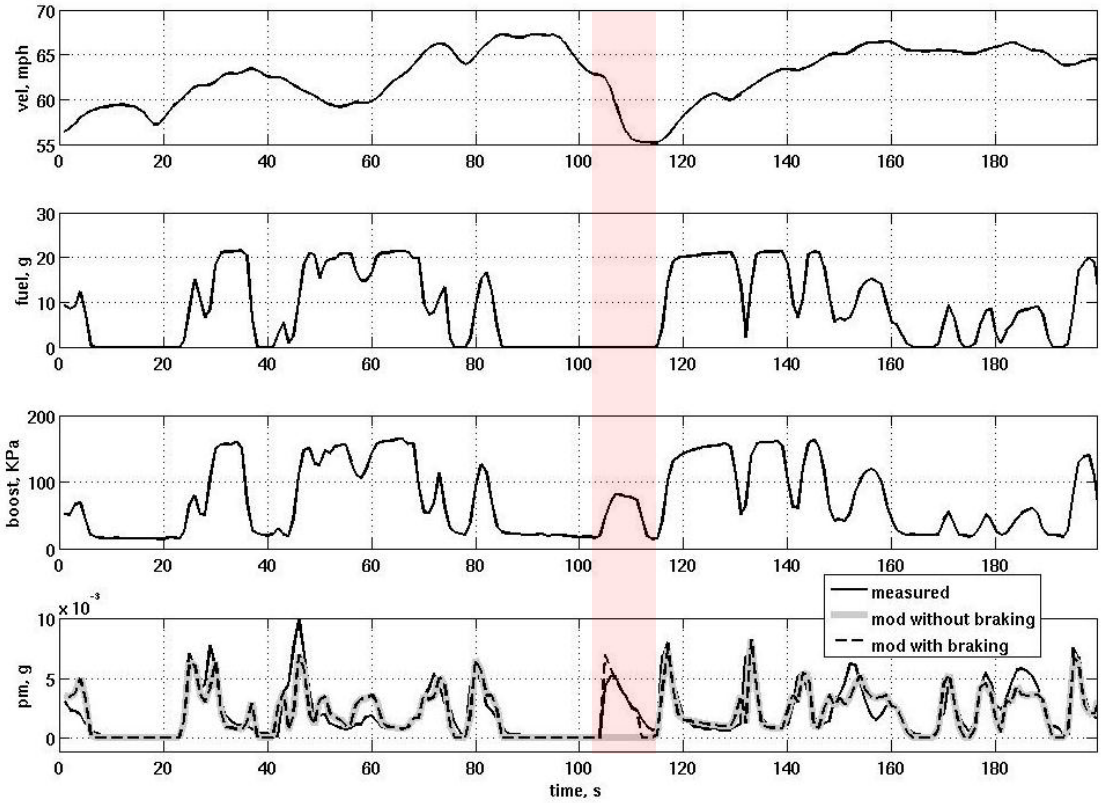

Figure 3-29 PM prediction over compression release braking event.

Further research is needed to determine the relationship of the magnitude of the compression release braking events with possible predictor variable such as prior vehicle activity, speed, and road grade. For model development work, aside from Section 3.9, the compression release braking events were omitted in order to concentrate on modeling the basic relationship between fuel and PM. It was estimated that the test truck spent roughly 1.7 % of its time in compression release braking mode and that this accounted for roughly 3% of the total PM emissions across 7.5 hours of vehicle activity described in the calibration and validation data set in 3.3.3. Although the total contribution of these emissions may be low, the nature of the emission event isolates the emissions to specific

areas. This may increase local concentrations of PM emissions and may be important in exposure studies, especially where more emission-sensitive areas are located next to downhill roadways.

3.10 Chapter 3 Summary

This chapter presented the development, calibration and validation of a second-by-second PM model. The developed PM model is based primarily on the rate of fuel use and parameters related to the rate of fuel use. Measured fuel from CE-CERT's MEL emission lab and calculations from measured fuel were used to calibrate the PM model. The data were processed and split into two portions: one for calibration and one for validation.

Correlation coefficients for various potential explanatory variables were calculated and evaluated to help identify predictors for PM modeling. Three variations of a PM model based on fuel rate and the positive portions of fuel rate were presented and evaluated. The final model is based on fuel rate and the positive changes in fuel rate broken into three speed ranges.

Intermediate variables from the calibration set were used to calibrate the fuel model which fit well with measured fuel in both the calibration and validation data sets. These two data sets combined consist of roughly 7 hours of vehicle activity over a wide range of driving conditions. The PM portion of the modeling work was developed and calibrated based on measured fuel data from the calibration data set. Once these coefficients were determined and following calibration of the fuel rate model, a

comparison between modeled PM using modeled fuel was performed on the validation data set. In this comparison, PM is modeled from the driving trace onward without any additional measured data.

Results for the selected PM model, calibrated to zero overall error on measured predictor values, shows an R^2 value of 0.72, a regression slope of 0.7 and an RMSE of 0.00104 g/s. The results of the selected PM model on the validation data set, using modeled predictor values, shows an R^2 value of 0.46 and an RMSE of 0.00197 g/s. A comparison between the DustTrak and the Dekati analyzers show slightly better R^2 and RMSE values (R^2 = 0.58, RMSE = 0.00172 g/s).

Additionally, compression release braking was identified as a significant source of PM emissions and the basis for a modeling approach was outlined. The test vehicle spent roughly 1.7% of its time in this mode which accounted for roughly 3% of the PM emissions. Further research is required for this potentially important area of study to quantify these braking events during normal driving, to study their contribution to human exposure and to improve the overall PM model.

4.0 Development of a Mesoscale HDD Emission Model

This work focuses on furthering the understanding of the effects of operational parameters on HDD emissions and on developing a methodology for mesoscale emission predictions using parameters not often incorporated at that level of emission modeling. As part of the modeling effort, an emission data set was populated for a broad range of conditions using the microscale model developed in previous work (Scora, 2007) and refined further in Chapter 0. The developed dataset is the foundation for energy and emission modeling work that can be applied in a variety of transportation applications as an improvement to traditional emission curves which only account for average speed and vehicle type. In order to demonstrate the effectiveness of the mesoscale model, it has been integrated with an EFNav application for route optimization which is discussed in Chapter 5.0.

4.1 Mesoscale Modeling Approaches

There are various approaches to modeling traffic energy use and emission production at the mesoscale level. The focus for mesoscale modeling is at the roadway link level and the input parameters used for analysis at this level are summary parameters that describe general characteristics such as average speed, number of vehicle stops, distance traveled, level of facility, etc.

A basic mesoscale modeling approach, aside from applying macroscale emission factors at the link level, is the use of average speed based emission factors. In this approach, the average traffic speed on a link is used to determine the emission rate on

that link. This emission rate can be developed for individual vehicles, for composite vehicles or by taking other factors into consideration such as road type or level of facility. With each additional consideration, a separate set of average speed based emission factors or a correction factor would have to be created. Average speed based factors can be applied from a binned lookup table using interpolation or as is commonly done, a relationship describing the emission factor as a function of average speed is developed to facilitate calculation and to visualize the emission trend with speed. Figure 4-1 presents a typical average speed based energy or emission curve with the characteristic dip at moderate speeds indicating the optimal driving range or "sweet spot" for the given dependent parameter. The average speed based curve is developed from data points representing individual drive cycles, characterized by their average speed and overall fuel use or emission production.

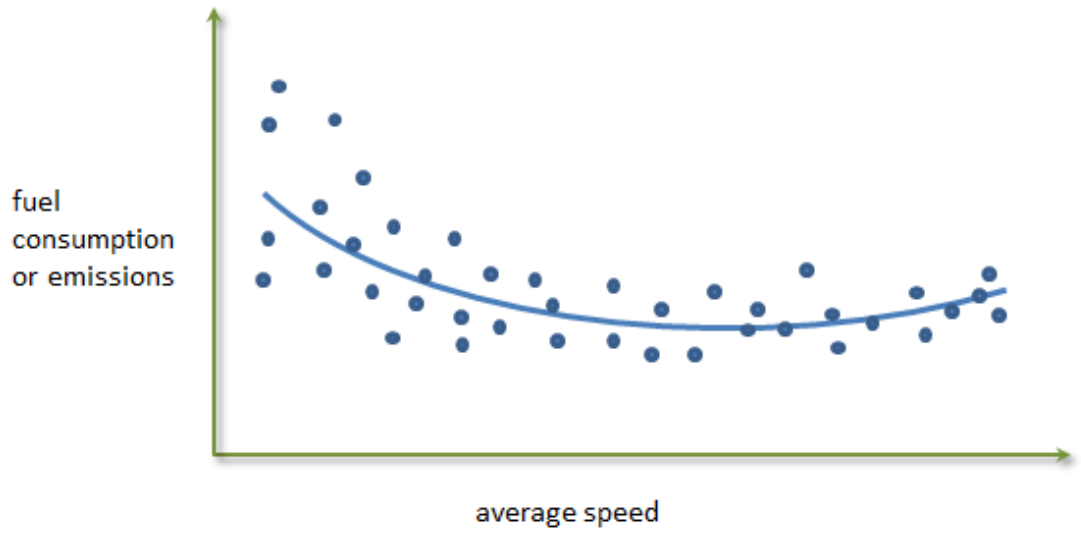

Figure 4-1 Example average speed based emission curve. Individual points represent separate drive cycles or snippets characterized by their average speed and overall fuel use or emission production.

There are several advantages to average speed based emission curves, namely that they are straightforward to implement and match well with transportation data and models. The main drawback, however, is that they cannot readily account for the additional effects of important operational parameters, most notably those relating to load. Operational parameters are discussed in further detail in the following section.

4.2 Operational Parameters

Operational parameters describe the conditions under which a vehicle is operating and include variables such as vehicle speed, acceleration, road grade, vehicle weight, road type, and congestion level. Energy and emission modeling in this section is at the mesoscale level, so only operational parameters that are mesoscale in nature will be available and relevant to the final model. The following subsections discuss several potential modeling parameters, their importance as mesoscale modeling inputs and how they are treated in the model.

4.2.1 Vehicle Speed and Acceleration

Vehicle speed and acceleration are related to fuel consumption and are important parameters especially for HDD vehicles. Earlier work has shown that increased vehicle speeds and aggressive acceleration are responsible for higher fuel use and consequently higher CO_2 emissions in light-duty vehicles (Kean, Harley, & Kendall, 2003) (Andre & Pronello, 1997). A similar, if not more pronounced, trend is expected for HDD vehicles since these normally have lower power to weight ratios. For the mesoscale modeling

work presented here, only average velocity is considered. Acceleration is often not available as a mesoscale modeling parameter and its effects can be subsumed indirectly through the road type and congestion level parameters discussed later.

4.2.2 Road Grade

Road grade is an important factor to consider when evaluating on-road fuel use and emissions (Fernandez & Long, 1995) (Park & Rakha, 2006) however it is not as important for light duty vehicles and has not been strongly considered for fuel consumption and emission modeling at the mesoscale level. For HDD vehicles, road grade is a significant factor (Scora, 2010). For example, sufficient road grade may result in a shorter route being less fuel efficient and less environmentally friendly than a flatter but longer route. Figure 4-3 presents measured HDD fuel consumption data as a function of road grade for vehicle activity greater than 10 mph and with zero acceleration. The data shows the strong relationship between fuel efficiency and road grade. The data shows that going from a flat road to one at 3 degrees grade results in a tripling of the fuel consumption rate. For this reason, it is important to included road grade in a fuel or emission analysis, yet it is often not incorporated at the mesoscale level. A recent review indicates that the major commercial navigation systems for trucks do not consider slope data for routing (Svensk & Sena, 2011).

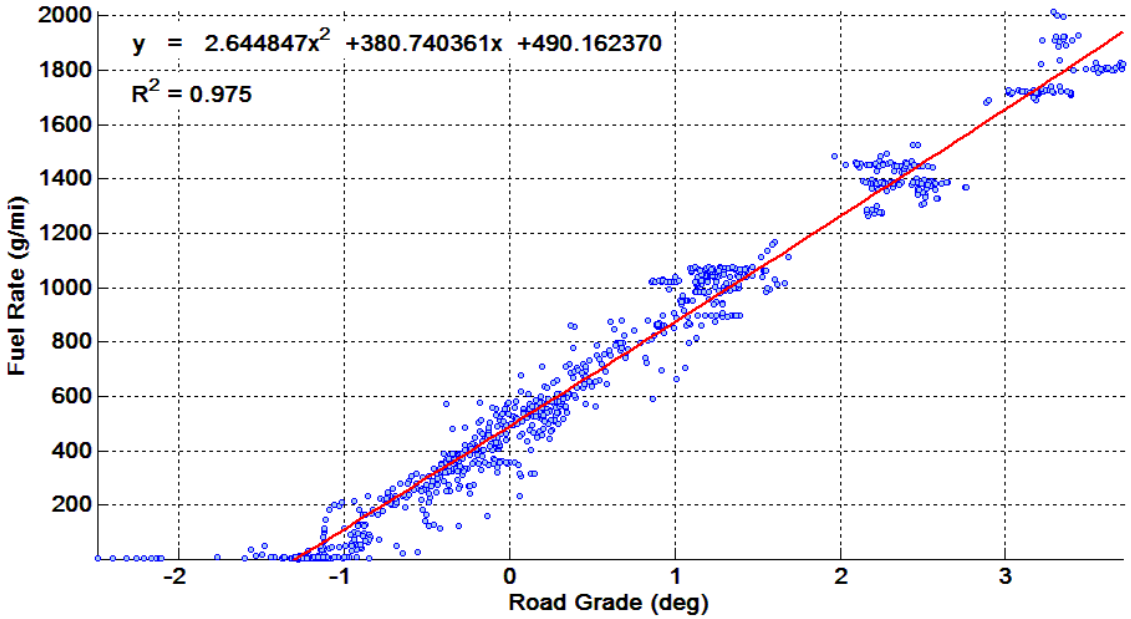

Figure 4-2 HDD fuel consumption as a function of road grade for zero acceleration activity at speeds greater than 10 mph.

Road Grade and Speed

It is also important to note that truck speed is correlated with grade. An analysis of over 57 hours of MEL test data, Figure 4-3, shows that the majority of high speed HDD driving in the data set occurs at negative grades. This is an important point to consider when limiting high-speed truck driving in order to reduce emissions (Scora, 2010). According to the American Trucking Association (ATA), a truck traveling at 75 mph consumes 27% more fuel than a truck traveling at 65 mph and bringing the speed limit for trucks down to 65 mph would save 2.8 billion gallons of diesel fuel over 10 years (ATA, 2011). The results in Figure 4-3 indicate that fuel savings may be significantly less than projected once grade is considered. There may even be a fuel

penalty in certain situations if trucks on a downgrade are required to brake to maintain a speed limit.

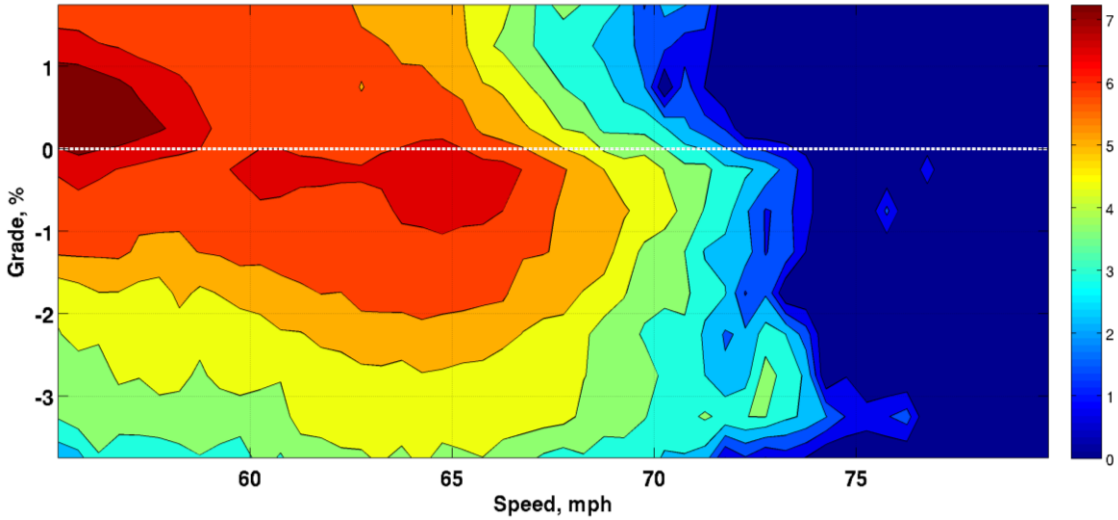

Figure 4-3 HDD vehicle speed activity by grade for over 57 hours of data (Scora, 2010).

To examine the effects of grade on fuel use in HDD further, the HDD microscale model was used. Figure 4-4 shows regression lines for simulated CO_2 emission results as a function of average cycle speed for over 130 highway snippets modeled at various grades using the HDD microscale model. The highway snippets used represent more than 17 hours of test data. Figure 4-4 shows that the CO_2 modeling results at 0% grade have the best goodness of fit and that the goodness of fit generally decreases toward extreme negative and positive grades. According to Figure 4-4, the modeled CO_2 g/m relationship with speed also becomes more linear as grade increases. For the HDD vehicle and trailer weight used in the modeling scenario shown in Figure 4-4, the minimum gram per mile emission rate occurs around 40 mph for 0% grade and closer to 55 mph for -6% grade. Figure 4-4 also shows that at larger negative grades, the emission penalty at high speed

driving beyond the point of minimum CO_2 g/m emissions is generally much less than at lower grades.

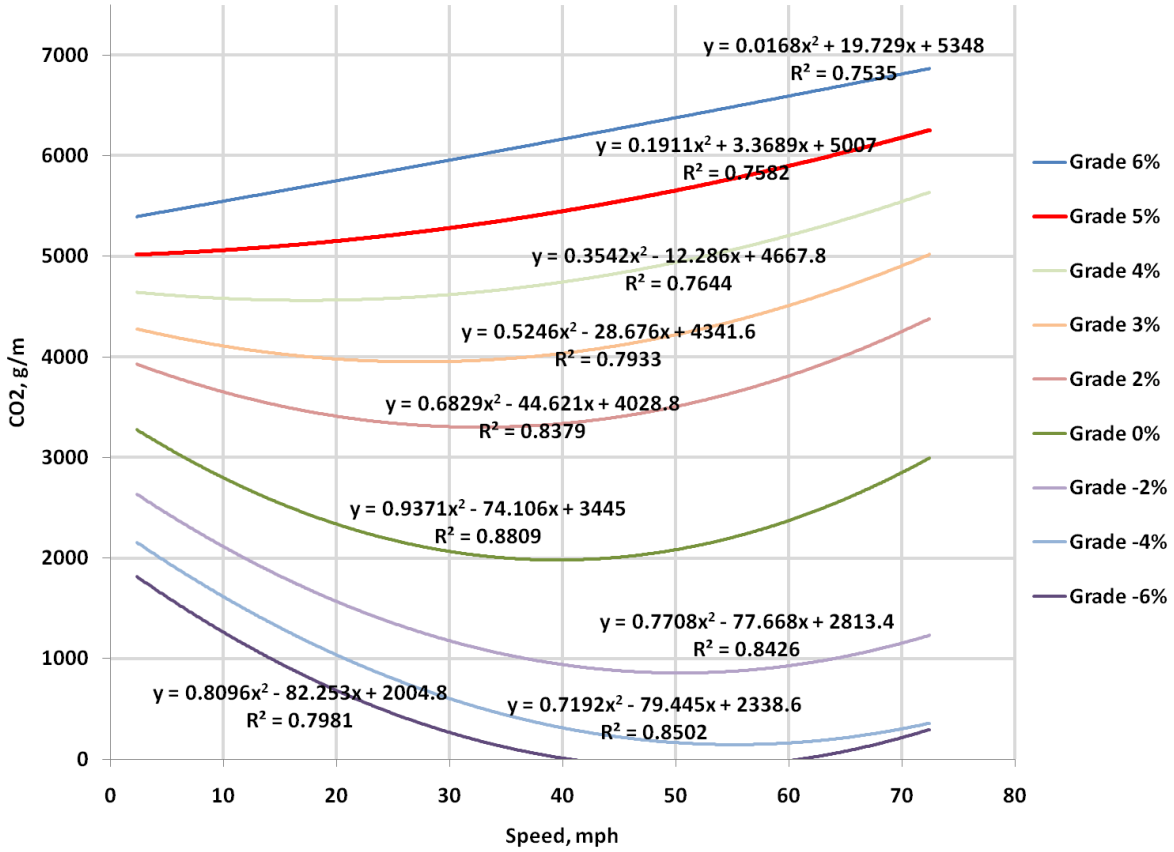

Figure 4-4 Microscale modeled CO_2 emissions as a function of speed for various grades

Road Grade Measurement

In many cases, road grade can be obtained from a transportation agency or third party graphical Information Systems (GIS) provider such as NAVTEQ (NAVTEQ, 2011). Without access to known road grade, road grade measurements can be performed in a number of ways with varying accuracy. Direct measurement using surveying tools is the gold standard, but this method is time consuming and cannot be applied easily or

safely especially for congested roadways. Other methods for estimating grade include the use of LIDAR (Light Detection and Ranging) data and the use of GPS (Global Positioning System) data (Zhang & Frey, 2005). The primary issue when using GPS data for road grade estimation is accuracy. Standard GPS receivers available commercially generate latitude, longitude and elevation data, but have limited accuracy, especially in the vertical direction. This method is not ideal for road grade estimations for emission analysis. Improved accuracy can be accomplished using carrier-phase differential techniques which incorporate a base station and position corrections (Farrell, Givargis, & Barth, 2000).

MEL records conventional GPS data along with vehicle and emission data. The collected GPS data stream is useful for vehicle positioning within five meters; however, relative elevation data from one second to the next is generally much more accurate. Separate from the MEL GPS measurements, CE-CERT's has an instrumented vehicle equipped with a carrier-phase differential GPS receiver that has collected data along many of the major routes and testing areas in Southern California. This high positioning accuracy GPS data (approximately 10 centimeters positioning accuracy) is post processed and provides elevation and grade information (Farrell, Givargis, & Barth, 2000). The MEL GPS dataset can be matched to the more accurate road grade data collected by carrier-phase differential GPS through map matching of the latitude and longitude coordinates.

4.2.3 Vehicle Weight

Vehicle weight is another important factor that influences HDD truck fuel consumption and emissions. The range of possible truck weights is roughly between 11,000 lbs. to 80,000 lbs. A truck tractor without a trailer can weigh as little as 11,000 lbs. depending on the truck and the federal weight limit for on-road HDD trucks is 80,000 lbs. without special permits. The MEL facility weighs approximately 44,360 lbs. and the HDD tractors tested typically weigh between 15,000 to 19,000 lbs. This puts most of the on-road MEL test weights between 59,000 and 63,000 lbs. On-road MEL testing is therefore limited to weights above 59,000 lbs. due to the weight of the MEL facility. Also, space limitations make adding weight to the MEL facility for on-road testing difficult. Various weight configurations can, however, be tested by MEL using CE-CERT's HDD chassis dynamometer. This usually requires on-road coast down testing with the test vehicle prior to chassis dynamometer testing in order to calibrate the dynamometer to reflect the vehicle's true road load. The calibration process ensures that the dynamometer absorbs the proper load to simulate various real-world power losses such as aerodynamic drag, tire rolling resistance, bearing losses, brake drag, transmission losses, and losses related to drivetrain inertia. Researchers at West Virginia University have demonstrated that dynamometer calibration can also be performed using simulated data (Wang, Lyons, Clark, & Luo, 1999). To date, the MEL data set contains limited test data to compare vehicle emissions at varying weights and the MEL data set contains no data which includes the combined effects of varying weight and grade. To simulate how

fuel consumption and emissions vary under various configurations of weight and grade, the HDD emission model was utilized and the simulated data is discussed in Section 4.4.

To examine CO_2 emissions variances with weight alone, the HDD microscale emission model was run for roughly 130 highway snippet cycles with varying weight and the results are presented in Figure 4-5. The data suggests that the effect of vehicle weight is greater at moderate average speeds with the effect decreasing at very low average speeds and very high average speeds. This is in line with the idea that at low speeds road friction plays a large role and that at higher speeds aerodynamic drag becomes an increasingly more important factor. Figure 4-5 also shows that as truck weight increases, the range in CO_2 emissions across all speeds for that weight decreases and that across all weights, CO_2 emissions are lowest at moderate average speeds and highest at low and high average speeds. The results in Figure 4-5 show that the optimal driving speed, where CO_2 g/m emissions are minimized, increases with increasing vehicle weight. For the modeled vehicle, the traveling speed at which CO_2 g/m are minimized is close to 23 mph when there is no additional trailer weight and closer to 45 mph with a large trailer weight of 64,000 lbs. This information is useful to modify truck driving behavior to maximize fuel economy.

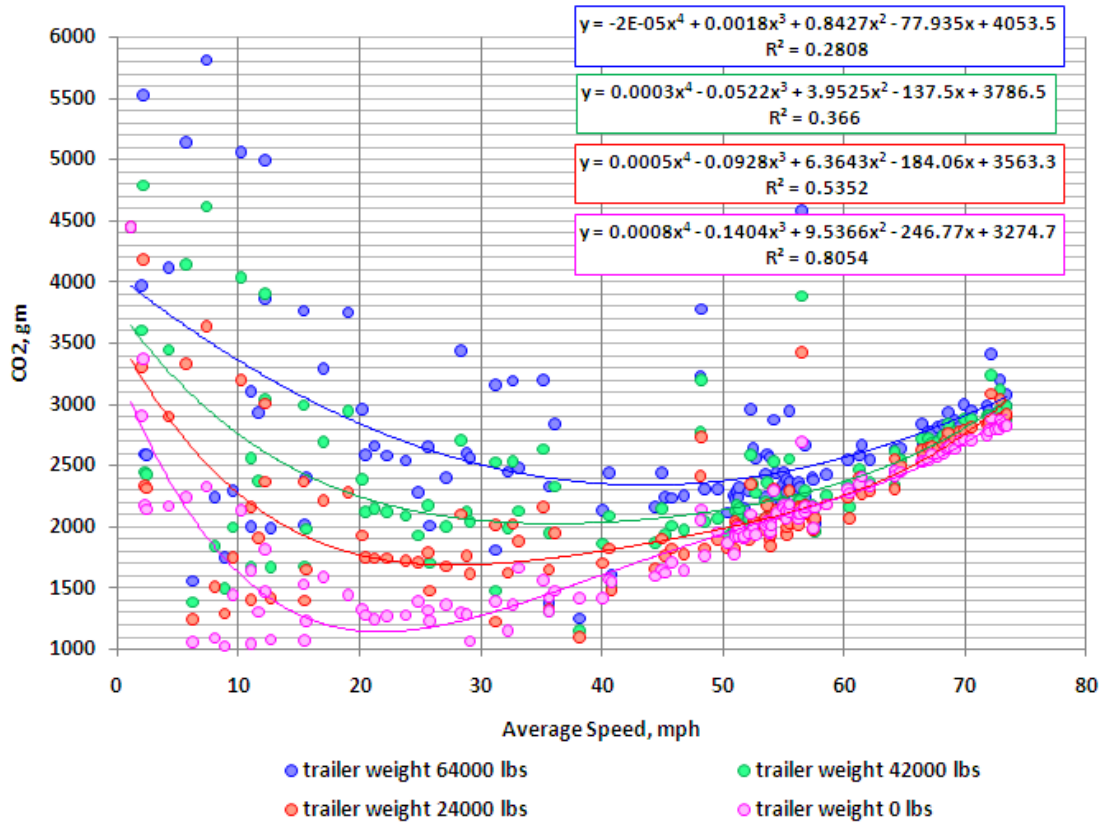

Figure 4-5 Modeled CO_2 emissions as a function of vehicle speed and vehicle weight.

4.2.4 Road Type and Congestion Level

The effect of congestion level indirectly accounts for the influence of acceleration on emissions. Free flow congestion level, for example, is characterized by higher speeds and milder acceleration and deceleration events, while higher congestion is characterized by lower speeds and more aggressive acceleration and deceleration events. The effect of road type is not as clear.

In order to determine the effect of road type on fuel use, roughly 130 highway snippets were identified ranging from a fraction of a mile in length to several miles. The

CO_2 emission factor versus average speed for these snippets was calculated and is presented in Figure 4-6 along with a second order polynomial regression line showing the CO_2 versus average speed emission curve. This same exercise was done for roughly 50 arterial snippets and the results are included in Figure 4-6. The results show that the CO_2 versus speed emission relationships look similar; it does, however, appear that at moderate speeds the arterial road types may show slightly higher emissions due to sharper stop-and-go activity. If this is true, this indicates that it is not enough to define CO_2 emission factors by average speed alone, but that some measure of driving pattern should be used. Further work is required to determine if CO_2 g/m emission rates truly differ by road type at comparable average speeds.

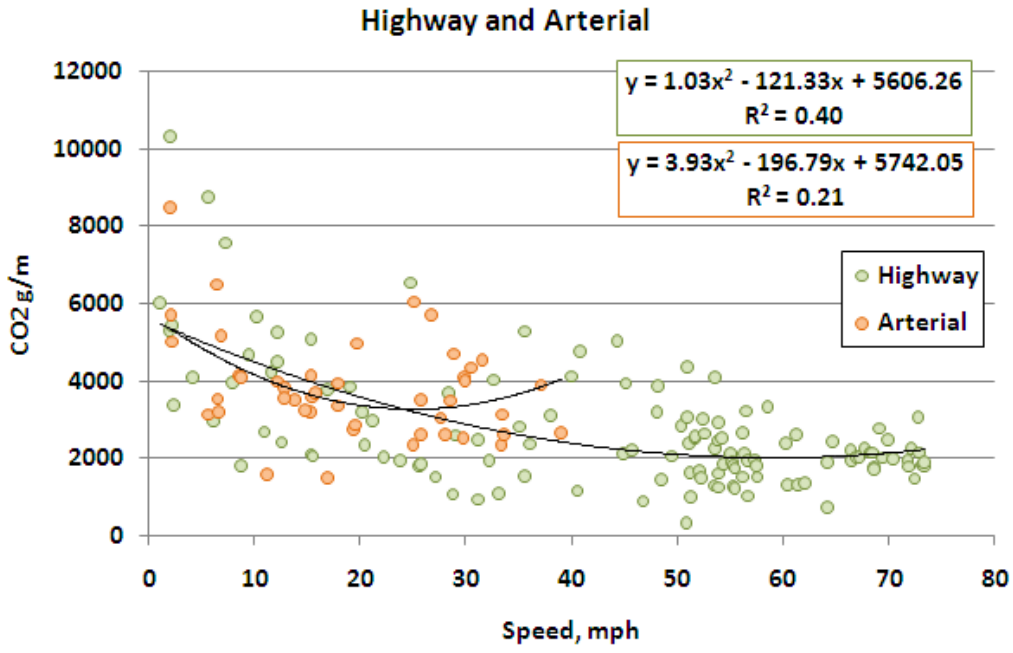

Figure 4-6 CO_2 emissions for highway and arterial driving snippets

4.3 Model Description

Several factors influence vehicle fuel consumption and emissions such as operational parameters, discussed in Section 4.2, and a vehicle's physical characteristics. This relationship is shown in equation 4.1.

$$mm_i \ \alpha \ \mathrm{f}(v, w, g, pc) \qquad 4.1$$

where:

mm = mesoscale model rate in g/m

i = fuel, CO_2, CO, HC, NO_x, PM

v = vehicle velocity

w = vehicle load

g = road grade

pc = physical characteristics of vehicle

The mesoscale model relates HDD energy and emissions with important operational parameters for a given vehicle. The operational parameters included are average velocity, road grade and vehicle load. A vehicle's physical characteristics such as aerodynamic shape, frontal area, and tire-road friction affect fuel use and emission production. These characteristics determine some of the major frictional forces that a vehicle encounters during real-world operation and are accounted for in the development of the modeling data set described in Section 4.4.

The mesoscale model fuel and emission model accounts for the input parameters described above, as well as interactions between these parameters. This is important

since, as the discussion and figures in Sections 4.2.2 and 4.2.3 indicate, the optimal truck speed for fuel consumption is not the same for every road grade or at every vehicle weight. The optimal speed for a truck with an empty container will be different than the optimal speed for the truck when it is fully loaded. Based on this, it may be best for this truck to use one route when carrying a load to a destination, and to use another route when returning empty.

To account for the interactions of multiple variables, Multiple Linear Regression (MLR) modeling is used. MLR modeling is discussed in Section 3.2.2. In MLR, a linear combination of multiple independent variables is used to predict a dependent variable. Although the combination of terms is linear, the terms themselves may be non-linear and include interaction terms such as equations 4.2 and 4.3.

$$Y_i = b_0 + b_1 v + b_2 v^2 + b_3 w + b_4 w^2 + b_5 g + b_6 g^2 + b_7 vw + b_6 vwg \ldots \quad 4.2$$

$$ln(Y_i) = b_0 + b_1 v + b_2 v^2 + b_3 w + b_4 w^2 + b_5 g + b_6 g^2 + b_7 vw + b_6 vwg \ldots \quad 4.3$$

where:

Y	= predicted energy and emission variables
i	= fuel, CO_2, CO, HC, NO_x, PM
v, w, g	= explanatory values such as velocity, weight, grade
$b_1, \ldots, b_n$	= regression parameters

The use of log data transformation, such as equation 4.3, is investigated. The log transformation is useful primarily if the residuals in the modeling results scale with increasing dependent variables and also to prevent the prediction of negative values.

4.4 Modeling Data Set

Calibration of the mesoscale model requires a comprehensive database covering all combinations of operational parameters. The MEL data set for a given vehicle does not provide this coverage and so a modeling data set is generated from on-road vehicle activity and the HDD microscale emission model developed in Chapter 0 for the test vehicle described in Section 3.3.3. Numerous vehicle activity snippets are identified from the MEL data set and are modeled under varying conditions using the microscale HDD emission model. Figure 4-7 presents a schematic for the development of the modeling data set.

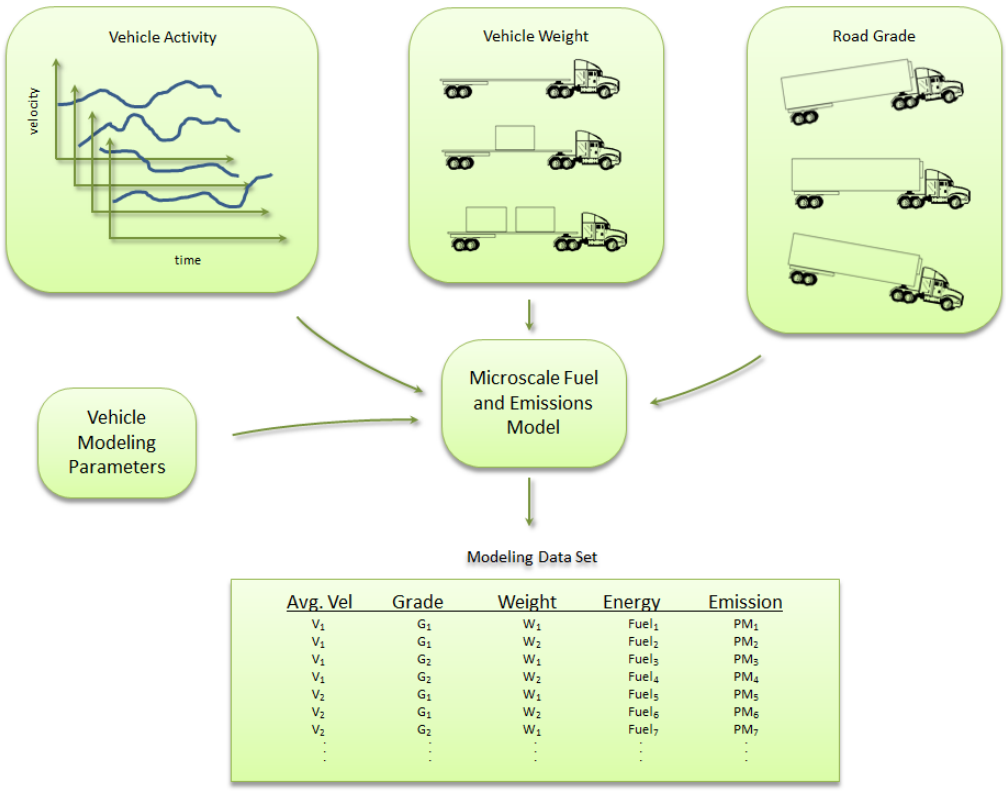

Figure 4-7 Schematic showing emission modeling data set development based on activity, vehicle weight and road grade.

The vehicle activity snippets used for the development of the modal data set are discussed in Section 4.4.1. The vehicle weight range that was modeled was 20,000 lbs. to 80,000 lbs. and the road grade range was -8 % to 8 %. Combinations of velocity, road grade and mass which exceeded the power threshold for the simulated vehicle were omitted from the modeled data set.

4.4.1 Vehicle Activity

The vehicle activity snippets used to generate the modeling data set for the development of the mesoscale model were taken from real-world truck highway activity from the MEL data set. Road type and congestion level were identified for much of the MEL data set using Google Earth, a spatial mapping tool. MEL data was processed into .kml files which mapped vehicle activity by location and colored vehicle activity by speed as illustrated by Figure 4-8 for a typical truck trajectory. In this figure, blue represents fast moving traffic and red represents slow moving traffic.

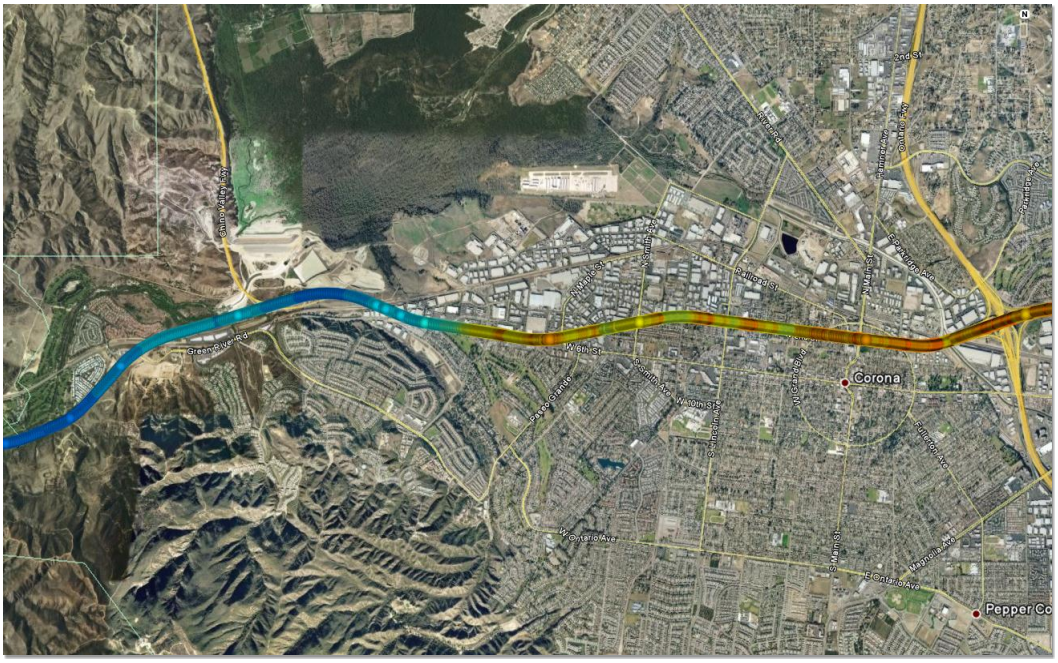

Figure 4-8 Example truck activity plotted in Google Earth. Red indicates congestion and blue indicates free flow.

Each data point in the .kml file, shown in Figure 4-8, contains specific trajectory information as well as source information. This allows the truck velocity trajectories to be examined and separated into different velocity snippets that represent different regimes of driving. The assumption is made that slow vehicle speeds on the freeway are a result of congestion. In Figure 4-8, the blue section of the trajectory represents uncongested freeway operation based on speed, and the yellow and orange parts of the trajectory represents stop-and-go congested highway traffic. Each velocity snippet and its associated data can be identified in this manner and separated out as depicted in Figure 4-9.

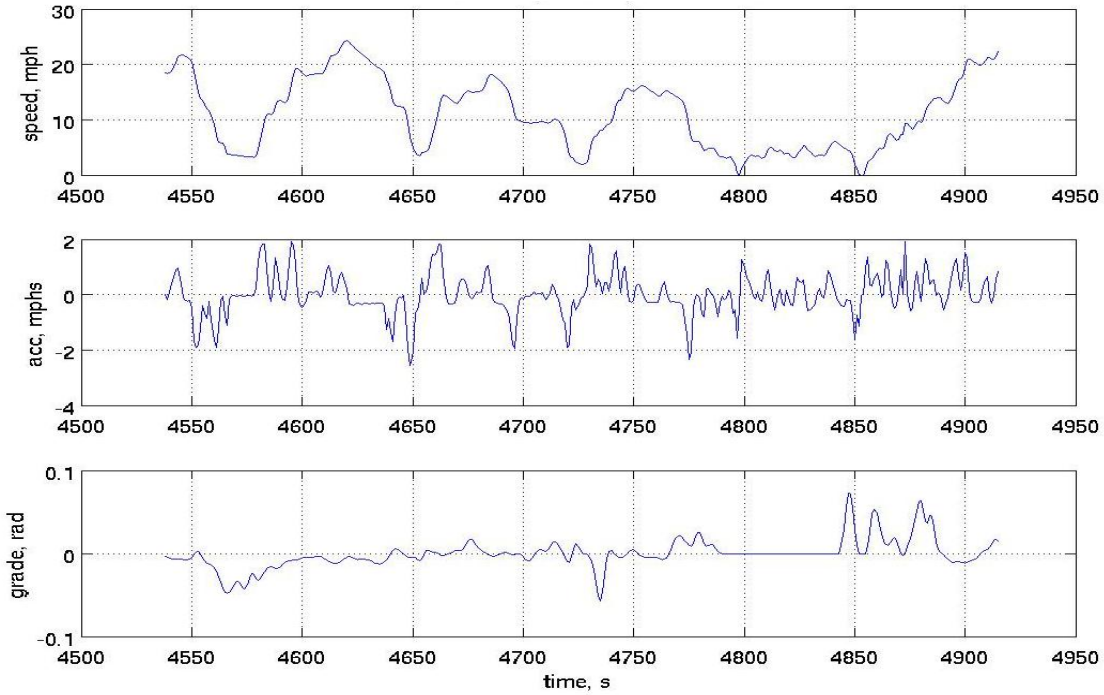

Figure 4-9 Example truck activity snippet.

The modeling data set consists of 158 snippets from highway driving under various levels of traffic congestion and covers a wide range of average speeds. The second-by-second velocity and acceleration distribution of the highway activity snippets is presented in Figure 4-10. Data for arterial roadways was also extracted from the data set and is presented in Figure 4-11. This data is reserved for validation purposes in Section 4.6. Data for the average velocities for the snippets is presented in Figure 4-12 and Figure 4-13.

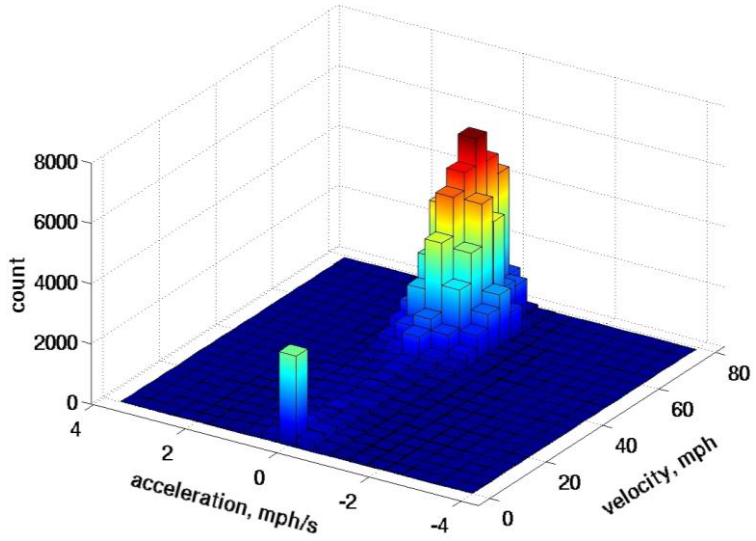

Figure 4-10 Distribution of activity in highway snippets excluding idle.

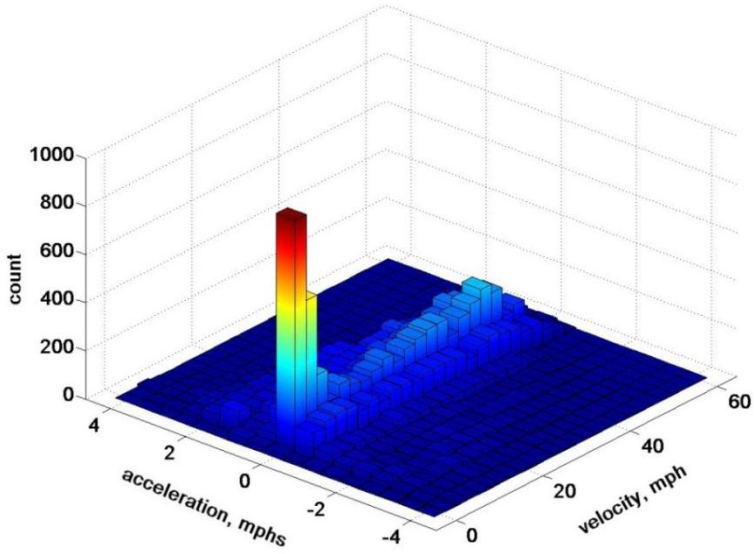

Figure 4-11 Distribution of activity in arterial snippets excluding idle.

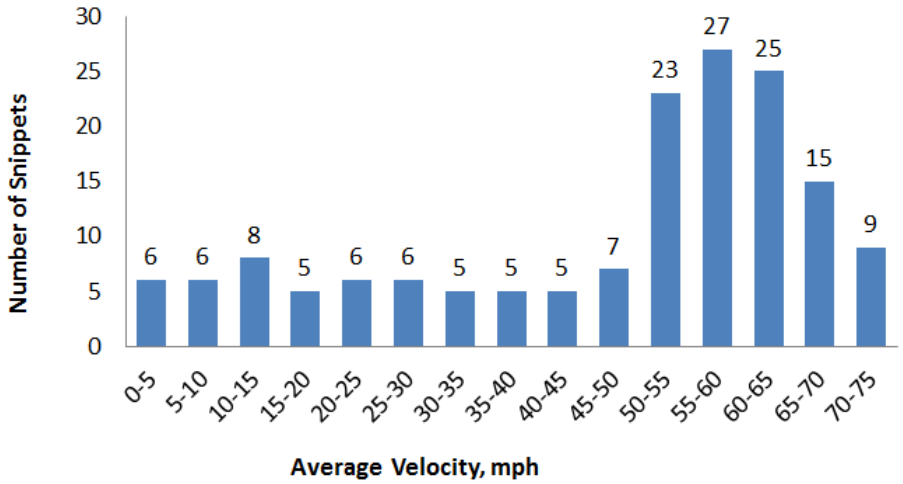

Figure 4-12 Average highway velocity snippet histogram.

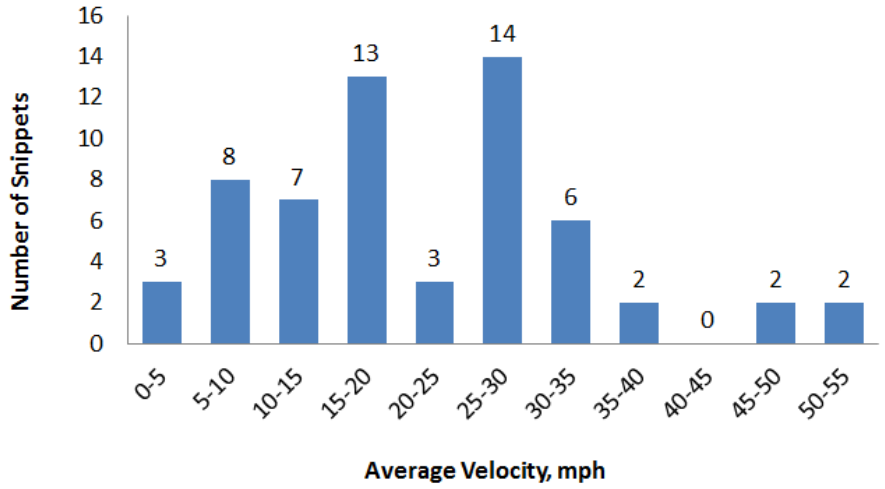

Figure 4-13 Average arterial cycle velocity histogram.

4.5 Model Development and Calibration

The mesoscale model is based on the MLR function presented in equation 4.2 and the modeling data set developed in Section 4.4. The modeling data set contains fuel use and PM data for over 3,800 combinations of average snippet velocity, grade and vehicle mass. This data is expanded to include all second and third order terms for these parameters and all possible interactions. This step increases the three independent terms to 63 terms. Initial analysis including fourth order terms found that they did not improve regressions, so fourth order terms were not considered in an effort to limit the complexity of the model.

Parameter fitting and calibration were performed using Matlab, discussed in Section 3.4, and R, a powerful and freely available statistical programming environment based on the "S" system developed by Bell Laboratories (Chambers, 2001). Regression analysis was performed using a stepwise regression method. Stepwise regression begins with an initial model and then adds or removes explanatory terms in a systematic way based on a measure of significance for that variable in the regression model. The preferred model characteristics were limited number of predictor terms and limited complexity. Since there are no constraints on the regression analysis, the resulting terms in the model were free to be non-hierarchical.

Regression results for a best model analysis for fuel and PM are presented in Figure 4-14 and Figure 4-15. These figures give the R^2 and RMSE values for the best model by the number of parameters included, not including the intercept. Figure 4-14

shows that roughly 90% of the variance in the fuel value is explained with 6 parameters and that improvements in R^2 and RMSE are slight beyond that. Figure 4-15 shows that with 6 parameters, the PM model has made its greatest gains in explanatory power (R^2 = 0.84), however incremental improvements in both R^2 and especially RMSE can still be had up to 9 or 10 parameters. It is important to note that the best model selection is not simply the addition of the next best parameter to the previous parameter set as in the step up approach and that higher number of parameter models may not include the same parameters used in lower number of parameter models.

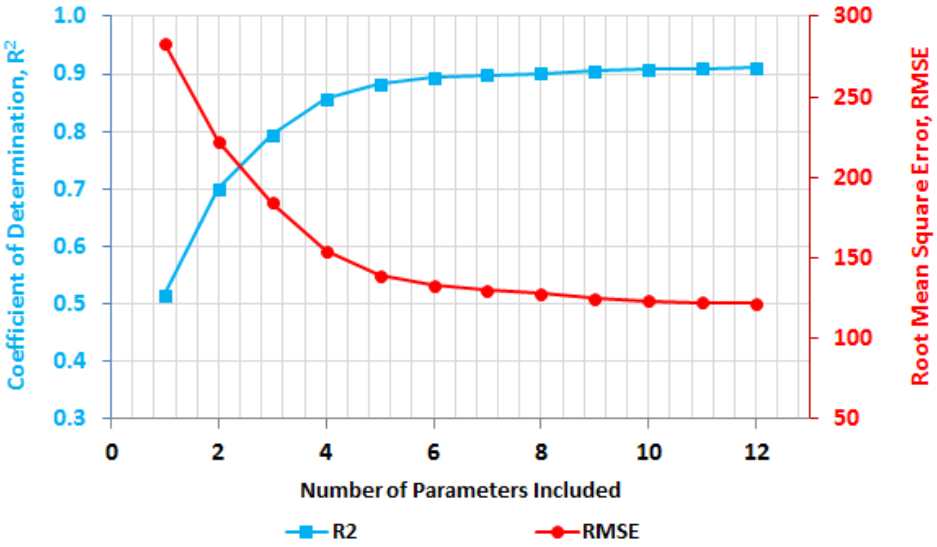

Figure 4-14 Regression statistics for best mesoscale fuel model based on number of predictor variables.

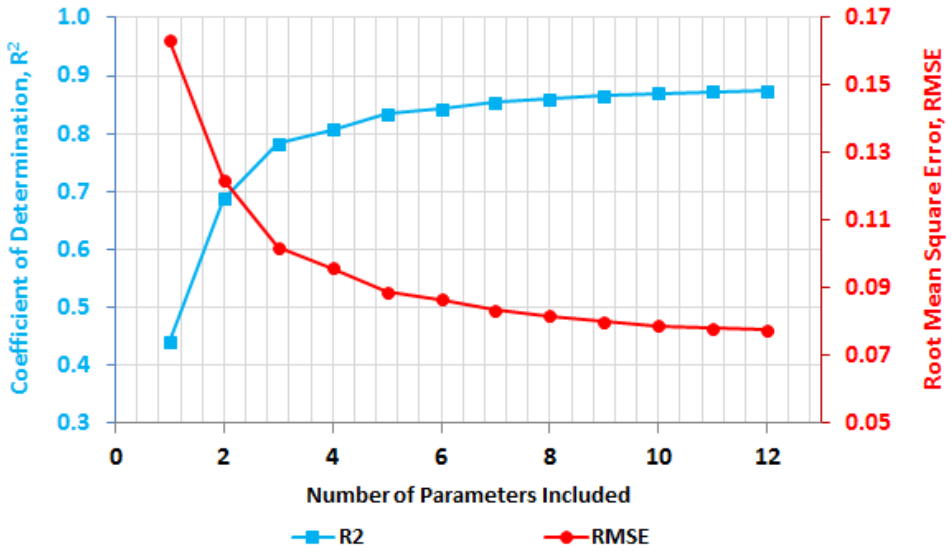

Figure 4-15 Regression statistics for best mesoscale PM model based on number of predictor variables.

Specific results and coefficients for the best fit models can be found in Table 4-1 through Table 4-4. For modeling work performed here and in Section 5.3, the 6 parameter fuel model and the 7 parameters PM model were chosen.

Table 4-1 Fuel models and coefficients for 1 to 6 parameters.

Number of Variables	1	2	3	4	5	6
R^2	0.516	0.701	0.794	0.856	0.883	0.893
RMSE	283.18	222.57	184.53	154.22	139.17	133.10
Intercept	638.36	937.74	850.48	457.13	624.90	747.25
g	9.3574E+01	7.7572E+01	1.2668E+02			3.2093E+01
g^2			9.1316E+00			
$g^2 \cdot m \cdot$				3.1536E-04	3.0007E-04	2.7834E-04
g·m				3.9707E-03	3.8187E-03	2.9933E-03
m				1.1120E-02	1.0689E-02	7.7958E-03
v		-8.3763E+00	-7.2986E+00	-6.8820E+00	-2.0064E+01	-2.0383E+01
v^2					1.7500E-01	1.8056E-01

Table 4-2 Fuel models and coefficients for 7 to 12 parameters.

Number of Variables	7	8	9	10	11	12
R^2	0.898	0.902	0.906	0.908	0.909	0.910
RMSE	130.21	127.71	125.02	123.36	122.57	121.88
Intercept	836.64	865.55	1015.77	931.67	890.49	764.58
g	3.3553E+01	4.1821E+01	8.5507E+01	5.2914E+01	5.9713E+01	4.5136E+01
$g^2 \cdot m \cdot$	2.7238E-04	2.3751E-04			1.4858E-04	2.5492E-04
$g^2 \cdot m^2$			4.9433E-09	4.5514E-09	2.4535E-09	
$g^3 \cdot m^2$			3.0773E-10		2.6779E-10	
$g^3 \cdot m^3$				4.0000E-15		
g·m	2.9051E-03	2.7023E-03		2.1341E-03	1.9504E-03	3.0063E-03
$g \cdot m^2$			2.3840E-08			
m	7.5038E-03	7.5497E-03	4.0617E-03	6.2097E-03	6.3523E-03	1.0214E-02
v	-3.3264E+01	-3.3226E+01	-3.4309E+01	-3.3619E+01	-3.2287E+01	-2.6510E+01
v^2	5.9208E-01	5.7951E-01	5.6989E-01	5.7195E-01	5.5756E-01	5.0073E-01
$v^2 \cdot g$						2.4531E-02
$v^2 \cdot g^2$		6.8252E-04				3.1429E-03
v^3	-3.5740E-03	-3.6514E-03	-3.4405E-03	-3.4525E-03	-3.3404E-03	-2.7122E-03
$v \cdot g^2$				9.4454E-02		
$v \cdot g^2 \cdot m$						-5.1466E-06
$v \cdot g^3$			-1.1415E-02		-9.5181E-03	
v·g·m						-5.6933E-05
v·m						-1.7325E-04
$v \cdot m^2$				-5.2266E-10	-4.7786E-10	

Table 4-3 PM models and coefficients for 1 to 6 parameters.

Number of Variables	1	2	3	4	5	6
R^2	0.439	0.688	0.782	0.807	0.834	0.842
RMSE	0.164	0.122	0.102	0.096	0.089	0.087
Intercept	0.323416	0.509514	0.608382	0.264766	0.396507	0.501771
g	4.636E-02	3.641E-02	6.731E-02			4.120E-02
$g^2 \cdot m$				1.341E-07		
$g^2 \cdot m^2$					1.546E-12	1.522E-12
$g \cdot m$				1.826E-06	1.744E-06	
$g \cdot m^2$						1.701E-11
m				5.874E-06	4.779E-06	
m^2						4.723E-11
v		-5.207E-03	-8.804E-03	-4.515E-03	-7.092E-03	-7.422E-03
$v^2 \cdot g$						-8.818E-06
$v^3 \cdot g$					-1.115E-07	
$v \cdot g$			-9.373E-04			

Table 4-4 PM models and coefficients for 7 to 12 parameters.

Number of Variables	7	8	9	10	11	12
R^2	0.854	0.86	0.866	0.87	0.872	0.874
RMSE	0.084	0.082	0.08	0.079	0.078	0.078
Intercept	0.556381	0.423301	0.34293	0.342284	0.3257	0.341431
g	4.601E-02	5.346E-02		2.610E-02	3.333E-02	2.903E-02
$g^2 \cdot m$				1.021E-07	1.084E-07	1.024E-07
$g^2 \cdot m^2$	1.439E-12	1.271E-12	1.700E-12			
$g \cdot m$			2.075E-06	1.529E-06	1.376E-06	1.491E-06
$g \cdot m^2$	1.592E-11	1.292E-11				
m		5.414E-06	7.303E-06	6.963E-06	7.085E-06	7.036E-06
m^2	4.399E-11					
v	-1.267E-02	-1.090E-02	-7.516E-03	-5.112E-03	-2.927E-03	-7.177E-03
v^2	7.616E-05	7.462E-05				
$v^2 \cdot g^3$					-6.305E-08	
v^3			5.773E-07	5.424E-07		5.365E-07
$v^3 \cdot m$					9.009E-12	
$v \cdot g$	-5.672E-04	-6.650E-04				-4.020E-04
$v \cdot g^2 \cdot m$				-5.048E-09	-5.914E-09	-3.678E-09
$v \cdot g^2 \cdot m^2$			-9.200E-14			-6.100E-14
$v \cdot g^3 \cdot m$			-2.968E-10	-2.840E-10	-2.744E-10	-4.336E-10
$v \cdot g \cdot m$				-3.902E-08	-4.135E-08	
$v \cdot g \cdot m^2$			-7.490E-13			-7.170E-13
$v \cdot m$		-4.514E-08		-1.393E-07	-1.750E-07	
$v \cdot m^2$			-1.933E-12			-1.986E-12

The final models did not use log data transformation as presented in equation 4.3 and select cases do result in slight negative predications. Other than eliminating negative values, the log transform resulted in slightly lower regression fits and its use was not warrented. To account for negative values, a minimum cutoff point is selected. The cutoff point for the fuel model is 20 g/m and the cutoff point for PM is 0.035 g/m. The effect of this is negligible on the calibration and validation results.

Calibration results for the 6 parameter fuel model and 7 parameter PM model are presented in Figure 4-16 and Figure 4-17. The calibration results for the fuel model show a good fit with and R^2 of 0.89 and an RMSE of 133 g/m. The calibration results for PM also show a good fit with and R^2 of 0.85 and an RMSE of 0.08 g/m.

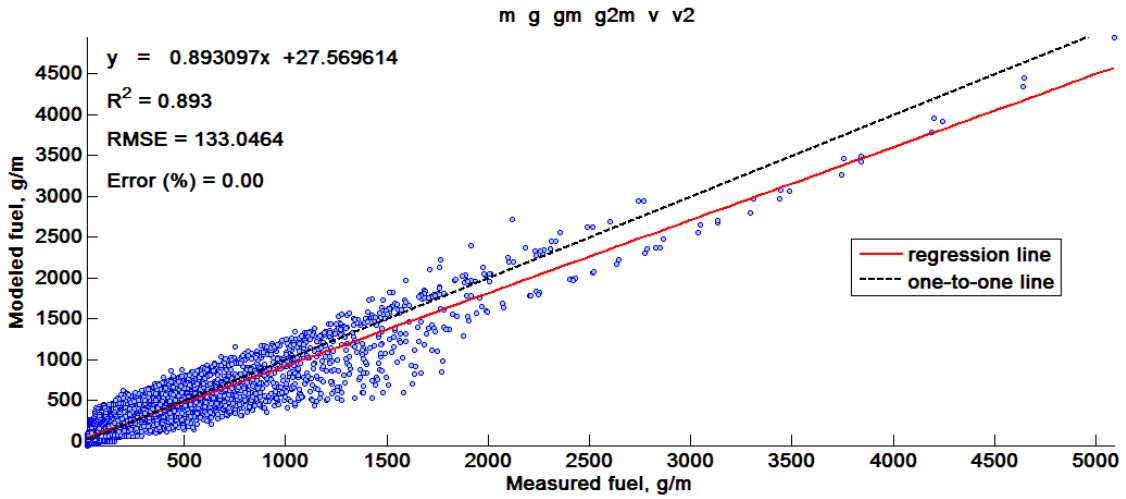

Figure 4-16 Parity plot for 6 parameter fuel model on calibration data set. Red line is one-to-one.

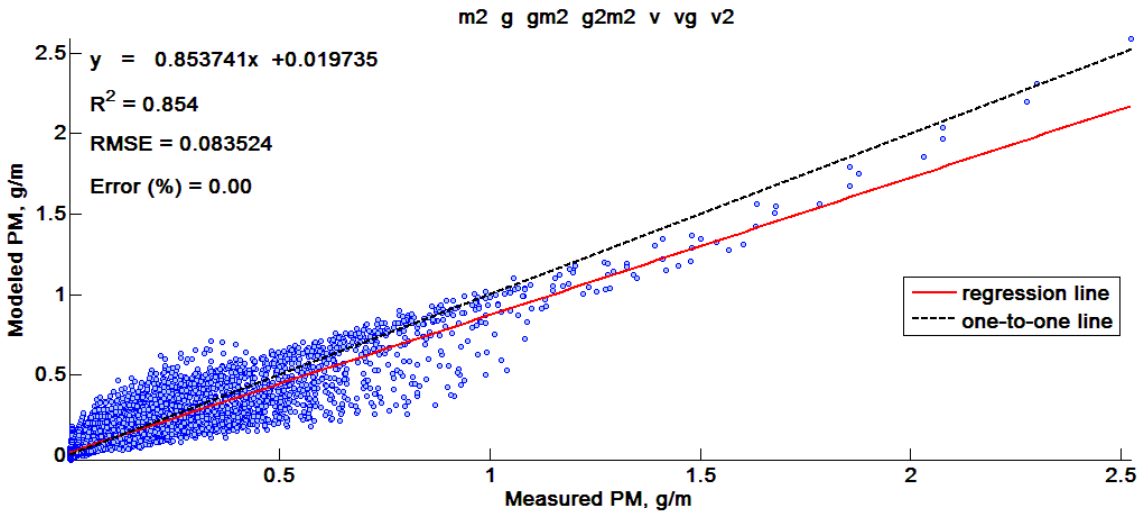

Figure 4-17 Parity plot for 7 parameter PM model on calibration data set. Red line is one-to-one

It is important to note that the regression results are dependent on the vehicle activity snippets used to generate the calibration and validation data set. The vehicle activity snippets for the calibration data set are exensive and range roughly from one tenth of a mile to over 30 miles in length. Reducing the vehicle activity snippet lengths typically reduces the variability in the vehicle speed distribution and it was found that regression results improve for both the fuel and PM model.

4.6 Validation

Validation of the mesoscale model was performed on the arterial data set presented in Section 4.4.1 using the 6 parameter fuel model described in Table 4-1 and the 7 parameter PM model described in Table 4-4. The arterial data set is independent of the highway data set that was used for calibration of the mesoscale model parameters. The results for fuel show no difference in R^2 (R^2 = 0.89) and an increase in RMSE from 133 g/m to 198 g/m. The results for PM show no significant decrease in R^2 (R^2 = 0.85) and an increase in RMSE from 0.084 g/m to 0.14 g/m.

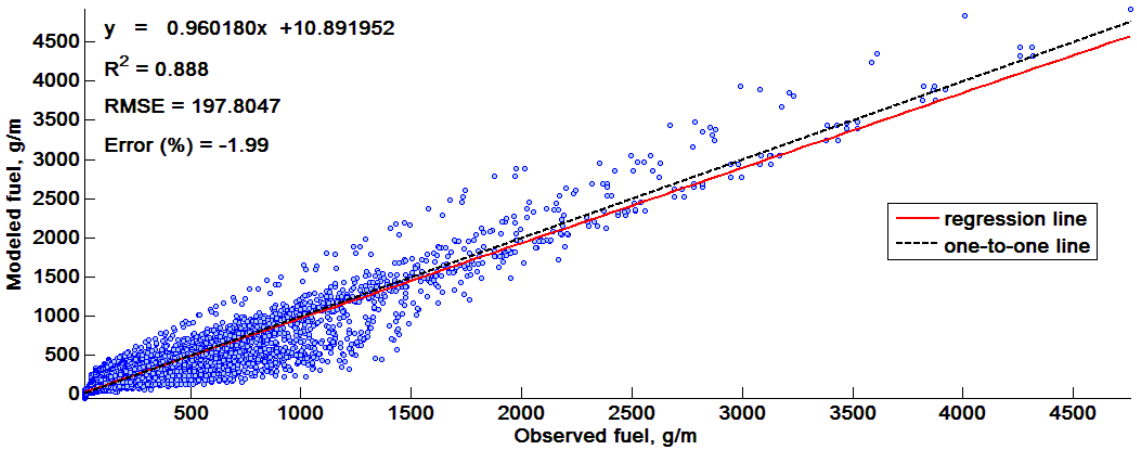

Figure 4-18 Parity plot for 6 parameter fuel model on arterial snippets.

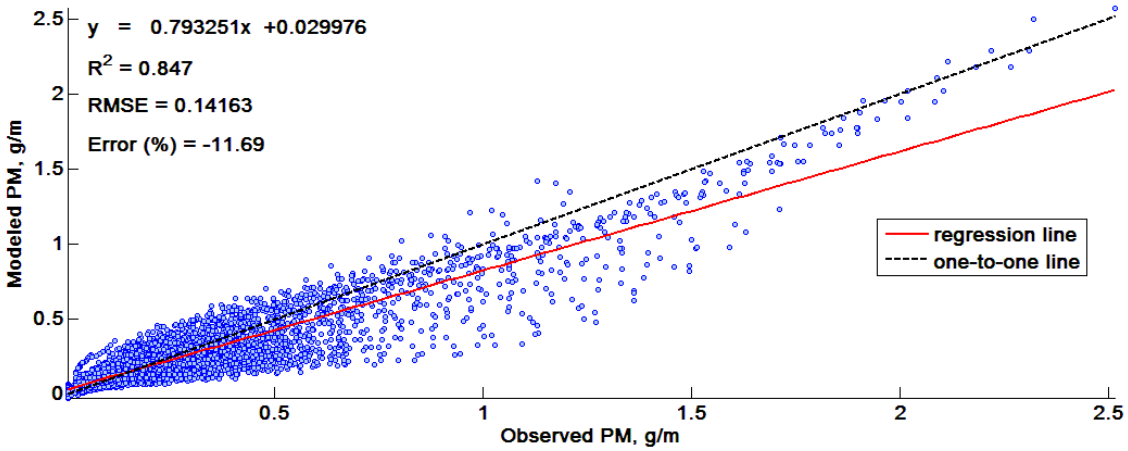

Figure 4-19 Parity plot for 7 parameter PM model on arterial snippets.

4.7 Section 4 Summary

This section presented the development, calibration and validation of the mesoscale model for a HDD vehicle. In order to develop the model, a unique modeling and validation data set was created based on a broad range of conditions using the microscale model and measured vehicle activity.

The mesoscale model is an MLR model based on average vehicle speed, road grade and vehicle load. These terms were tested in many combinations to account for higher order effects and interactions. Stepwise regression methods were used to determine several best models by number of parameters. Final models based on 6 terms for fuel use and 7 terms for PM were selected and validated.

The explanatory variables which the mesoscale model is based on are important operational parameters that greatly impact fuel use and emissions. Relationships between these parameters, fuel use and emissions were demonstrated with simulated data and

discussed in this section. The mesoscale model is integrated with an EFNav application for route optimization in Chapter 5.0.

Currently, the model does not account for road type or congestion level directly. The road type variable, although available, did not provide a discernible effect in our data set. The effects of congestion level are accounted for to a large extent by average speed, however if a parameter for congestion level is available, including it as an explanatory variable or splitting the model up by congestion level may improve the modeling fits. Validation results on the independent set of arterial snippets through a wide range of weights and grades show fuel prediction error to within 2% of the target value and PM prediction error to within 12% of the target value, with R^2 values of 0.89 to 0.85 respectively.

5.0 Environmentally Friendly Navigation with Developed Mesoscale Model

Environmentally friendly navigation for heavy-duty trucks (EFNav-HDT) has many potential benefits. The key objective of EFNav is to optimize vehicle routing in order to minimize vehicle fuel consumption, vehicle emission production, human exposure to vehicle emissions, or other negative environmental effects. The purpose of this portion of work is to demonstrate the use of the mesoscale HDD emission modeling tool in an EFNav system.

The framework for the EFNav system was developed in previous work with light duty vehicles by CE-CERT's Transportation Systems Research (TSR) group (Barth, Boriboonsomsin, & Vu, 2007). The EFNav system performs route selection based on algorithms that minimize some type of cost function for a link-node roadway network. A classical solution to the route optimization problem in a link-node network is given by Dkjkstra's algorithm (Chabini & Lan, 2002), however more efficient algorithms exist (Ghiani, Guerriero, Laporte, & Musmanno, 2003) (Frazzoli & Bullo, 2004). The work presented here does not focus on the improvement of these algorithms, but rather on the improvement of the cost functions which are used by these algorithms. The typical cost functions for routing are based on distance or time. In this work the focus is on reducing fuel use based on the combination of the operational parameters of weight, grade and the average speed on the link (Ahn & Rakha, 2007). The following sections describe the

general EFNav methodology, the application of the mesoscale emission model and initial in-use test results.

5.1 EFNav Dynamic Roadway Network

The EFNav application consists of several components: (1) a digital dynamic roadway network with grade and integrated real-time traffic information as available; (2) link weighting factors or cost functions; (3) routing and optimization algorithms; and (4) a user interface for receiving user defined origin and destination inputs as well as for displaying route selection, energy and emission estimates, and various outputs. The basic function of the EFNav application is described here briefly.

EFNav relies on the Dynamic Roadway Network (DynaNet) which was developed by CE-CERT for the Bay Area and Southern California (Boriboonsomsin, Barth, Zhu, & Vu, 2010). Current research efforts are focused on expanding this network to the entire state of California. DynaNet consists of several layers of information that are fused together in a MySQL database including roadway characteristics such as link length and link grade, as well as real-time or historic data from multiple sources for roadway speed, traffic conditions, etc. The primary source for the real-time traffic information is from California's Freeway Performance Measurement System (PEMS, see (Chao, Jia, Petty, Shu, Skarbardonis, & Varaiya, 2000)) and the traffic information provider, INRIX (INRIX Inc., 2011). Truck speed in the network is estimated as 82% of the general traffic speed (Boriboonsomsin, Zhu, & Barth, 2011). Certain parameters that

impact fuel use and emissions, such as vehicle acceleration, are not directly available for roadway links and cannot be used for fuel or emission estimation directly.

The network data including real-time roadway information are used to calculate cost factors for each link in the network. Based on user defined origin and destination points as well as the calculated cost factors applied to each link, the EFNav application will calculate the optimal route for minimizing the route cost using existing route planning network-wide routing algorithms. The optimized route information, along with trip characteristics such as fuel use and estimated emission production are displayed to the user through the user interface.

5.2 EFNav Interface

CE-CERT's EFNav application is a research tool that has been developed for multiple platforms including the iPhone, the Android operating system and as a web application. For this research, the EFNav web application was configured for HDD routing using the mesoscale model fuel equation to update the network link cost factors based on real-time traffic velocity information as well as network grade and vehicle weight. The updated weighting factors are then used for route optimization.

Figure 5-1 shows the EFNav web application interface and route estimation for an example route, optimized for minimum fuel use, from the Port of Long Beach to the Fontana area in Southern California. The window frame on the left of the application allows the user to input origin and destination points by the latitude and longitude coordinates, and to select the criteria for minimization which includes time, distance, and

fuel. In some cases, optimizing by these criteria will route along similar paths since minimizing distance tends to minimize fuel and trip length. In cases with heavy congestion or steep road grades, the shortest distance path may no longer be the most economical. This is more of an issue as vehicle weight increases.

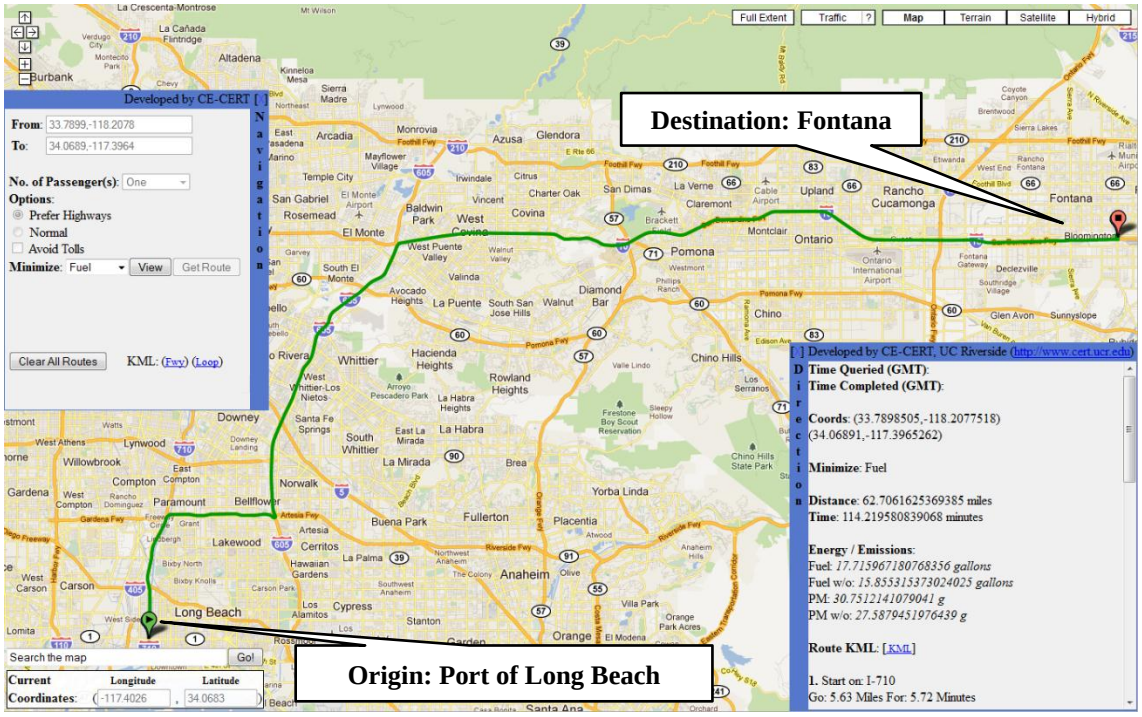

Figure 5-1 CE-CERT's EFNav web application interface.

The window frame on the right of the EFNav screen displays output results for route optimization including starting and ending coordinates, route minimization criteria, route length, estimated route travel time, estimated fuel consumption and estimated emission production, as well as route directions. The EFNav web application is built on the Google Maps web service and the user has access to several Google Map overlays such as real-time traffic, terrain, satellite and hybrid maps.

5.3 EFNav-HDT Application

This section describes the application of the EFNav-HDT in an example scenario. In this exercise, the mesoscale model is calibrated for a test truck, origin and destination points are chosen for routing, the EFNav-HDT route choice is calculated and the models performance in the EFNav application is evaluated.

5.3.1 Mesoscale Model Calibration

The mesoscale model fuel use model developed in Chapter 4.0 was recalibrated for the HDD truck used for the EFNav testing scenario. Data for the test truck, shown in Figure 5-2, is presented in Table 5-1.

Table 5-1 EFNav test vehicle details

Engine Make	Engine Model	Engine Displacement	Rated Power	Engine Year	Tractor Weight	Odometer	Test Location
-	-	liters	hp@RPM	year	lbs.	miles	
Caterpillar	C15	14.7	500	2,000	15,760	42,963	on-road

Figure 5-2 EFNav test vehicle image

The calibration of the mesoscale fuel model requires three basic steps outlined in Section 0. These steps are the calibration of the microscale model for the test vehicle, the development of a mesoscale modeling data set using the microscale model and the calibration of the mesoscale model on the modeling data set.

Microscale Model Calibration

The HDD microscale emission model was calibrated for nearly 2 hours of on-road test data to a total error of less than 1%. The results of the calibration process are presented in Figure 5-3 and show that the microscale model performs well on the calibration data with an R^2 of 0.95 and RMSE of 1.5 g/s. Figure 5-4 shows the results of the calibrated model on an independent data set of nearly 1 hour of on-road activity. The validation results show that model performs just as well on the validation data set. These results do not account for errors introduced by unknown conditions such as wind and varying road surfaces conditions.

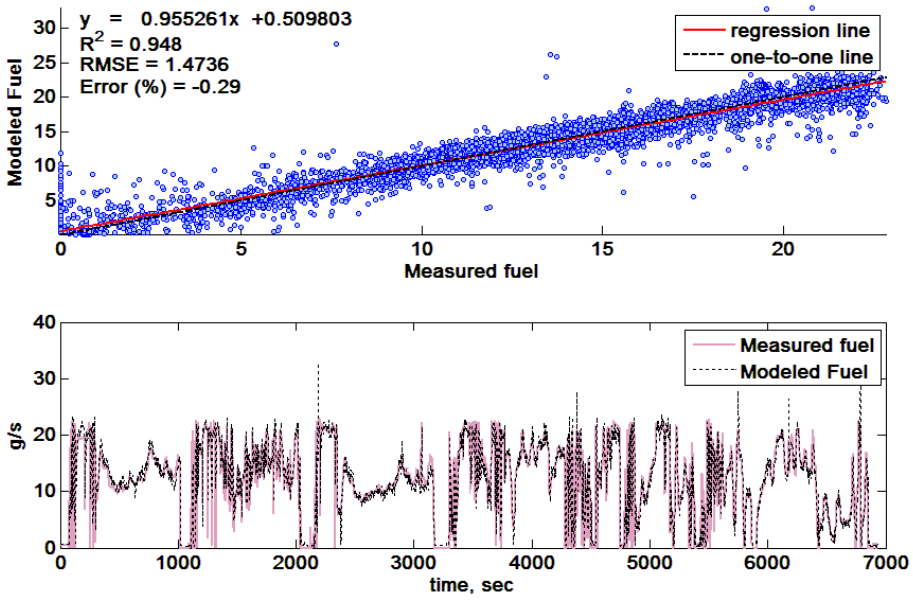

Figure 5-3 EFNav vehicle microscale model calibration results. Top plot presents scatterplot of modeled vs. measured second-by-second fuel use. Bottom plot presents time series of modeled vs. measured second-by-second fuel use.

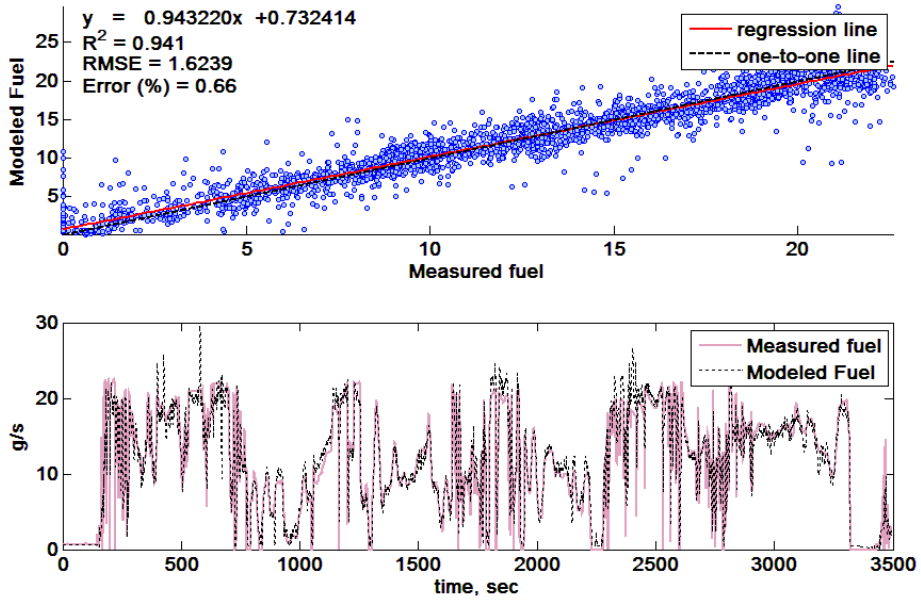

Figure 5-4 Microscale model validation results for EFNav vehicle. Top plot presents scatterplot of modeled vs. measured second-by-second fuel use. Bottom plot presents time series of modeled vs. measured second-by-second fuel use.

Mesoscale Modeling Data Set and Mesoscale Model Calibration

Mesoscale model calibration and validation modeling data for the test vehicle was created following the methodology presented in Section 0 using the vehicle activity snippets discussed in Section 4.4. Mesoscale model calibration results for the EFNav test vehicle are presented in Figure 5-5 which shows that the 6 parameter mesoscale fuel model developed in Section 0 predicts nearly 88% of the variance in the target fuel values with a RMSE of 155.5 g/m. Model parameters are presented in Table 5-2.

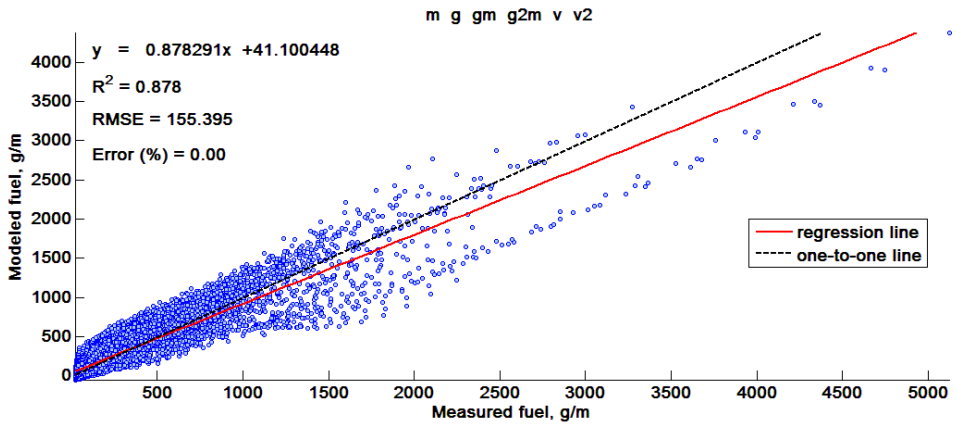

Figure 5-5 Parity plot of mesoscale model calibration results for EFNav vehicle.

Table 5-2 Mesoscale model coefficients for EFNav vehicle

Intercept	Minimum Fuel	m	g	g·m	g^2·m	v	v^2
7.14E+02	2.30E+01	9.82E-03	4.34E+00	2.86E-03	2.04E-04	-2.84E+01	2.82E-01

Results of the calibrated mesoscale model on the independent validation data are presented in Figure 5-6. The results show that the model performance remains similar to

that of the calibration data with an R^2 of 0.87 and an RMSE of 196.5. The total error across the validation data set was 2.02%.

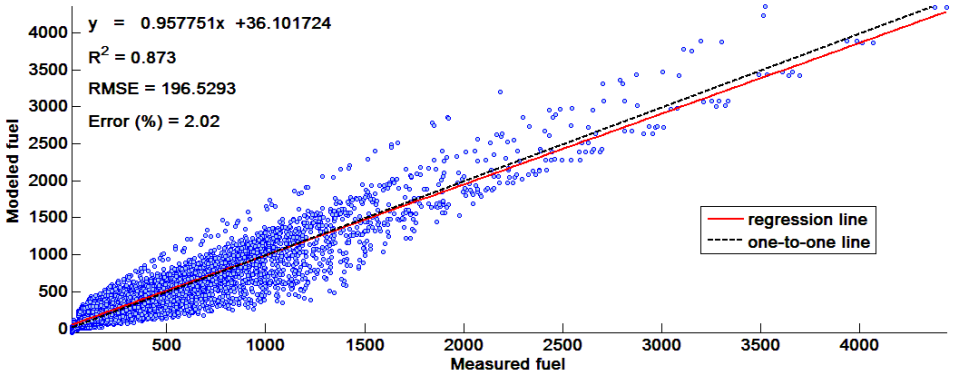

Figure 5-6 Parity plot of the mesoscale model validation results for EFNav vehicle.

As an additional point of comparison, the calibrated mesoscale model was applied to the summary parameters of the measured data used to calibrate and validate the microscale model. The results in Table 5-3 indicate that the model performs well in this exercise with an error of less than 8% for both data sets.

Table 5-3 The mesoscale model calibration and validation results for EFNav vehicle

	Length	Distance	Avg. Velocity	Avg. Grade	Measured Fuel	Mesoscale Model Fuel	Error
	seconds	miles	mph	%	g/m	g/m	%
Calibration Data Set	7012	119.9639	61.5902	0.1521	704.3179	648.35	-7.95
Validation Data Set	3509	60.8	62.36	0.0489	665.007	634.91	-4.53

5.3.2 Network Routes

The origin and destination points that were chosen for the EFNav test scenario were near the Port of Long Beach (POLB) by the I-710 and the city of Fontana California

on the I-10. The POLB is the second busiest port in the nation (Port of Long Beach, 2011) and is situated in close proximity to the Port of Los Angeles (POLA), ranked the number one port in the nation for the last 10 years. Combined, the POLB and the POLA are the 6th busiest port in the world (The Port of Los Angeles: America's Port, 2011).The I-710 highway leading away from the POLB is a major artery for truck traffic. The areas in and around Fontana California are home to numerous warehouses, distribution centers and small manufacturers, making it a popular HDD truck destination. There are various highway routing options between the ports and the Fontana area which make that origin/destination pair useful for EFNav route analysis.

5.3.3 Test Procedure and Results

The EFNav mesoscale model application was tested against measured data. A fuel minimized route from the POLB to Fontana was determined for a 72,000 lb. test truck using the web based EFNav mesoscale model application. The predicted route was based on real-time traffic data presented in Figure 5-1. The test truck described in Section 5.3.1 was weighted with a flatbed trailer loaded with six 7,800 lb. K-rails for a combined weight near 72,000 lbs. The test truck was instrumented with a specially developed data logger that records selected parameters at a frequency of 1 Hz from the truck's ECM following the J1939 vehicle bus standard. The data logger also collects streaming data from an attached GPS unit at each second.

Testing was performed on a weekday morning at 10:30 am on the predicted route from the POLB to Fontana. Comparison data for the test trip with measured data is

presented in Figure 5-7. Plot one in Figure 5-7 shows the comparison of the EFNav predicted speed and the measured speed for the test route by distance. The blue line in Figure 5-7 in the first plot shows the measured speed. The red line shows the general traffic speed for the route as available from the DynaNet database at the start of travel time and the green line shows the same real-time general traffic speed adjusted by 0.82 to estimate truck speeds (Boriboonsomsin, Zhu, & Barth, 2011). This comparison shows that in this case, the given speeds at the start of travel time were a good indicator of trip speeds throughout the test run with a few notable deviations. The EFNav application can be updated repeatedly to reroute based on more recent data, but for this analysis only the initial route was considered. The second plot from the top in Figure 5-7 shows the travel time comparison as a function of distance for the measured data and for the DynaNet data for the test route. This data shows that the time on the network is overestimated by almost 11 %. The rise in both the truck and general traffic travel time around the 30 mile mark are a result of the decrease in travel speed at that distance on the route.

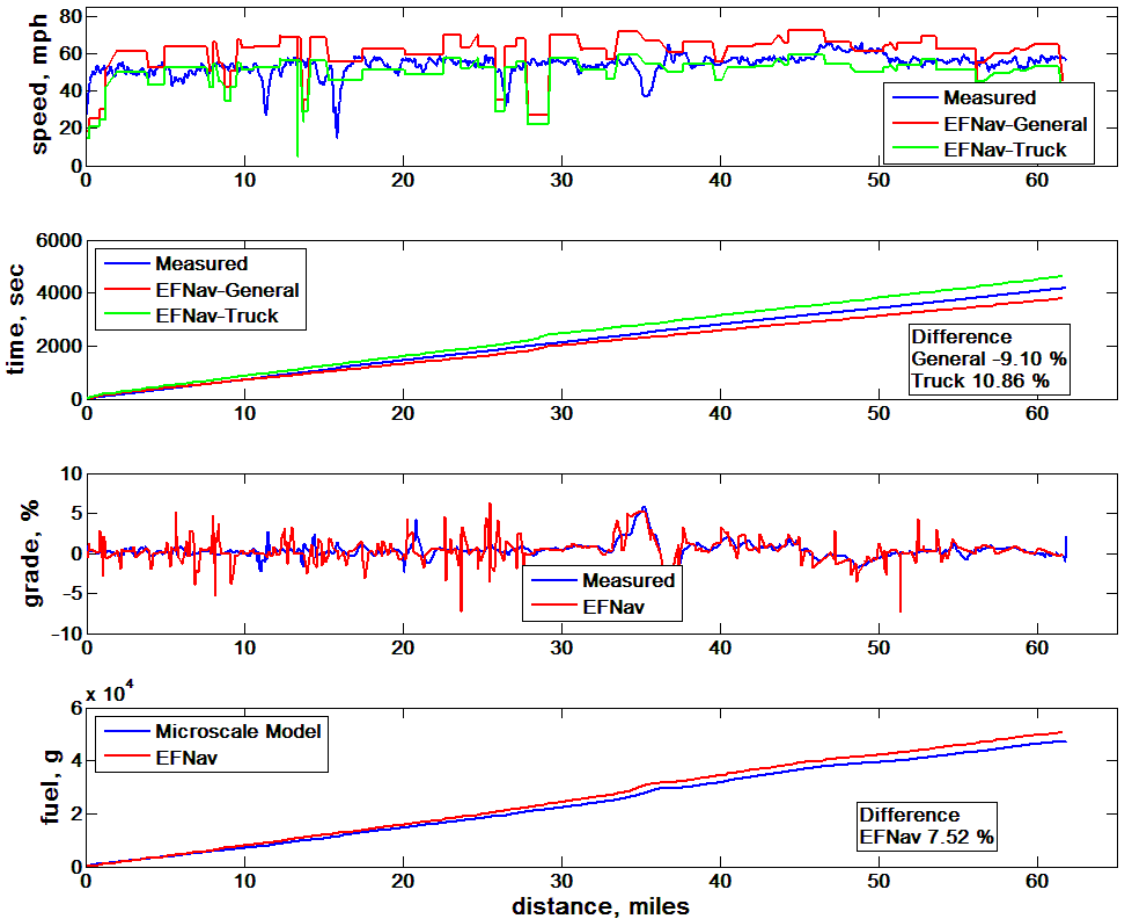

Figure 5-7 EFNav mesoscale model comparisons against measured data. 1) vehicle speed by distance; 2) travel time by distance; 3) road grade by distance; 4) fuel consumption by distance

A comparison of measured grade data and data from the DynaNet network are presented in the third plot in Figure 5-7 for reference. The grade data from the DynaNet network is the average grade on a link with links being anywhere from 25 feet to 1.2 miles in length. Measured grade is approximated from GPS data for every second. A comparison of predicted cumulative fuel consumption for the entire test route with measured data is shown in the fourth plot in Figure 5-7. This plot indicates that the EFNav application overestimates fuel use by about 7.5 % for the test trip in comparison

to the fuel calculation from the microscale model. This plot also shows that EFNav cumulative fuel consumption looks very similar in profile to the cumulative measured fuel consumption, showing similar sensitivity to grade along the route. The strong performance of the EFNav mesoscale model in predicting fuel consumption over a route indicates that the EFNav mesoscale model application should do well with comparisons of routes based on fuel use.

A comparison of EFNav mesoscale model fuel predictions along the test route for varying conditions, presented in Figure 5-8, demonstrates the sensitivity of the EFNav mesoscale model application to the operational parameters of grade and weight. The blue line shows the EFNav mesoscale model fuel prediction at a test weight of 72,000 lbs. using the link based network grade. The red line presents the same prediction at a minimum test weight of 20,000 lbs. and the green line presents the same prediction at a maximum test weight of 80,000 lbs. These values show that the difference in fuel prediction due to weight change alone can vary by as much as 240 %. The magenta line presents the same prediction as the base EFNav mesoscale model case with the exception of network grade which was set to zero. The results show that in this case the inclusion of network grade decreases the fuel prediction by 13 % and the resulting prediction is much more linear with distance.

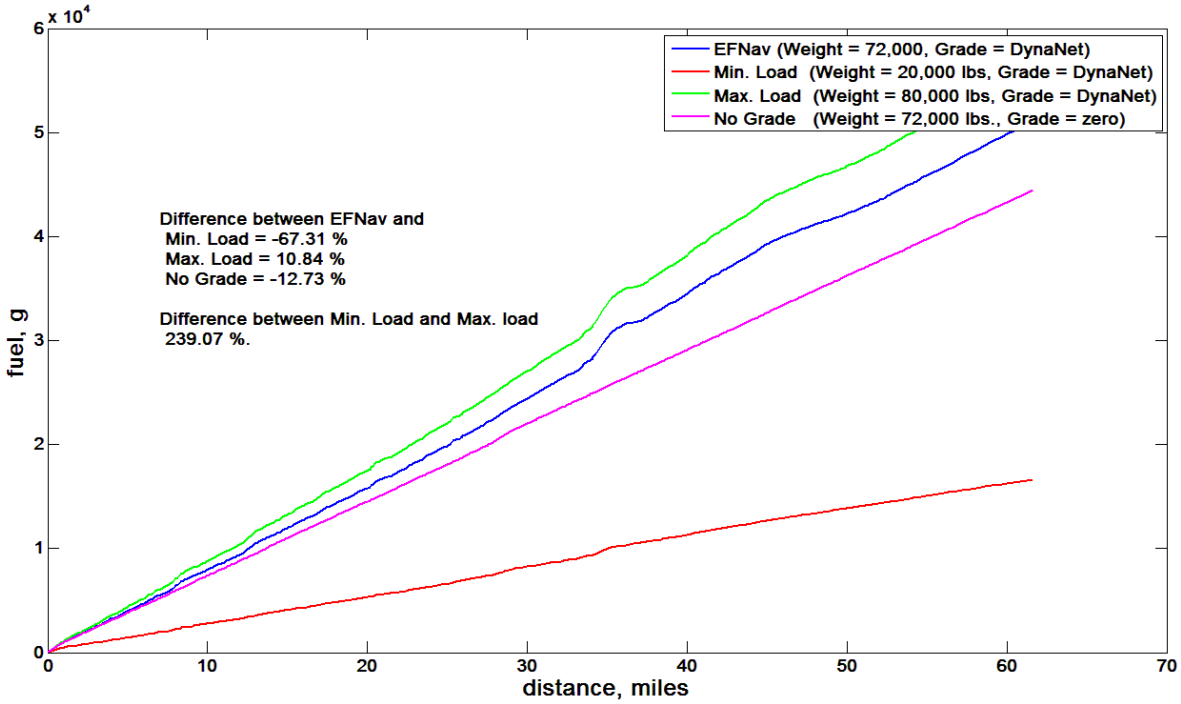

Figure 5-8 Mesoscale model sensitivity to operational parameters of grade and weight

5.4 Chapter 5 Summary

This chapter presented an example application of the developed mesoscale model in an HDD EFNav application. The key objective of EFNav is to optimize vehicle routing to minimize some of the negative environmental effects associated with transportation such as fuel consumption and GHG emissions. The optimization of routes based on fuel use requires the accurate estimation of fuel use across links in a roadway network. The mesoscale fuel model was integrated into the EFNav application to provide a more accurate projection of fuel use than the standard average speed based estimation by accounting for roadway grade and vehicle mass, two important parameters affecting engine load and consequently fuel consumption.

The mesoscale fuel model was calibrated for a HDD test truck following the steps presented in Chapter 4.0. This process involved the calibration of the HDD microscale model, the generation of a mesoscale modeling data set and the fitting of the mesoscale model to the mesoscale modeling data set. Calibration and validation results for the microscale model were similar with a RMSE error between 1.45 g/s and 1.6 g/s, an R^2 of 0.94 and total error of less than 1 %. The mesoscale fuel model was calibrated to zero overall error which resulted in an R^2 of 0.88 and a RMSE of 155.4 g/m. The mesoscale fuel model validation resulted in an R^2 of 0.87, the RMSE rose to 196.5 g/m, and the total error was roughly 2 %.

Measured vehicle activity and location data were collected for the HDD test truck loaded to 72,000 lbs. on a fuel minimized route from the POLB to Fontana. Predicted fuel from the EFNav mesoscale model application using average link data was compared to calculated fuel from the microscale model using second-by-second vehicle activity. The results show that the EFNav mesoscale model application is within 7.5 % of the calculated value and that cumulative fuel use tracks very well over the route. This demonstrates that the EFNav mesoscale model is an effective tool for fuel based route minimization.

EFNav mesoscale model predictions for the test route at selected weights and with road grade and no road grade show that fuel predictions can vary by as much as 240 % between a fully loaded truck and an empty truck and that the omission of road grade reduces the fuel estimation by as much as 12.7 % for the selected route.

6.0 Conclusions and Recommendations for Further Research

This dissertation consists of major components: 1) the development of an advanced microscale HDD PM model derived from unique real-world measured activity and emission data sets; 2) the development of a mesoscale fuel and PM model which utilizes key operational parameters such as vehicle weight and road grade, and is developed from a specially generated comprehensive set of simulated data; and 3) the application of the mesoscale model in a unique EFNav application providing robust fuel use estimation for route minimization. This chapter discusses key conclusions from this work and provides suggestions for possible areas of future research.

6.1 Conclusions

Key conclusions from this work are split up under the three components of research and are presented here.

6.1.1 Microscale PM Model Development

A microscale HDD PM emissions model was developed and calibrated from a unique set of measured second-by-second on-road test data. Various explanatory variables were evaluated for their predictive power for PM emissions. PM was found to correlate strongly with fuel consumption and the positive change in fuel consumption. These two parameters formed the basis of the PM model. Splitting the model into positive and negative acceleration regions was not found to improve PM predictions; however, splitting the model into velocity ranges did show a marked improvement in PM

predictions decreasing the RMSE by 20% (0.0013303 g/s to 0.0010473 g/s) in the calibration data set and by 10% (0.002194 g/s to 0.0019687 g/s) in the validation data set with significant improvements in R^2 as well.

Results for the selected PM model, calibrated to zero overall error on measured predictor values, show an R^2 value of 0.72 and an RMSE of 0.00104 g/s. The results of the selected PM model on the validation data set, using modeled predictor values, shows an R^2 value of 0.46 and an RMSE of 0.00197 g/s. A comparison between the DustTrak and the Dekati analyzers show slightly better R^2 and RMSE values (R^2 = 0.58, RMSE = 0.00172 g/s). The performance of the model based on known data from the ECU in the calibration data set indicates that the model performance may be greatly improved in an onboard vehicle application such as real-time on-board emission predictions. In the calibration step, model performance matches PM emissions from the Dekati far better than the scaled DustTrak data; with an improvement in RMSE of nearly 40% and an increase in R^2 from 0.58 to 0.72.

Compression release braking was identified as a source of PM emissions. It was estimated that the test truck spent roughly 1.7% of its time in compression release braking mode and that this accounted for roughly 3% of the total PM emissions across 7.5 hours of vehicle activity. It was noted that compression release braking is isolated to specific areas and may be of particular interest in exposure studies, especially with sensitive areas located next to downhill roadways. A PM emission modeling approach

using an exponential decay equation was presented for compression release braking events.

6.1.2 Mesoscale Model Development

A mesoscale fuel and PM model which utilizes key operational parameters such as vehicle weight and road grade was developed for a HDD truck. The mesoscale model was developed and calibrated from a specifically generated set of simulated emission data that encompasses a comprehensive range of vehicle speeds, vehicle weights, and road grades.

A 6 parameter MLR fuel model and a 7 parameter MLR PM model were developed from the modeled data set. Validation results on the independent set of arterial snippets through a wide range of weights and grades show fuel prediction error to within 2% of the target value and PM prediction error to within 12% of the target value, with R^2 values of 0.89 to 0.85 respectively.

Several operational parameters were considered. Analysis of measured data shows that road grade has a strong positive linear relationship with fuel consumption when acceleration is near zero. Truck speed was found to be negatively correlated to road grade. An analysis of over 57 hours of truck driving data showed that truck speeds above 60 mph were occurring predominantly at increasingly larger negative grades. This result may be important when considering limiting truck speeds to reduce fuel use and emissions since it indicates that projected fuel savings may be considerably less than expected if the influence of grade is not considered.

HDD CO_2 emission data was simulated for various average speeds and grades. The results show that the optimal vehicle operating speed decreases as road grade increases and that the relationship between CO_2 emissions and vehicle speed becomes linear with increasing road grade.

Vehicle weight was also examined in detail. Simulated HDD CO_2 emission data for various average speeds and truck loads indicates that not only do CO_2 emissions increase with vehicle load as expected, but that the optimal vehicle speed also increases with vehicle load.

6.1.3 EFNav with the Developed Mesoscale Model

The mesoscale model, developed for a variety of transportation/emission analyses, was integrated with an EFNav application and compared against test data. The results show that truck speed predictions were very reasonable and that truck travel time on the route was overestimated by 11 %. Fuel estimation from the EFNav mesoscale model application for the trip was over estimated by 7.5 % and matches well in profile with measured data. Comparison of EFNav mesoscale model predictions for different weights showed that cumulative fuel use varied by 240 % between an empty truck and a fully loaded truck weight for the examined route. Comparisons of EFNav mesoscale model predictions with and without grade information show that grade information increased the fuel prediction by 12.7 %. The ability of the EFNav mesoscale model application to accurately predict fuel use and the sensitivity of the application to the

parameters of grade and vehicle weight show that EFNav mesoscale model is an effective tool for evaluating routes based on fuel use.

6.2 Recommendation for Further Work

This section presents several areas for future work which are relevant to the topics presented in this dissertation.

Variable Time Alignment – Time alignment of PM emissions to vehicle activity data in this research was performed statistically to within fractions of a second using a constant time shift. True alignment of measured tailpipe mass emissions depends in part on variances in the exhaust flow rate. Data analysis as well as model development may benefit significantly from a variable time shift or similar corrections which account for these variances.

Compression Release Braking – Compression release braking was identified as a significant source of PM emissions and one which is localized to specific conditions, namely on greater or lengthy negative road grades (i.e., downhill). Further research is required to determine the occurrence, magnitude and influences of these emissions. Compression release braking should be analyzed geospatially and in relation to human exposure. Once further refined, the compression release braking module can be integrated with the HDT PM emission model.

Application of On-Board PM Model – Calibration results from the microscale PM model using ECM data indicate that the microscale PM model performance based on fuel data from the ECM is significantly improved relative to modeled fuel from the physical model.

This indicates that the model would lend itself well in an onboard vehicle application such as real-time on-board emission predictions. In this application, the fuel parameter is unaffected by unknown conditions such as wind, road grade or variances in weight. Access to the ECM module would also provide additional parameters that are useful for modeling such as an indicator for compression release braking, the number of cylinders being used in compression release braking or an indicator for diesel particulate filter regeneration.

Additional Operational Parameter Evaluation – The developed mesoscale model accounts for road grade, vehicle weight and vehicle speed which are the driving operational parameters in HDD fuel consumption. Additional research is required to identify and incorporate the effects of further operational parameters such as road type, congestion level, stop-and-go characteristics, idle time and driver behavior.

Developed Mesoscale Model Across Vehicle Types – The mesoscale model was developed for a single type of vehicle, however it is applicable to a wide-range of vehicle. Further research is required to continue to expand this modeling effort to a wider variety of vehicle types.

Link Length Analysis – The mesoscale modeling data set was developed from vehicle activity snippets that varied from 0.1 miles to over 40 miles in length. This results in a desired wide range of activity characteristics. For particular applications that require fuel or emission estimations over shorter distances or times, such as EFNav whose link lengths are predominantly less than 0.2 miles, the development of the mesoscale model

from shorter activity cycles may reduce modeling error. Further research is required to characterize the optimal cycle characteristics for the applied application.

References

AEI. (2010, August). *Annual Energy Review 2009.* Retrieved September 2011, from U.S. Energy Information Administration: http://www.eia.gov/totalenergy/data/annual/pdf/aer.pdf

Ahn, K., & Rakha, H. (2007). Field Evaluation of Energy and Environmental Impacts of Driver Route Choice Decisions. *2007 IEEE Intelligent Transportation Systems Conference.* Seattle, WA.

Ahn, K., Rakha, H., Trani, A., Aerde, V., & M. (2002). Estimating vehicle fuel consumption and emissions based on instantaneous speed and acceleration levels. *Journal of Transportation Engineering, 128(2),* 182-190.

ALK Technologies Inc. (2011). *PC-Miler*. Retrieved 10 10, 2011, from PC-Miler: http://pcmiler.com/

Amsden, A. (1999). *KIVA A-3V, Release 2, Improvements to KIVA A-3V.* Los Alamos National Laboratory.

An, F., & Ross, M. (1993). A Model of Fuel Economy with Applications to Driving Cycles and Traffic Management. *Transportation Research Record 1416*, 105-114.

An, F., Barth, M., Norbeck, J., & Ross, M. (1997). Development of comprehensive modal emissions model: operating under hot-stabilized conditions. *Transportation Research Record: Journal of the Transportation Research Board, No. 1587*, 52-62.

An, F., Barth, M., Scora, G., & Ross, M. (1998). Modeling enleanment emissions for light-duty vehicles. *Transportation Research Record No. 1641*, 48-57.

An, F., Barth, M., Scora, G., & Ross, M. (1999). Modal-based intermediate soak time emissions modeling. *Transportation Research Record No. 1664, National Academy of Science.,* 58-67.

Andre, M., & Pronello, C. (1997). Relative influence of acceleration and speed on emissions under actual driving conditions. *International Journal of Vehicle Design, 18,* 340-353.

ARB. (2008, December 12). ARB adopts landmark rules to clean up pollution from "big rigs". *California Environmental Protection Agency News Release: Release 08-103*.

ArcLogistics. (2009). *ArcLogistcs 9.3*. Retrieved October 2010, from ArcLogistics Website: www.arclogistics.info

ATA. (2011). *Recommendation 1: Speed Limits and Speed Governing*. Retrieved October 2011, from Trucks Deliver a Cleaner Tomorrow: http://www.trucksdeliver.org/recommendations/speed-limits.html

Barth, M., & Boriboonsomsin, K. (2008). Real-World CO2 Impacts of Traffic Congestion. *Transportation Research Record, Journal of the Transportation Research Board, No. 2058*.

Barth, M., An, F., Norbeck, J., & Ross, M. (1996). Modal emissions modeling: a physical approach. *Transportation Research Record: Journal of the Transportation Research Board, No. 1520*, 81-88.

Barth, M., An, F., Younglove, T., Scora, G., Levine, C., Ross, M., et al. (2000, April). NCHRP Web-Only Document 122,Contractor's final report for NCHRP Project 25-11, National Cooperative Highway Research Program. *The development of a comprehensive modal emissions model*.

Barth, M., Boriboonsomsin, K., & Vu, A. (2007). Environmentally-Friendly Navigation. *2007 IEEE Intelligent Tansportation Systems Conference.* Seattle, WA.

Barth, M., Malcolm, C., & Scora, G. (2001, May). PATH Technical Report (MOU-381), California PATH Program. *Integrating a comprehensive modal emissions model into ATMIS transportation modeling frameworks* , 51.

Barth, M., Scora, G., & Younglove, T. (2004). A Modal Emission Model for Heavy Duty Diesel Vehicles. *Transportation Research Record Number 1880,Journal of the Transportation Research Board*, 10-20.

Barth, M., Wenzel, T., Scora, G., An, F., Ross, M., & Norbeck, J. (1997). Analysis of modal emissions from diverse in-use vehicle fleet. *Transportation Research Record: Journal of the Transportation Research Board, No. 1587*, 73-84.

Bonnet, C., & Fritz, H. (2000). Fuel Consumption Reduction in a Platoon: Experimental Results with two Electronically Coupled Trucks at Close Spacing. *SAE International*(2000-01-3056).

Boriboonsomsin, K., Barth, M., Zhu, W., & Vu, A. (2010). ECO-Routing Navigation System based on Multi-Source Historical and Real-Time Traffic Information. *IEEE ITSC2010 Workshop on Emergent Cooperative Technologies in Intelligent Transportation Systems.*

Boriboonsomsin, K., Zhu, W., & Barth, M. (2011). A Statistical Approach to Estimating Truck Traffic Speed and its Application to Emission Inventory Modeling. *Transportation Research Record*.

Browand, F., McArthur, J., & Radovich, C. (2004). *Fuel Saving Achieved in the Field Test of Two Tandem Trucks.* California PATH Research Report UCB-ITS-PRR-2004-20, University of California Berkeley.

CARB. (1998, October). The Toxic Air Contaminant Identification Process:Toxic Air Contaminant Emissions from Diesel-fueled Engines. *Fact Sheet*. Sacramento, CA.

CARB. (2000, October). Risk Reduction Plan to Reduce Particulate Matter Emissions from Diesel-Fueled Engines and Vehicles. http://www.arb.ca.gov/diesel/documents/rrpfinal.pdf, (accessed November 2009).

CARB. (2000). *Risk Reduction Plan to Reduce Particulate Matter Emissions from Diesel-Fueled Engines and Vehicles.*

CARB. (2009, 12 7). *AB 32 Fact Sheet-California Global Warming Solutions Act of 2006.* Retrieved October 2010, from California Air Resources Board Web Site: www.arb.ca.gov/cc/factsheets/ab32factsheet.pdf

CARB. (2010). *Greenhouse Gas Inventory Data - 2000 to 2008.* Retrieved 10 2010, from CARB Web Site: http://www.arb.ca.gov/cc/inventory/data/data.htm

Chabini, I., & Lan, S. (2002). Adaption of A* Algorithm for the Computation of Fastest Path in Deterministic Discrete-time Dynamic Networks. *IEEE Transactions on Intelligent Transportation Systems, 3*(1).

Chambers, J. (2001). *The S System*. Retrieved 10 10, 2011, from S: http://stat.bell-labs.com/S/

Chao, C., Jia, Z., Petty, K., Shu, J., Skarbardonis, A., & Varaiya, P. (2000). FREEWAY PERFORMANCE MEASUREMENT SYSTEM (PEMS) SHOWS BIG PICTURE. *Intellimotion, 9*(2).

Clark, N., Gautam, M., Wayne, S., Lyons, D., Thompson, G., & Zielinska, B. (2007). *Heavy-duty Vehicle Chassis Dynamometer Testing for Emissions Inventory, Air Quality Modeling, Source Apportionment and Air Toxics Emissions Inventory E-55/59 All Phases.* Alpharetta, GA: Coordinating Research Council, INC.

Cocker, D., Shah, S., Johnson, K., Miller, W., & Norbeck, J. (2004). Development and Application of a Mobile Laboratory for Measuring Emissions from Diesel

Engines. 1. Regulated Gaseous Emissions. *Environmental Science & Technology, 38*, 2182-2189.

Cocker, D., Shah, S., Johnson, K., Zhu, X., Miller, W., & Norbeck, J. (2004). Development and Appliation of a Mobile Laboratory for Measuring Emissions from Diesel Engines. 2. Sampling for Toxics and Particulate Matter. *Environmental Science & Technology, 38*, 6809-6816.

Dekati Ltd. (2010, 1). *Dekati DMM Mass Monitor.* Retrieved from Dekati Web site: www.dekati.com/cms/files/File/PDF/DMMbrochure.pdf

EIA. (2010, August 19). *Total Energy - Annual Energy Review.* Retrieved February 2011, from U.S. Energy Information Administration: www.eia.doe.gov/emeu/aer/ep/ep_frame.html#9

EPA. (1997, September). Emission Standards Reference Guide for Heavy-Duty and Nonroad Engines. *EPA420-F-97-014*.

EPA. (2002). *User's Guide to MOBILE6.1 and MOBILE6.2: Mobile Source Emission Factor Model.*

EPA. (2005). *Emission Facts: Average Carbon Dioxide Emissions Resulting from Gasoline and Diesel Fuel.* OTAQ.

EPA. (2010). *PM-PEMS Measurement Allowance Determination: Final Report.*

EPA. (2011). *Regulatory Announcement: EPA Finalizes Transportation Conformity Rule: MOVES Regional Grace Period Extension.*

Farrell, J., Givargis, T., & Barth, M. (2000). Real-Time Differential Carrier Phase GPS-Aided INS. *IEEE Transactions on Control Systems Technology, 8*(8).

Fernandez, P., & Long, J. (1995). Grades and other load effects on on-road emissions: an on-board analyzer study. *Fifth CRC On-Road Vehicle Emission Workshop.* San Diego.

FHWA. (2011). *Chapter 2: National Freight Transportation Trends and Emissions.* Retrieved October 2011, from Federal Highway Administration Web Site: http://www.fhwa.dot.gov/environment/air_quality/publications/effects_of_freight_movement/chapter02.cfm

FHWA. (2011, January). *Federal Highway Administration Web Site.* Retrieved September 2011, from Freight Facts and Figures 2010:

http://ops.fhwa.dot.gov/freight/freight_analysis/nat_freight_stats/docs/10factsfigures/table2_1.htm

Frazzoli, E., & Bullo, F. (2004). Decentralized algorithms for vehicle routing in a stochastic time-varying environment. *Decision and Control*, 3357-3363.

Ghiani, G., Guerriero, F., Laporte, G., & Musmanno, R. (2003). Real-time vehicle routing: Solution concepts, algorithms and parallel computing strategies. *European Journal of Operational Research*, 1-11.

Hausberger, S., Rodler, J., Sturm, P., & Rexeis, M. (2003). Emission Factors for HDV andValidation by Tunnel Measurements. *Atmospheric Environment 37*, 5237-5245.

Heywood, J. (1988). *Internal Combustion Engine Fundamentals.* New York: McGraw-Hill.

Huang, W., Bevly, D., & Li, X. (2007). 3D Road Geometry Based Optimal Truck Fuel Economy. *Proceedings of ASME International.* Seattle, Washington.

INRIX Inc. (2011). *Home*. Retrieved 10 10, 2011, from INRIX go anywhere: http://www.inrix.com/

ISSRC. (2008). *IVE Model Users Manual Version 2.0.*

Johnson, T. (2006). Diesel Emission Control Review. *SAE Technical Paper Series*(2006-01-0030).

Kean, A., Harley, R., & Kendall, G. (2003). Effects of Vehicle Speed and Engine Load on Motor Vehicle Emissions. *Environmental Science and Technology*, 3739-3747.

Kear, T., & Niemeier, D. (2006). On-Road Heavy-Duty Diesel Particulate Mass Emissions Modeled Using Chassis Dynamometer Data. *Environ. Sci. Tchnol.*, 40:7828-7833.

Koupal, J. (2001). Beyond MOBILE6: EPA's Plan for Developing a New Generation Mobile Source Emissions Model. *Proceedings of the CRC 11th On-Road Vehicle Emission Workshop.* San Diego, California.

Koupal, J., Cumberworth, M., Michaels, H., Beardsley, M., & Brzezinski, D. (2002). *Draft Design and Implementation Plan for EPA's Multi-Scale Motor Vehicle and Equipment Emission System (MOVES).* U.S. EPA Technical Report #420-P-02-006.

Liu, H., He, K., Lents, J., & Wang, Q. (2008). *Methodology for Developing Microemission Model Based on On-Board Heavy-Duty Truck Tests in China.*

Lloyd, A., & Cackette, T. (2001, June). Diesel Engines: Environmental Impact and Control. *Air & Waste Management Association, 51*, 809-847.

MathWorks. (2009). *MATLAB-The Language of Technical Computing.* Retrieved May 2010, from MathWorks Web Site: www.mathworks.com/products/matlab/technicaliterature.html

Nam, E., Giannelli, B., & Koupal, J. (2003). Speed Anomalies in VSP Based Emissions. *13th CRC On-Road Vehicle Emission Workshop.* San Diego.

NAVTEQ. (2011). Retrieved September 2011, from NAVTEQ website: http://www.nn4d.com/site/global/home/p_home.jsp

ORTEC. (2011). *ORTEC*. Retrieved 10 10, 2011, from ORTEC: http://www.ortec.com/US

Palacios, J. (1999). *Understanding and Quantifying Motor Vehicle Emission with Vehicle Specific Power and TILDAS Remote Sensing.* PhD Thesis, MIT.

Park, K., Cao, F., Kittelson, D., & McMurray, P. (2003). Relationship between Partical Mass and Mobility for Diesel Exhaust Particles. *Environmental Science and Technology*.

Park, S., & Rakha, H. (2006). Energy and environmental impacts of roadway grades. *85th Annual Meeting of Transportation Research Board.* Washington D.C.

Parks, J., & Huff, S. (2007). Characterization of In-Cylinder Techniques for Thermal Management of Diesel Aftertreatment. *SAE International*(2007-01-3997).

Port of Long Beach. (2011). *Facts at a Glance*. Retrieved October 2011, from Port of Long Beach: Green Port: http://www.polb.com/about/facts.asp

Rakha, H., Ahn, K., & Trani, A. (2004). Evelopment of VT-Micro Model for Estimating Hot Stabilized Light Duty Vehicle and Truck Emissions. *Transportation Research Part D-Transport and Environment 9(1)*, 49-74.

Rakha, H., Van Aerde, M., Ahn, K., & Tran, A. (2000). Requirements for Evaluating Traffic Signal Control Impacts on Energy and Emissions Based on Instantaneous Speed and Acceleration Measurements. *Transportation Research Record 1738*, 56-67.

Rand McNally. (2011). *Truck GPS*. Retrieved 10 10, 2011, from RAND McNally: http://www.randmcnally.com/trucking/

Razi, M., & Athappilly, K. (2005). A comparative predictive analysis of neural networks (NN), nonlinear regression and classification and regression tree (CART) models. *Expert Systems with Applications 29*, 65-74.

Scora, G. (2007, September). *Development of a Heavy Duty Diesel Emissions Model and Transportation Model Integration.* MS Thesis, UCR.

Scora, G. (2010). Effects of Operational Variability on Heavy-Duty Truck Greenhouse Gas Emissions. *Proceedings, Transportation Research Board 89th Annual Meeting.*

Scora, G., Morris, B., Barth, M., & Trivedi, M. (2011). Real-Time Roadway Emission Estimation using Visual Traffic Measurements. *IEEE Trans. Intelligent Transportation Systems.*

Seinfeld, J., & Pandis, S. (1998). *Atmospheric Chemistry and Physics.* New York: John Wiley & Sons, Inc.

Stone, C. (1996). *A Course in Probability and Statistics.* Belmont: Wadsworth Publishing.

Svensk, P.-O., & Sena, M. (2011). Energy Efficient Navigation for Heavy Vehicles. *18th ITS World Congress on Intelligent Transportation Systems.* Orlando.

TeleType Co. (2010). *Truck GPS*. Retrieved 10 10, 2011, from WorldNav Satellite Navigation System: http://www.teletype.com/c/portable-truck-gps.html

The Port of Los Angeles: America's Port. (2011). *About the Port*. Retrieved October 2011, from The Port of Los Angeles: http://www.portoflosangeles.org/idx_about.asp

TSI. (2006). *DustTrak DRX Aerosol Monitor Theory and Operation. Application Note EXPMN-002.*

TSI. (2009). *Measuring Total Suspended Particulates (TSP) with Aerosol Photometers. Application Note ITI-058.* Shoreview, MN: TSI Incorporated.

TSI. (2011). *Precision Measurement Tools with Unsurpassed Accuracy and Reliability*. Retrieved 10 10, 2011, from TSI Trust. Science. Innovation.: http://www.tsi.com/

TU Graz. (2009). *Emission Factors from the Model PHEM for the HBEFA Version 3.* Report Nr. I-20a/2009 Haus-Em 33a/08/679.

Twigg, M., & Phillips, P. (2009). Cleaning the Air We Breathe - Controlling Diesel Particulate Emissions from Passenger Cars. *Platinum Metals Rev., 53*(1), 27-34.

Wang, W., Lyons, W., Clark, N., & Luo, J. (1999). Energy consumption analysis of heavy-duty vehicles for transient emissions evaluation on chassis dynamometer. *Journal of Automobile Engineering*, 205-214.

Warila, J., Nam, E., Landman, L., & Kahan, A. (2011). Light-Duty Exhaust Emission Rates in MOVES2010. *MOVES Workshop.* Ann Arbor.

Wark, K., & Warner. (1981). *Air Pollution: Its Origin and Control: Second Edition.* New York, New York: Harper Collins.

Yanowitz, J., McCormick, R., & Graboski, M. (2000, January). In-Use Emissions from Heavy Duty Diesel Vehicles. *Environmental Science & Technology, 34*(5), 729-740.

Zhang, K., & Frey, C. (2005). Road Grade Estimation for On-Road Vehicle Emissions Modeling Using LIDAR Data. *Proceedings, Annual Meeting of the Air and Waste Management Association.* Minneapolis.

Appendix A – VSP Equations for Transportation Analysis

$$\mathrm{VSP} = v(1.1a + \mathrm{g}\sin(\theta) + \mathrm{g}C_r) + \frac{\rho_a C_d A_f v^3}{2M} \quad \text{A-1}$$

where

v = vehicle speed in m/s

a = vehicle acceleration in m/s^2

g = gravity (m/s^2)

θ = grade

C_r = coefficient of rolling resistance

ρ_a = density of air (kg/m^3)

(~1.2 kg/m^3 at sea level and 20 °C)

C_d = coefficient of aerodynamic drag

A_f = frontal area of vehicle (m^2)

M = mass of vehicle (kg)

Typical values for some of the coefficients can be assumed and the equation can be simplified for general use. Some variable approximations are presented in Table A-1 for seven vehicle classes.

Table A-1 Approximation of vehicle category characteristics

Type	Mass (kg)	Frontal Area (m^2)	C_r	C_d
Sedan	1360	2.0	0.0135	0.34
Pickup	2340	3.3	0.0135	0.43
SUV	3035	3.44	0.0135	0.41
Van	2270	3.46	0.0135	0.38
Bike	230	0.65	0.0250	0.9
Truck	11360	6.6	0.0094	0.7
Semi	27300	10.0	0.0094	0.85

Using the approximated values from the Table A-1, the terms in equation A-1 can be reduced, for ease of use, to the equations found in the Table A-2 (Scora, Morris, Barth, & Trivedi, 2011).

Table A-2. VSP equations for vehicle classes.

Type	VSP Equation (kW/metric ton)
Sedan	$\text{VSP} = v(1.1a + \text{g}\sin(\theta) + 0.1323) + 0.000300v^3$
Pickup	$\text{VSP} = v(1.1a + \text{g}\sin(\theta) + 0.1323) + 0.000364v^3$
SUV	$\text{VSP} = v(1.1a + \text{g}\sin(\theta) + 0.1323) + 0.000279v^3$
Van	$\text{VSP} = v(1.1a + \text{g}\sin(\theta) + 0.1323) + 0.000348v^3$
Bike	$\text{VSP} = v(1.1a + \text{g}\sin(\theta) + 0.24500) + 0.001526v^3$
Truck	$\text{VSP} = v(1.1a + \text{g}\sin(\theta) + 0.09212) + 0.000244v^3$
Semi	$\text{VSP} = v(1.1a + \text{g}\sin(\theta) + 0.09212) + 0.000187v^3$

Appendix B – Correlation Matrices for Calibration Data

The following tables show correlations between some of the explanatory variables which were considered for microscale modeling discussed in Chapter 0. The correlation tables are split into three speed groups discussed in Sections 2.6.1 and 3.6.

Table 6-1 Correlation matrix of explanatory variables for speeds between 0 and 25 mph.

	vel	acc	acc-	acc+	jerk	jerk+	grade	fuel	$fuel^2$	$fuel^3$	VSP	dfdt	dfdt+	dfdt-	RPM	PM
vel	1	0.06	0.02	0.12	-0.21	-0.22	-0.02	0.43	0.45	0.41	0.08	0.05	0.21	-0.17	0.4	0.34
acc	0.06	1	0.95	0.74	-0.06	-0.2	-0.06	0.6	0.43	0.34	0.01	0.18	0.42	-0.2	0.62	0.52
acc-	0.02	0.95	1	0.49	-0.08	-0.24	-0.05	0.41	0.27	0.2	-0.01	0.08	0.27	-0.19	0.53	0.36
acc+	0.12	0.74	0.49	1	0.01	-0.05	-0.04	0.76	0.61	0.5	0.07	0.31	0.57	-0.15	0.58	0.68
jerk	-0.21	-0.06	-0.08	0.01	1	0.92	0.05	-0.04	-0.02	-0.01	0.03	0.28	0.18	0.27	-0.23	-0.03
jerk+	-0.22	-0.2	-0.24	-0.05	0.92	1	0.06	-0.1	-0.07	-0.05	0.04	0.16	0.1	0.17	-0.24	-0.09
grade	-0.02	-0.06	-0.05	-0.04	0.05	0.06	1	0.15	0.16	0.16	0.62	0.04	0.08	-0.03	-0.1	0.12
fuel	0.43	0.6	0.41	0.76	-0.04	-0.1	0.15	1	0.94	0.85	0.28	0.37	0.64	-0.14	0.63	0.83
$fuel^2$	0.45	0.43	0.27	0.61	-0.02	-0.07	0.16	0.94	1	0.98	0.31	0.37	0.55	-0.02	0.45	0.71
$fuel^3$	0.41	0.34	0.2	0.5	-0.01	-0.05	0.16	0.85	0.98	1	0.3	0.33	0.45	0.03	0.35	0.58
VSP	0.08	0.01	-0.01	0.07	0.03	0.04	0.62	0.28	0.31	0.3	1	0.06	0.15	-0.09	-0.04	0.22
dfdt	0.05	0.18	0.08	0.31	0.28	0.16	0.04	0.37	0.37	0.33	0.06	1	0.83	0.73	0	0.45
dfdt+	0.21	0.42	0.27	0.57	0.18	0.1	0.08	0.64	0.55	0.45	0.15	0.83	1	0.23	0.31	0.73
dfdt-	-0.17	-0.2	-0.19	-0.15	0.27	0.17	-0.03	-0.14	-0.02	0.03	-0.09	0.73	0.23	1	-0.39	-0.1
RPM	0.4	0.62	0.53	0.58	-0.23	-0.24	-0.1	0.63	0.45	0.35	-0.04	0	0.31	-0.39	1	0.59
PM	0.34	0.52	0.36	0.68	-0.03	-0.09	0.12	0.83	0.71	0.58	0.22	0.45	0.73	-0.1	0.59	1

Table 6-2 Correlation matrix of explanatory variables for speeds between 25 and 50 mph.

	vel	acc	acc-	acc+	jerk	jerk+	grade	fuel	$fuel^2$	$fuel^3$	VSP	dfdt	dfdt+	dfdt-	RPM	PM
vel	1	-0.02	0.08	-0.2	0.04	-0.07	-0.04	0.08	0.07	0.05	0.15	0	-0.13	0.09	0.08	-0.16
acc	-0.02	1	0.92	0.68	0.32	-0.15	-0.12	0.59	0.51	0.47	-0.02	0.09	0.21	-0.04	0.46	0.41
acc-	0.08	0.92	1	0.33	0.38	-0.18	0.06	0.49	0.4	0.35	0.09	0.06	0.14	-0.03	0.43	0.28
acc+	-0.2	0.68	0.33	1	0.06	-0.03	-0.41	0.48	0.48	0.48	-0.22	0.11	0.25	-0.04	0.29	0.46
jerk	0.04	0.32	0.38	0.06	1	0.6	0.04	0.13	0.12	0.1	0	0.42	0.29	0.36	-0.14	0.2
jerk+	-0.07	-0.15	-0.18	-0.03	0.6	1	-0.1	-0.12	-0.12	-0.12	-0.1	0.29	0.32	0.15	-0.25	0.15
grade	-0.04	-0.12	0.06	-0.41	0.04	-0.1	1	0.44	0.42	0.39	0.55	0.02	-0.12	0.12	0.05	0
fuel	0.08	0.59	0.49	0.48	0.13	-0.12	0.44	1	0.97	0.92	0.31	0.16	0.09	0.15	0.39	0.39
$fuel^2$	0.07	0.51	0.4	0.48	0.12	-0.12	0.42	0.97	1	0.99	0.31	0.17	0.02	0.22	0.36	0.31
$fuel^3$	0.05	0.47	0.35	0.48	0.1	-0.12	0.39	0.92	0.99	1	0.29	0.17	-0.02	0.24	0.35	0.26
VSP	0.15	-0.02	0.09	-0.22	0	-0.1	0.55	0.31	0.31	0.29	1	-0.02	-0.05	0.01	0.1	0.03
dfdt	0	0.09	0.06	0.11	0.42	0.29	0.02	0.16	0.17	0.17	-0.02	1	0.7	0.85	-0.24	0.45
dfdt+	-0.13	0.21	0.14	0.25	0.29	0.32	-0.12	0.09	0.02	-0.02	-0.05	0.7	1	0.21	-0.09	0.73
dfdt-	0.09	-0.04	-0.03	-0.04	0.36	0.15	0.12	0.15	0.22	0.24	0.01	0.85	0.21	1	-0.26	0.07
RPM	0.08	0.46	0.43	0.29	-0.14	-0.25	0.05	0.39	0.36	0.35	0.1	-0.24	-0.09	-0.26	1	0.03
PM	-0.16	0.41	0.28	0.46	0.2	0.15	0	0.39	0.31	0.26	0.03	0.45	0.73	0.07	0.03	1

Table 6-3 Correlation matrix of explanatory variables for speeds greater than 50 mph.

	vel	acc	acc-	acc+	jerk	jerk+	grade	fuel	$fuel^2$	$fuel^3$	VSP	dfdt	dfdt+	dfdt-	RPM	PM
vel	1	0.02	0.1	-0.14	-0.04	-0.11	-0.23	-0.14	-0.15	-0.15	-0.21	-0.1	-0.11	-0.05	0.77	-0.23
acc	0.02	1	0.91	0.64	0.61	0.02	-0.22	0.31	0.27	0.24	-0.18	0.11	0.08	0.09	-0.02	0.22
acc-	0.1	0.91	1	0.27	0.72	0.02	-0.1	0.22	0.18	0.15	-0.07	0.09	0.04	0.09	0.05	0.11
acc+	-0.14	0.64	0.27	1	0.09	0.01	-0.32	0.32	0.31	0.29	-0.28	0.09	0.11	0.04	-0.13	0.31
jerk	-0.04	0.61	0.72	0.09	1	0.46	0.01	0.08	0.06	0.05	0.02	0.28	0.19	0.23	-0.13	0.13
jerk+	-0.11	0.02	0.02	0.01	0.46	1	-0.09	-0.04	-0.05	-0.05	-0.08	0.28	0.3	0.14	-0.12	0.17
grade	-0.23	-0.22	-0.1	-0.32	0.01	-0.09	1	0.68	0.65	0.61	0.94	0.01	0.02	-0.01	-0.3	0.27
fuel	-0.14	0.31	0.22	0.32	0.08	-0.04	0.68	1	0.96	0.91	0.69	0.09	0.07	0.08	-0.22	0.48
$fuel^2$	-0.15	0.27	0.18	0.31	0.06	-0.05	0.65	0.96	1	0.99	0.67	0.09	0	0.13	-0.21	0.45
$fuel^3$	-0.15	0.24	0.15	0.29	0.05	-0.05	0.61	0.91	0.99	1	0.63	0.08	-0.03	0.14	-0.2	0.41
VSP	-0.21	-0.18	-0.07	-0.28	0.02	-0.08	0.94	0.69	0.67	0.63	1	0	0.01	-0.01	-0.26	0.27
dfdt	-0.1	0.11	0.09	0.09	0.28	0.28	0.01	0.09	0.09	0.08	0	1	0.69	0.82	-0.13	0.42
dfdt+	-0.11	0.08	0.04	0.11	0.19	0.3	0.02	0.07	0	-0.03	0.01	0.69	1	0.17	-0.13	0.64
dfdt-	-0.05	0.09	0.09	0.04	0.23	0.14	-0.01	0.08	0.13	0.14	-0.01	0.82	0.17	1	-0.08	0.07
RPM	0.77	-0.02	0.05	-0.13	-0.13	-0.12	-0.3	-0.22	-0.21	-0.2	-0.26	-0.13	-0.13	-0.08	1	-0.26
PM	-0.23	0.22	0.11	0.31	0.13	0.17	0.27	0.48	0.45	0.41	0.27	0.42	0.64	0.07	-0.26	1